THE VISUALIZATION OF STRANGE ATTRACTORS IN THREE DIMENSIONS

by

Tracy Stauffer Halsey

Thesis submitted to the Faculty of the

Virginia Polytechnic Institute and State University

in partial fulfillment of the requirements for the degree of

MASTER OF SCIENCE

in

Engineering Mechanics

APPROVED:

Scott L. Hendricks, Chairman

Ronald D. Kriz

Mark S. Cramer

April 1993

Blacksburg, Virginia

c.2

S655
V855
1993
H357
c.2

THE VISUALIZATION OF STRANGE ATTRACTORS IN THREE DIMENSIONS

by

Tracy Stauffer Halsey

Dr. Scott L. Hendricks, Chairman

Engineering Mechanics

(ABSTRACT)

The existence of strange attractors for dynamical systems with three variables is discussed. The structure and dimensionality of these attractors are observed with computer packages that have three dimensional viewing capabilities. The importance of visualizing these attractors is discussed. Some new visual tools developed for this purpose are introduced. These tools are then used to observe strange attractors for the Lorenz, Rössler, and Silnikov systems of equations. The solutions to the Lorenz equations are followed in detail for certain parameter values. Figures of the attractors are included to attempt to show the benefits of the new tools. There is an accompanying video that contains visualizations of the strange attractors to illustrate the three dimensional capability of the new tools. A comparison is made of current methods used to view attractors with the new tools. It is concluded that the three dimensional visualization of the structures is very important and beneficial for learning about the attractors.

Acknowledgements

I would first of all like to thank the Department of Engineering Science and Mechanics for the financial assistance which made the pursuit of my Master's Degree possible. I would also like to thank the department for the Help Session position, the experience was not only enjoyable but fulfilling.

My next thank you is for Doug, Mike, and especially John. The visualization lab was so much easier to go to with all three of them always cheerful, fun, and willing to lend a hand. But John deserves special thanks, for all his help in putting together the modules for visualization of the strange attractors. I will always be grateful for his help, which he so willingly gave, even when he was tremendously busy himself.

Next I would like to thank Dr. Kriz for his constant enthusiasm and dedication to scientific visualization, without which this thesis would have never started. Also, thanks for always being willing to lend a hand.

I cannot begin to thank my advisor, Dr. Hendricks, for everything. His patience, understanding, guidance, and confidence helped me to not only deal with the pressures of writing a thesis but the pressures of life. I hope to one day teach and advise students in the same outstanding manner as he does.

Thanks, Benny, for all your help in the past two years, for always keeping things interesting, and for being such a good friend.

Thanks to the "nabes", MaryBeth and Chris for their fun and friendship,

without which the past two years would have been very dull.

A special thank you goes to my parents, who were always there for me, especially for all the phone calls home (and there were lots). I hope they know how much more bearable the past six years were with them on my side.

Last but not least, I want to thank my husband Andy for everything. He was always there for me, through good times and even more importantly the bad times, and I thank him for this and all the happiness he has brought me over the years.

Table of Contents

Abstract ii

Acknowledgements iii

List of Figures viii

1. Introduction 1

    1.1 Background and Motivation 1

    1.2 Scope of Thesis 3

2. Definitions and Examples 4

    2.1 Dynamical Systems and Phase Space 4

        2.11 Point Attractor 10

        2.12 Limit Cycle 12

        2.13 Strange Attractor 15

        2.14 Fractal Dimensions 23

    2.2 Examples of Strange Attractors 29

        2.21 Lorenz Equations 30

        2.22 Rössler Equations 34

        2.23 Silnikov Equations 35

3. Visualization 37

3.1 Scientific Visualization 38

3.2 AVS Tool 40

3.21 AVS 41

3.22 Development of New Modules 42

4. Theory and Application 52

4.1 Lorenz Equations 53

4.11 Properties of the Lorenz equations 53

4.12 Lorenz solutions for 0<r<24.74 60

4.13 Lorenz strange attractor 70

4.14 Lorenz solutions for 24.74<r<∞ 70

4.2 Rössler equations 89

4.3 Silnikov Equations 97

5. Conclusion 103

5.1 Discussion and Literature Review 103

5.11 Poincaré maps 104

5.12 Other Available Software Packages 104

5.13 Other attempts 110

5.2 Conclusion 113

5.3 Suggestions for Future Work 114

References 116

Vita 119

List of Figures

Figure 2.1: A damped oscillator 6

Figure 2.2: Position and velocity plots for the underdamped oscillator 7

Figure 2.3: Phase trajectory for the damped oscillator 9

Figure 2.4: A damped pendulum 11

Figure 2.5: Phase trajectories approaching a point attractor for the damped pendulum 13

Figure 2.6: Periodic orbits in phase space for the undamped pendulum 14

Figure 2.7: Limit cycle of the Van der Pol Oscillator for a=2.5 16

Figure 2.8: Lorenz strange attractor for r=28, σ=10, b=2.66667 18

Figure 2.9: Area contraction in a point attractor 21

Figure 2.10: Process of finding the dimension of a square 24

Figure 2.11: Process of finding the dimension of the Cantor middle-thirds set 26

Figure 2.12: Process of finding the dimension of Siérpinski's Triangle 28

Figure 2.13: Rayleigh-Benard model of convecting fluid between two plates 32

Figure 3.1: Network Editor screen in AVS 43

Figure 3.2: User interface screen for the Lorenz module 45

Figure 3.3: Dial Editor box for the parameter r in the Lorenz module 46

Figure 3.4: User interface screen for the Colorpolyline module 48

Figure 3.5: User interface screen for the Colorpolyline-2 module 49

Figure 4.1: Lorenz solution for r=.5, initial (x,y,z)=(1,1,1) 58

Figure 4.2: Phase portrait near the origin for 1<r<13.92.. 61

Figure 4.3: "Crossover" of trajectories to the opposite equilibrium point 63

Figure 4.4: Homoclinic orbit for r=13.926.. 64

Figure 4.5: Trajectory near the homoclinic orbit 65

Figure 4.6: Local box enclosing origin 67

Figure 4.7: Two trajectories for 24.5 - blue attracted to strange attractor, green attracted to fixed point c1 69

Figure 4.8: A rotated view of the Lorenz strange attractor for r=28 71

Figure 4.9: A rotated view of the Lorenz strange attractor for r=28 72

Figure 4.10: Lorenz attractor for r=28, blue initial (x,y,z)=(1,1,1), green initial (x,y,z)=(1.01,1.01,1) 73

Figure 4.11: An x^2y periodic orbit for r=100 75

Figure 4.12: An x^2yx^2y periodic orbit for r=99.7 77

Figure 4.13: A y^2xy^2x periodic orbit for r=99.7 78

Figure 4.14: An x^2y^2xy periodic orbit for r=126.52 79

Figure 4.15: An x^2yxy periodic orbit for r=114.0 80

Figure 4.16: An x^2yxy^2xy periodic orbit for r=132.5 81

Figure 4.17: An x^5y^5 periodic orbit for r=58.7 83

Figure 4.18: An x^4y^4 periodic orbit for r=69.8 84

Figure 4.19: An x^3y periodic orbit for r=71.5 85

Figure 4.20: A y^2xyx^3 periodic orbit for r=86.4 86

Figure 4.21: An x^3y^3 periodic orbit for r=92.2 87

Figure 4.22: Semi-periodicity in the Lorenz attractor for r=199 88

Figure 4.23: Final xy periodic orbit for r>315 90

Figure 4.24: Periodic orbit of the Rössler system for c=2.4 92

Figure 4.25: Rössler strange attractor for c=4.26 93

Figure 4.26: A rotated view of the Rössler strange attractor for c=4.26 94

Figure 4.27: A periodic orbit of the Rössler system for c=5.3 95

Figure 4.28: A periodic orbit of the Rössler system for c=30 96

Figure 4.29: Funnel-like structure of the Rössler system for c=150 98

Figure 4.30: Silnikov strange attractor for a=.4, b=.65, c=1, d=1 99

Figure 4.31: Silnikov strange attractor for a=.37, b=.65, c=1, d=1 100

Figure 4.32: Silnikov strange attractor for a=.4, b=.7, c=2, d=1 101

Figure 5.1: Poincaré map of the Lorenz strange attractor for the plane z=r-1, with r=28, σ=10, b=2.6667 105

Figure 5.2: Poincaré map of the Rössler strange attractor for the plane x=0, with a=b=.2, c=5.7 106

Figure 5.3: Poincaré map of the Silnikov strange attractor for the plane x=.2 107

Figure 5.4: Six different rotated views of the Lorenz strange attractor 109

Figure 5.5: The projection of the Lorenz attractor onto the x-y plane, with color representing the variation of z; from Novak [32] 111

Chapter 1

Introduction

1.1 Background and Motivation

Within the past thirty years, scientists have become more and more interested in the study of chaos. Because numerous parts of nature behave chaotically, many different branches of science are part of the ongoing search for understanding of this phenomenon. The book *Chaos: The Making of a New Science* by James Gleick [1] presents a wonderful introduction into the discoveries and path of chaos over the past three decades. The article "Chaos: The Ultimate Assymmetry" by Arthur Fisher [2] is a much shorter version of Gleick's story, but is also a good introduction to the world of chaos.

Why the big interest and popularity of this subject? The fascination with chaos is that beneath apparent randomness and disorder lies a certain type of order. It was due to the computer that this observation was made

possible, since the study of chaos involves solving systems of nonlinear differential equations. The solutions to these systems generate large data sets that are difficult to study. Therefore, as the capabilities of computers has progressed, so has the interest in visualizing these large data sets.

In the past few years, there have been many software packages introduced to view the solutions of equations that describe dynamical systems, including equations that behave chaotically. Some of these include Phaser [3] and PhasePlane [4]. Unfortunately, the capabilities of these programs are limited to two dimensional views. Chaos occurs in only three or more dimensions, so the present systems make it difficult to visualize the structure of objects in this higher dimensional space.

This problem provided the motivation for this thesis. A new way to view chaos for three dimensional systems was developed with the use of powerful graphics tools. The package involves the use of an existing software called AVS with specicalized portions designed for the problem of viewing chaos. With this new software package, a few specific systems are explored to understand their behavior, including a famous system called the Lorenz equations. The package is also used with other visual tools to create an educational video.

1.2 Scope of Thesis

As was mentioned, there are at present several tools that can be used to visualize systems that exhibit chaos. Unlike other theses, the review of the literature about these systems and their capabilities will be most beneficial as a part of the discussion at the end. The thesis is organized in the following manner. First, in Chapter Two, terms and concepts associated with dynamics and chaos will be defined. Next, in Chapter Three, the importance of visualization for dynamical systems will be discussed, and then the new tools that were developed will be introduced. In Chapter Four, a study of some of the solutions to the Lorenz equations will be discussed with references to the way the tools were used to aid in the understanding of these solutions. Also in this chapter, the Rössler and Silnikov equations and the visualization of some of their solutions will be discussed.

After these chapters, the reader will have an understanding of chaos, and will have been introduced to the new system and its usage. In Chapter Five a literature review is presented which compares currently available methods to view chaos to the new system developed in this thesis. This last chapter will also make a conclusion about the new system as well as suggestions for future expansion of the software.

Chapter Two

Definitions and Examples

In order to discuss chaos and its visualization, it is necessary to describe associated terms. This chapter will define the basic ideas of chaos theory and introduce examples of chaotic systems. Many of the following descriptions and definitions are due to Baker and Gollub [5], Bergé, Pomeau, Vidal [6], Drazin [7], and Jackson[8]. However, they can usually be found in any introductory book about chaos.

2.1 Dynamical Systems and Phase Space

Dynamical systems are represented as a system of differential equations

of the form

$$\frac{d\mathbf{X}}{dt} = \mathbf{f}(\mathbf{X},t) \tag{2.1}$$

where $\mathbf{X}$ is a vector of variables. This set of first order ordinary differential equations is called the state space form of the equations. These equations describe the way variables in the system evolve in time. The behavior of the system can be viewed in various forms. For example, consider a simple damped oscillator illustrated in Figure 2.1. This system is represented by the second order differential equation

$$\mathrm{m}\frac{d^2\mathrm{x}}{dt^2} + \mathrm{c}\frac{d\mathrm{x}}{dt} + \mathrm{kx} = 0 \tag{2.2}$$

in which the coefficients m, c, and k represent the mass of the object, the damping constant, and the spring constant respectively. This second order equation can be put into its state space form,

$$\begin{aligned} \frac{d\mathrm{x}}{dt} &= \mathrm{y} \\ \frac{d\mathrm{y}}{dt} &= -\frac{\mathrm{c}}{\mathrm{m}}\mathrm{y} - \frac{\mathrm{k}}{\mathrm{m}}\mathrm{x} \end{aligned} \tag{2.3}$$

If $c^2<4km$ then the system is said to be underdamped. The position x can be plotted as a function of time, and the velocity $\mathrm{y} = \frac{d\mathrm{x}}{dt}$ can also be plotted as a function of time. Both of these plots are illustrated in Figure 2.2 for the underdamped case.

There is another way to see the behavior of the system by using the idea

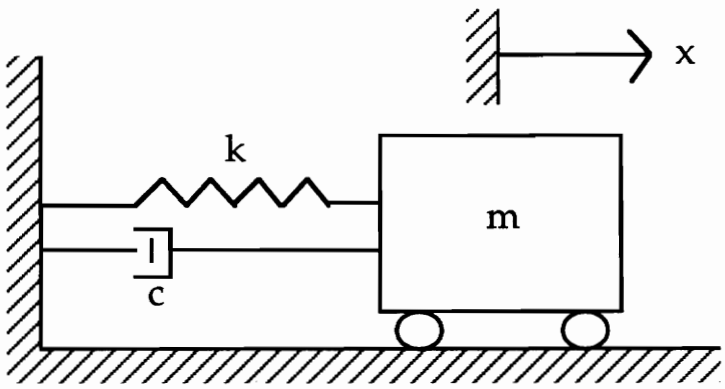

Figure 2.1: A damped oscillator

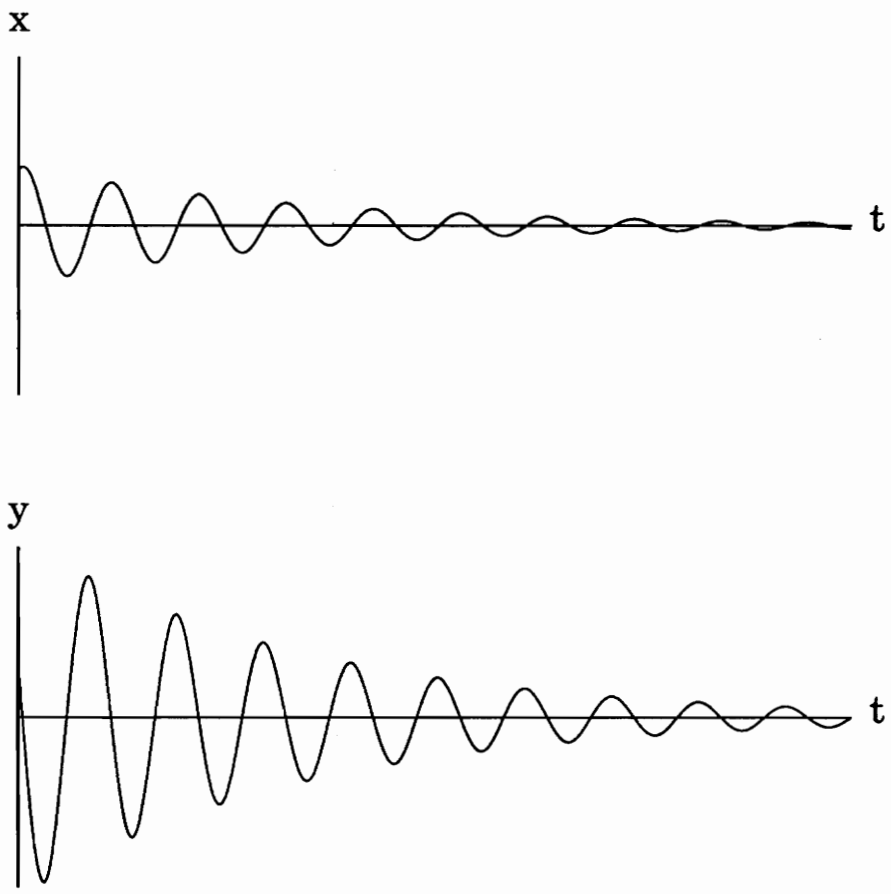

Figure 2.2: Position and velocity plots for the underdamped oscillator

of phase space. Phase space consists of orthogonal directions for which each of the axes represents one of the variables that are needed to define the instantaneous state of the dynamical system. In the case of the oscillator, the instantaneous state of the system is represented by the position x and the velocity y. Time can be eliminated between the two solutions for position and velocity, and then a plot of x versus y can be made as shown in Figure 2.3. This figure shows one example of a phase trajectory, a particular orbit that illustrates the development of the system for one specific set of initial conditions.

A collection of the different types of orbits for a system is called a phase portrait. It should include at least one each of all possible types of solutions to the system. Phase portraits are revealing because they give a complete picture of all the kinds of motion for the system.

From this picture, it can easily be seen whether or not the trajectory will settle down to some state. A system will settle down only if it is dissipative, that is, energy is not conserved. In dynamics, the behavior that a system settles to after it has begun its motion is called an attractor. Any initial condition within the domain of the attraction will eventually be pulled into the motion exhibited by the attractor. There are three main types of attractors - point attractors, limit cycles, and strange attractors.

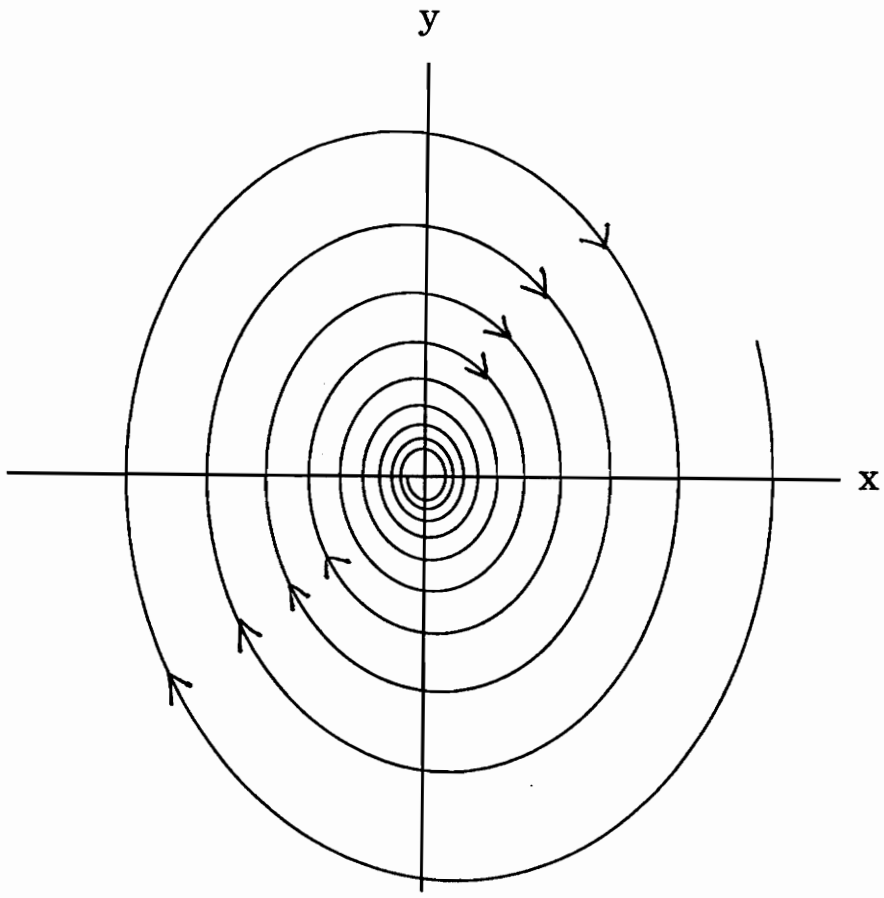

Figure 2.3: Phase trajectory for the damped oscillator

2.11 Point Attractor

Equilibrium points of a set of differential equations are those points at which the first time derivatives of all the variables go to zero. That is,

$$\frac{d\mathbf{X}}{dt} = \mathbf{f}(\mathbf{X},t) = 0 \qquad \text{if } \mathbf{X} = \mathbf{X}_{\text{equilibrium}} \tag{2.4}$$

If the equilibrium point is stable and the long term behavior of the motion decays to this point then it is called a point attractor. Figure 2.3 shows an example of a phase trajectory that approaches a point attractor at the origin. The orbit is asymptotic and spirals into the attracting point. Another good physical example of this type of motion is given by a damped pendulum as illustrated in Figure 2.4. This system is represented by the following second order equation

$$\frac{d^2\theta}{dt^2} + \frac{c}{m}\frac{d\theta}{dt} + \frac{g}{l}\sin\theta = 0 \tag{2.5}$$

which also can be written in its state space form

$$\frac{d\theta}{dt} = \omega$$
$$\frac{d\omega}{dt} = -\frac{c}{m}\omega - \frac{g}{l}\sin\theta \tag{2.6}$$

The instantaneous state of this system would be represented by the angular position θ of the mass and its angular velocity $\omega = \frac{d\theta}{dt}$. The motion of this damped system is attracted to the position where x is zero, that is the mass is

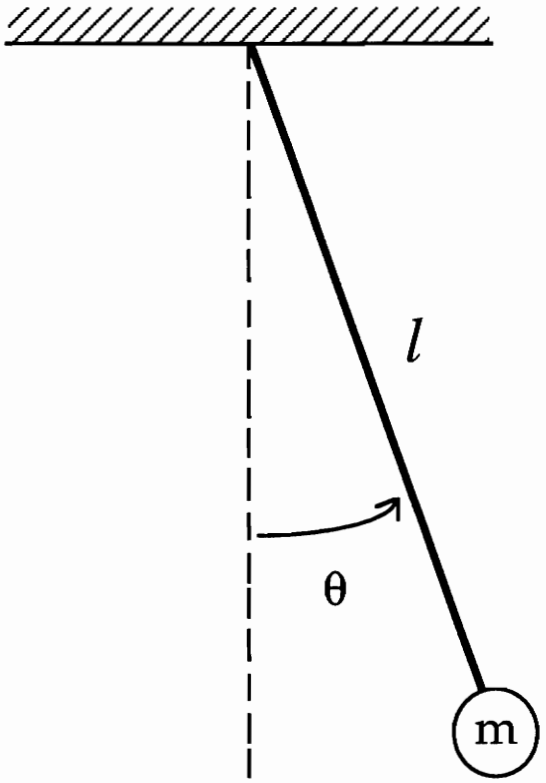

Figure 2.4: A damped pendulum

hanging straight down. The phase trajectories about this equilibrium point are shown in Figure 2.5. This figure illustrates that the pendulum's position upon release, i.e. its initial conditions, does not change its final destination.

2.12 Limit Cycle

In many systems the initial conditions will affect the future behavior, such as systems that oscillate with a constant periodic motion. For the example of the pendulum, if the damping force is removed, then the mass will tend to swing back and forth with a constant amplitude. This amplitude, however, depends on the position from which the pendulum is released. If the pendulum is released from a large angle it will have a much larger amplitude motion than if it is released from a smaller one. In Figure 2.6 a few of these periodic orbits can be seen. The larger the amplitude, the larger the orbit. In this example each orbit has a different period.

Nonlinear systems can exhibit the following different type of behavior. Sometimes the solutions of the system will be attracted to one unique periodic orbit. This attracting orbit is called a limit cycle. For this type of behavior, the initial conditions of the system have no effect on the final amplitude or period of the motion. All trajectories within the domain of the attractor will terminate on the limit cycle and therefore have the same final amplitude as this specific periodic orbit. The undamped pendulum system does not exhibit limit cycle behavior. Although the undamped pendulum has periodic orbits,

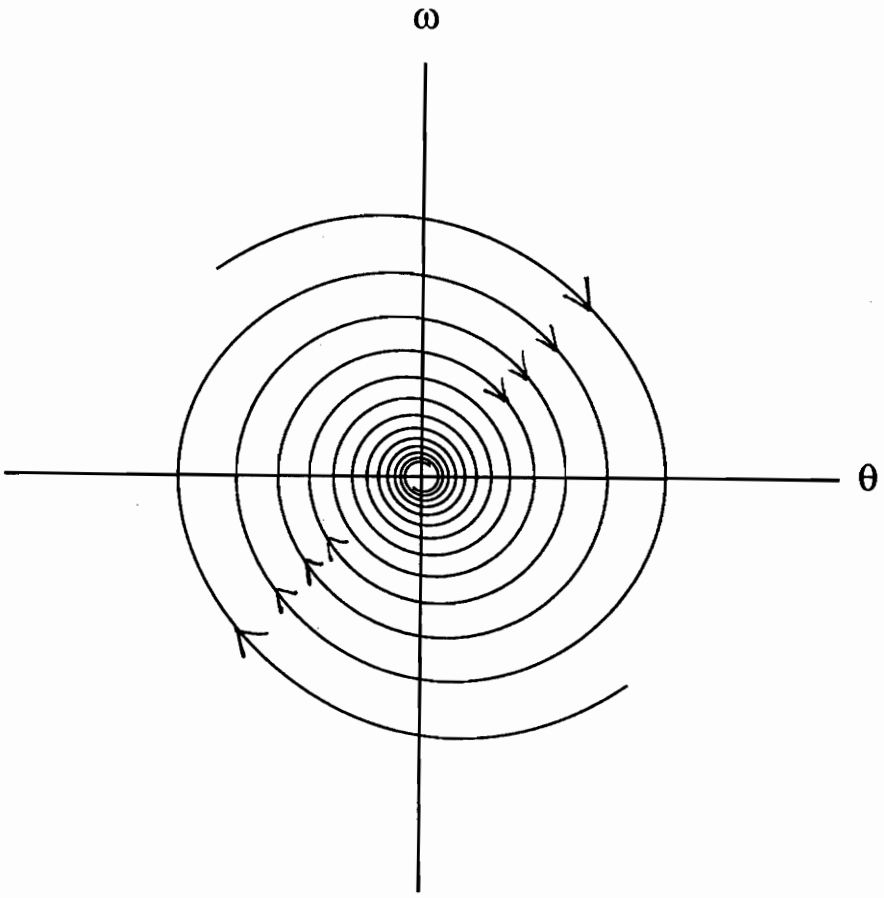

Figure 2.5: Phase trajectories approaching a point attractor for the damped pendulum

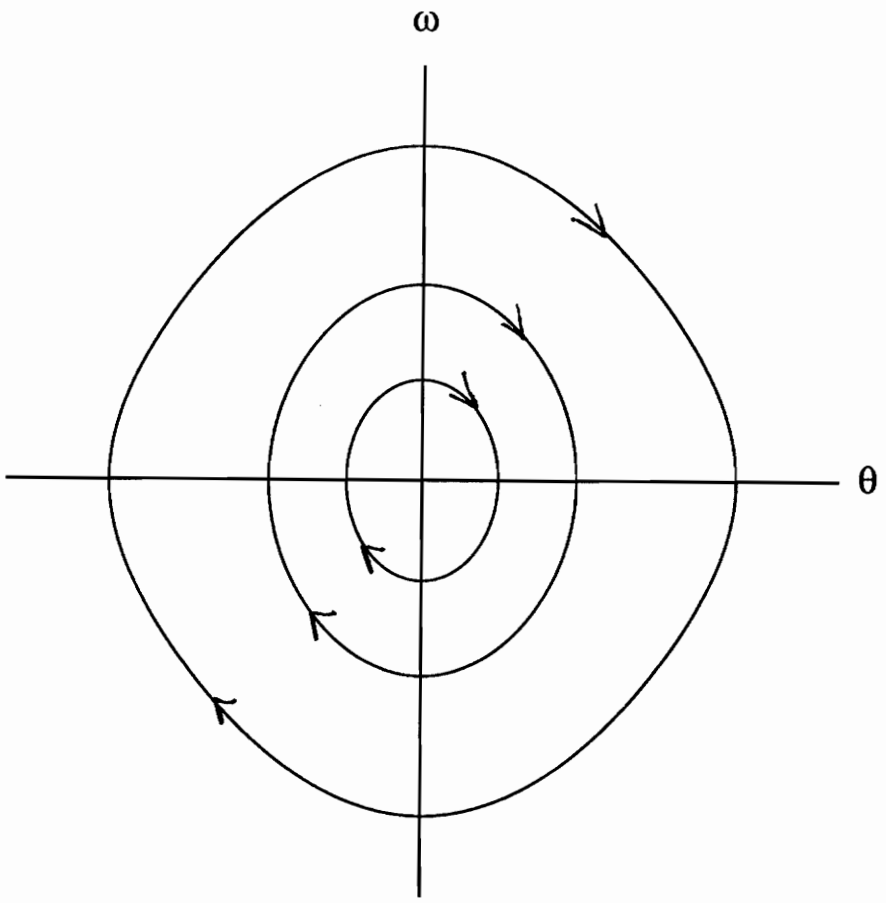

Figure 2.6: Periodic orbits in phase space for the undamped pendulum

the final amplitude of the motion depends on the initial conditions. Therefore there are many possible periodic orbits, not a unique attracting one.

An example of a system with a limit cycle is the Van der Pol oscillator. This nonlinear system is described by the second order equation

$$\frac{d^2x}{dt^2} + a(x^2 - 1)\frac{dx}{dt} + x = 0 \tag{2.7}$$

Equation (2.7) can be put in its state space form

$$\begin{aligned} \frac{dx}{dt} &= y \\ \frac{dy}{dt} &= -a(x^2 - 1)y - x \end{aligned} \tag{2.8}$$

If a>0 then this system has an attracting limit cycle. The phase portrait for a=2.5 is illustrated in Figure 2.7. No matter what the initial conditions are, the trajectory will always end up in the same periodic motion. Once the trajectory is in this cycle, it will stay in the motion for all time. A physical example of a limit cycle is the human heartbeat. It has a natural pace that it works to maintain. Things like stress or anxiety may speed it up past its regular period, but eventually it will settle back down into its normal rhythm.

2.13 Strange Attractor

Recently, it has been discovered that certain systems have attractors that are not point attractors or limit cycles. The trajectory in phase space is attracted to an unusual type of orbit which is now known as a strange

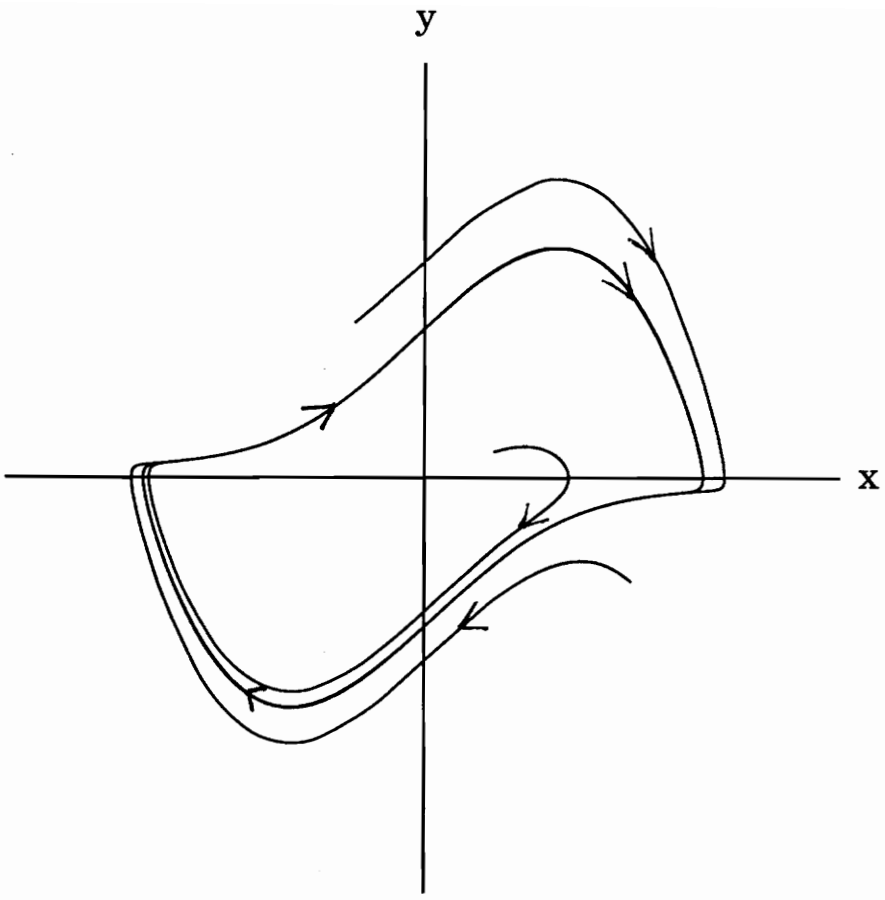

Figure 2.7: Limit cycle of the Van der Pol Oscillator for a=2.5

attractor. The Lorenz equations are a good example of a system that has a strange attractor. This three dimensional system is represented by the following set of equations:

$$\begin{aligned} \frac{dx}{dt} &= \sigma(y - x) \\ \frac{dy}{dt} &= rx - y - xz \\ \frac{dz}{dt} &= xy - bz \end{aligned} \tag{2.9}$$

For certain values of the parameters r,σ, and b, a strange attractor is present. Figure 2.8 shows a two dimensional projection of an orbit that is part of the Lorenz strange attractor. In Chapter Four, the Lorenz attractor will be studied in more detail.

The most unique feature about the strange attractor is the following phenomenon. Once a trajectory is on the attractor, its future position a short time later cannot be predicted. The trajectory will remain on the attractor, but where it will be is unknown. This position is not computable no matter what method is used to solve the equations or how powerful the computers are that integrate the system. A system that exhibits this type of behavior is said to be chaotic. The strange attractor illustrates the fact that chaos can indeed have order within disorder.

In order for a system to have a strange attractor, the system of equations must be nonlinear and there must be at least three variables in the equations. Ruelle and Takens [9] were among the first to prove that at least

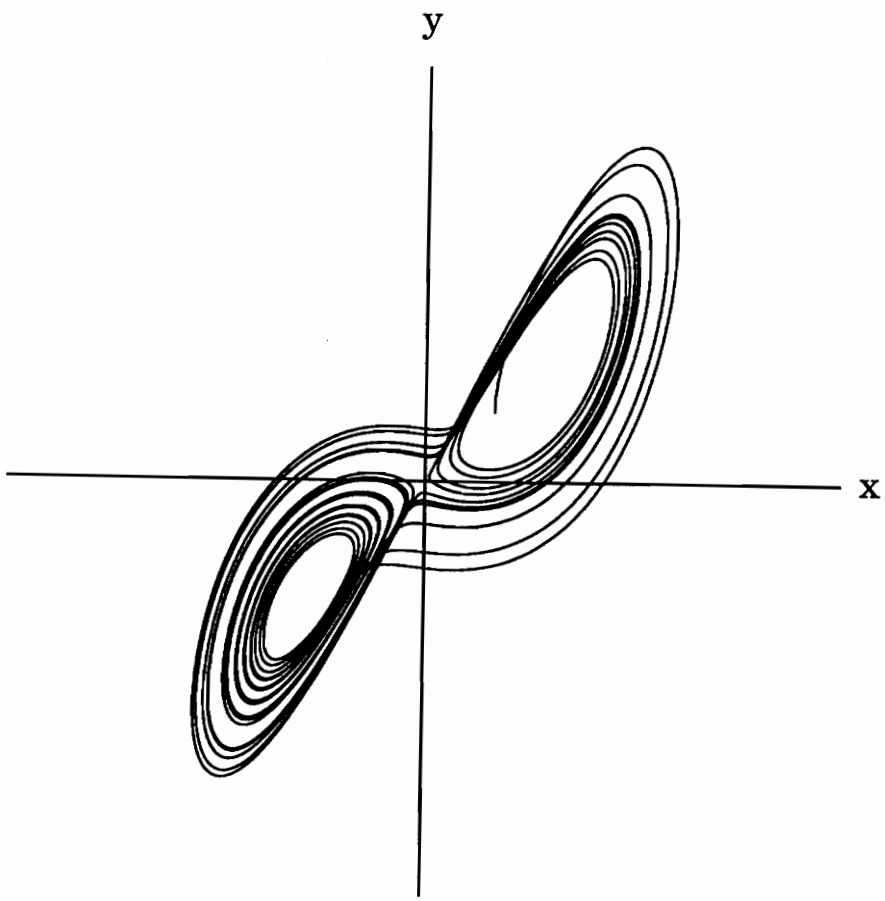

Figure 2.8: Lorenz strange attractor for r=28, σ=10, b=2.66667

three variables are needed for chaotic attractors. Three dimensions are enough to allow the existence of a strange attractor because the phase trajectories describing the path of the motion can have the following important qualities simultaneously.

First, since the equations governing this type of motion are deterministic, any one trajectory is unique and different from another. This uniqueness condition describes an important condition that solutions to a chaotic system must exhibit. A trajectory's path cannot cross itself or cross the paths of other trajectories. If it did intersect, then at the point where crossing occurred, the motion could have two possible past histories which would be a contradiction to the uniqueness condition.

A second condition that is needed in order for a strange attractor to exist is that the motion must be bounded and dissipative. By use of a Liapunov function [10], it can be shown that for a bounded system every trajectory eventually enters some finite region and stays there. In order for the system to enter an attractor within this finite region the system must be dissipative. A system is dissipative if the divergence of the flow is negative. For a system with n independent variables the value of

$$\mathbf{D} = \frac{\partial}{\partial x_1}\left(\frac{dx_1}{dt}\right) + \frac{\partial}{\partial x_2}\left(\frac{dx_2}{dt}\right) + \ldots + \frac{\partial}{\partial x_n}\left(\frac{dx_n}{dt}\right) \tag{2.10}$$

represents the divergence. If this value is negative, then phase space - such as area or volume - is not preserved, so the space shrinks as time evolves. For

example, in the case of the point attractor, area (two dimensional phase space) is not preserved and shrinks to a point as Figure 2.9 illustrates. For a system with three variables, the phase space is three dimensional. Therefore, if the system is dissipative, volume will not be preserved. This means that a strange attractor in this space will have zero volume.

The final and most important quality of a strange attractor is divergence of any two trajectories. This means that any two different trajectories starting close together will end up far apart. This main feature of chaos is known as sensitivity to initial conditions. In a nonlinear system that exhibits chaos, even very slight changes initially will lead to exponentially diverging trajectories as time progresses. As a result of this phenomenon, it becomes impossible to predict a trajectory's future location on the strange attractor.

The method used to measure this separation of trajectories is the calculation of what is called the Lyapunov exponent [7]. This exponent is a mathematical quantity that represents the distance between two trajectories initially very close together. For discrete systems, when $x_{k+1}=f(x_k)$,or

$$\begin{aligned} f^2(x) &= f(f(x)) \\ f^3(x) &= f(f^2(x)) = f(f(f(x))) \\ f^n(x) &= f(f(\cdots f(x)\cdots)) \end{aligned} \tag{2.11}$$

the idea is that very close trajectories a distance ε apart are separated

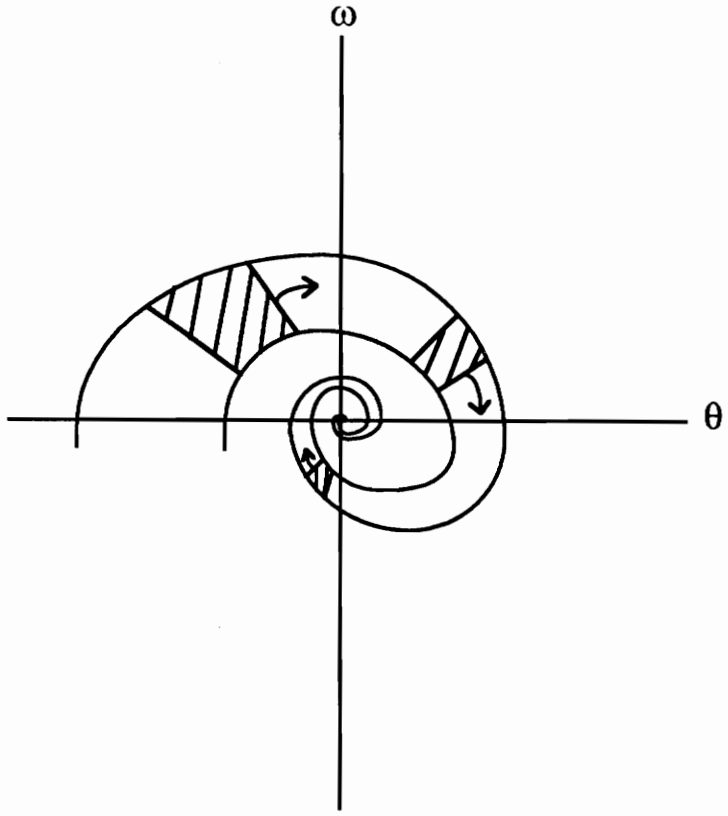

Figure 2.9: Area contraction in a point attractor

exponentially by

$$e^{n\lambda(x_o)} \approx \frac{f^n(x_o+\epsilon) - f^n(x_o)}{\epsilon} \tag{2.12}$$

The value of λ is known as the Lyapunov exponent and is expressed by

$$\lambda(x_o) = \lim_{n\to\infty} \frac{1}{n} \ln \left| \frac{df^n(x_o)}{dx_o} \right| \tag{2.13}$$

Equation (2.12) shows that if λ is positive, the trajectories are diverging, and if it is negative, then they are converging. These equations are for discrete systems, however there is a similar, more complicated way to find Lyapunov exponents for continuous systems [11]. For the three dimensional case, there are three Lyapunov exponents. When the motion is chaotic and converging to a strange attractor, two of the exponents will be negative, and one will be positive. The positive exponent represents the sensitivity to initial conditions, while the negative exponents are a result of the dissipation which causes trajectories to approach the attractor.

In order for this divergence as well as the other above properties to exist all at once, the orbit must be determined by three or more variables. That is, the phase space must be of three dimensions or more. Hirsch and Smale [12] rigorously prove the Poincare-Bendixon theorem which states that a bounded region in two-dimensional space cannot have chaotic flow. For a discussion less rigorous but easier to follow, see Bergé et al p.115-116 [6].

2.14 Fractal Dimensions

How can a strange attractor have all of the above properties at once? It must maintain the uniqueness of all trajectories. It also has to have sensitivity to initial conditions, so two initially close trajectories must diverge. Furthermore, the motion must be bounded. As was mentioned, the orbit must be determined by three or more variables for these to occur. Therefore the dimension of an attractor must be larger than two. However, for a system with three variables, the phase space will be three dimensional. Recall that dissipation causes the attractor to have zero volume, therefore its dimension must be less than three. Then what dimension can the attractor have?

In order to continue with the discussion on the dimension of a strange attractor, it is necessary to define mathematically what is meant by dimension. The formula used in determining dimension can be represented by

$$d = \lim_{\beta \to 0} \frac{\log [N(\beta)]}{\log \left[\frac{\beta_o}{\beta}\right]} \qquad (2.14)$$

where $N(\beta)$ represents the number of cubes of side β needed to cover the object which has dimension d, and β_o is some reference length. To demonstrate the use of Equation (2.14), consider a square with sides β_o as in Figure 2.10. If only one box is used to cover the square then the sides of the box would have length β_o . If squares with side $\frac{\beta_o}{2}$ are used then four boxes are necessary. In general, if squares of side $\frac{\beta_o}{2^n}$ are used then 2^{2n} boxes are needed to cover

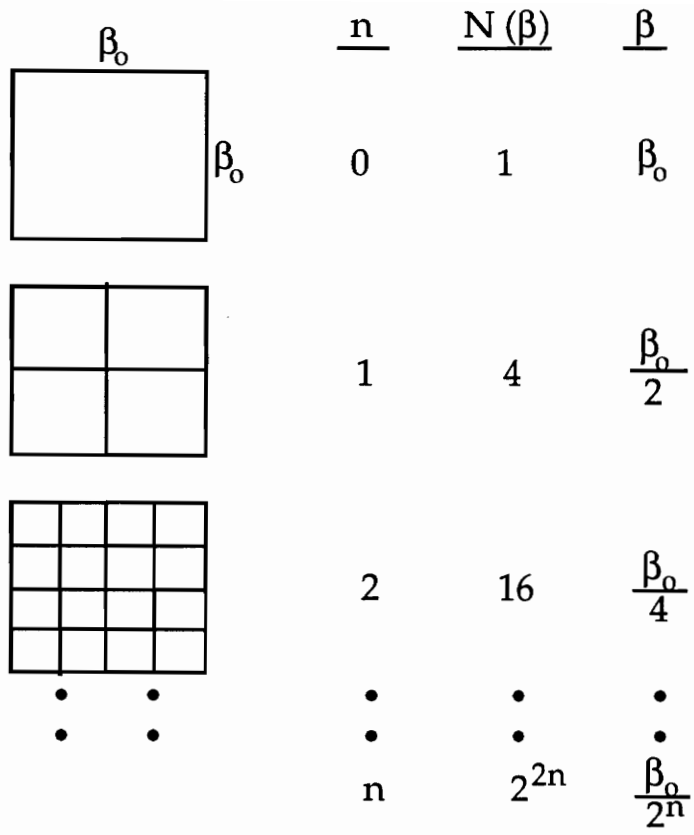

Figure 2.10: Process of finding the dimension of a square

the square (see Figure 2.10). Therefore the dimension of the box is

$$\begin{aligned} d &= \lim_{n\to\infty} \frac{\log [2^{2n}]}{\log [2^{n}]} \\ &= \lim_{n\to\infty} \frac{2n\log [2]}{n\log [2]} \\ &= 2 \end{aligned} \tag{2.15}$$

This gives back the expected dimension of two for a square. Equation (2.14) similarly returns a dimension of one for a line and a dimension of three for a cube.

There are less simple sets for which non-integer dimensions are calculated. If Equation (2.14) is used and calculates a dimension that is not an integer, then the object is said to have a fractal dimension. This term was created by Benoit Mandelbrot, whose book *The Fractal Geometry of Nature* [13] was the first to introduce and explore structures exhibiting this idea.

An example of a set with fractal dimension is Cantor's middle-thirds set. The idea of this set is shown in Figure 2.11. Start with a line of reference length β_o and then take out the middle third. Then take out the middle third of each of the remaining two thirds. Continue this process n times, and let n go to infinity. The result is an infinite set known as Cantor Dust. This collection is not a line, so it does not have dimension one. However, it is not a finite collection of points so the dimension is not zero.

Equation (2.14) can be used to determine the fractal dimension of Cantor's set. Consider the first line of the set. The length of a line used to

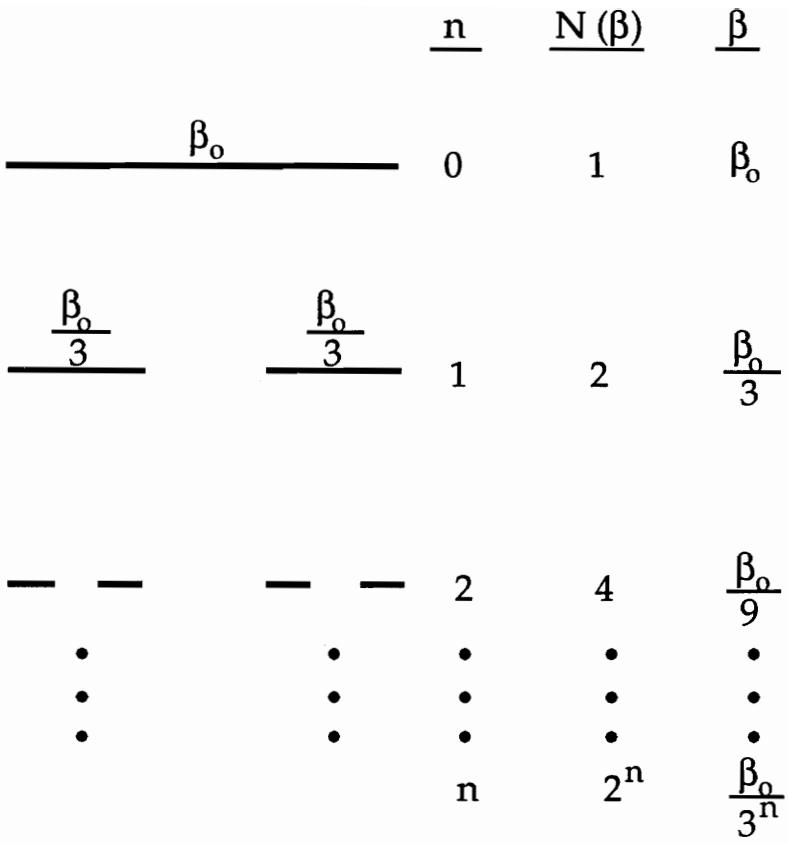

Figure 2.11: Process of finding the dimension of the Cantor middle-thirds set

cover the first line of the set would be β_o and the number of lines would be one. After the first third is removed, the remaining object can be covered with two lines, each of side $\frac{\beta_o}{3}$. As Figure 2.11 shows, the length of the lines needed after the nth removal is $\frac{\beta_o}{3^n}$. The number of lines needed is 2^n. Equation (2.14) would then be

$$\begin{aligned} d &= \lim_{n\to\infty} \frac{\log[2^n]}{\log[3^n]} \\ &= \lim_{n\to\infty} \frac{n\log[2]}{n\log[3]} \\ &= \lim_{n\to\infty} \frac{\log[2]}{\log[3]} \\ &= 0.6309... \end{aligned} \tag{2.16}$$

The dimension of the Cantor middle thirds set is fractal, somewhere in between dimension zero and one.

Another example of an object with fractal dimension is the Siérpinski Triangle. Consider an equilateral triangle with sides β_o . Connect the midpoints of each side to take out the "middle" triangle of the original figure. Do this an infinite number of times to get the Siérpinski Triangle. (See Figure 2.12). Equation (2.14) can be used to determine the dimension of this object. As Figure 2.12 shows, after n removals, 3^n triangles of side $\frac{\beta_o}{2^n}$ are needed to

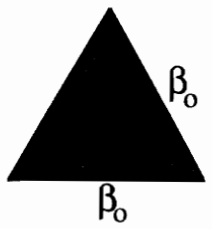

n	N (β)	β
0	1	β_o
1	3	$\frac{\beta_o}{2}$
2	9	$\frac{\beta_o}{4}$
•	•	•
•	•	•
n	3^n	$\frac{\beta_o}{2^n}$

Figure 2.12: Process of finding the dimension of Siérpinski's Triangle

cover the remaining structure. Equation (2.14) would then be

$$d = \lim_{n\to\infty} \frac{\log[3^n]}{\log[2^n]}$$
$$d = \lim_{n\to\infty} \frac{n\log 3}{n\log 2} \qquad (2.17)$$
$$d = 1.5849$$

Thus, Siérpinski's Triangle has a fractal dimension between 1 and 2.

Recall that the strange attractor needed to have dimension bigger than two and yet less than three. Using the same idea of dimension as above, it can be shown that strange attractors do indeed have fractal dimension. The dimension of the Lorenz attractor has been found to be approximately 2.06 [14]. It is this fractal property that allows the conditions of uniqueness and sensitivity to initial condition to exist in a structure that is bounded and also attracts all orbits. This property is universal for strange attractors.

2.2 Examples of Strange Attractors

The first section discussed the type of attractors that could exist for a nonlinear, dissipative system of differential equations. A main point was that a strange attractor exhibiting chaos can only occur for systems with three or more variables. This section will introduce some systems that display chaos.

2.21 Lorenz Equations

During the 1950's and 1960's many scientists were working on the problem of long-range weather forecasting. Models of weather patterns were simulated on computers and theories were tested about the possibilities of long-range prediction. In 1963, a meteorologist by the name of Edward Lorenz noticed a strange condition in his weather simulating computer results. During a simulation, Lorenz decided he wanted to see a particular sequence of numbers again. Instead of starting the run all over, he typed in the initial conditions from an earlier printout midway through a previous run of the program. Lorenz expected the results to duplicate the old sequence. Instead, the numbers diverged rapidly. Lorenz checked the initial conditions he typed in and noticed that they were rounded off to three digits compared to the six digits stored in the computer's memory. He thought that this slight difference between the initial conditions was of no consequence. He was wrong.

The small difference in the initial conditions led to a tremendous divergence in the later results. For weather prediction, this was bad news. Any small change in initial conditions was enough to seriously alter the future weather. Lorenz referred to this as the Butterfly effect. The flap of a butterfly's wings can cause just enough change in initial conditions to cause a totally different weather pattern than expected. This phenomenon is now known as sensitivity to initial conditions.

Lorenz wanted to study this effect mathematically, but the system he

was modelling involved many variables and equations. In order to display the same complex behavior but with less complication, Lorenz needed to find a simple system of nonlinear differential equations. He started with the problem of Rayleigh-Benard that modelled convection of a fluid between two plates (see Figure 2.13). The plate on the bottom is heated, while the top plate is held at a constant temperature. As the fluid begins to be heated from below, heat moves toward the top plate by conduction, without disturbing the fluid which remains still. The temperature difference is small enough to allow the heat to diffuse from the bottom to the top without causing any motion in the fluid.

As the heat is turned up, there is a critical temperature at which the fluid begins to move. The fluid on the bottom becomes much warmer than the fluid on the top. It becomes lighter through expansion and rises, while the heavier, cooler fluid on top falls under gravity. The motion develops into cylindrical rolls, known as convection rolls. The fluid rises and falls in a circular pattern in the same direction, with the hot fluid losing its heat at the top to the cool plate and the cooler fluid gaining heat at the bottom from the hot plate.

If the temperature on the bottom plate is increased further, the motion becomes unstable and the convection rolls start to wobble. Eventually the fluid becomes wild and turbulent. The equations that describe this behavior, though, were still more complex then Lorenz wanted, so he developed a set of equations that would model the following type of behavior. Suppose the rolls

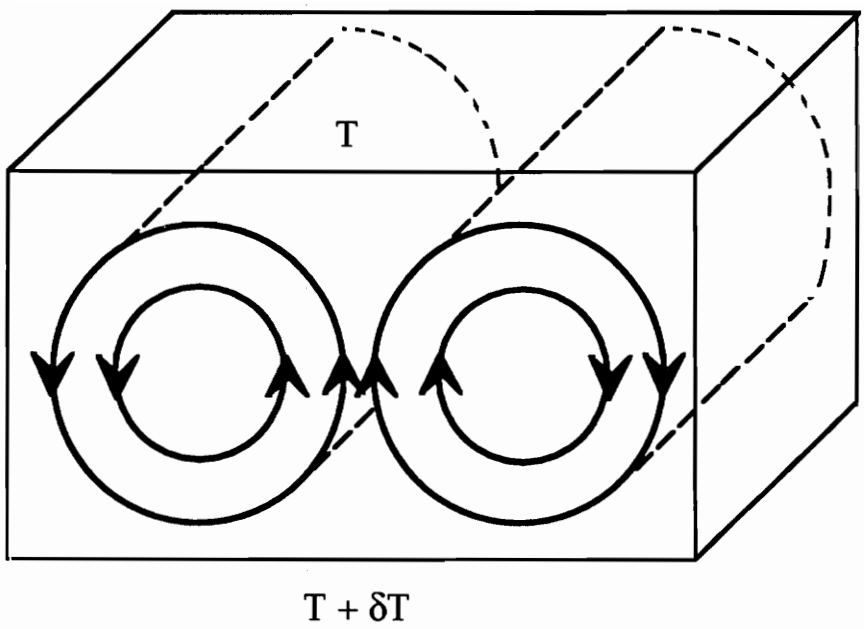

Figure 2.13: Rayleigh-Benard model of convecting fluid between two plates

start to rotate too fast, then the fluid may not have enough time to absorb enough heat at the bottom. Therefore instead of heading up to the cool plate to dissipate heat, it will turn around and reverse the flow, pushing back against the momentum of the fluid behind it. After a certain value of temperature, the fluid will reverse its spin many times, without any predictable pattern.

The system of equations that Lorenz devised would model this type of behavior in the fluid, but with only three variables. Even though these equations do not fully model physical convection due to the severe simplifications, it should be noted that there are real systems that can be accurately represented by these equations, such as dynamo systems that exhibit magnetic reversals [8], and a water wheel [1]. The equations as developed by Lorenz are

$$\begin{aligned} \frac{dx}{dt} &= \sigma(y - x) \\ \frac{dy}{dt} &= rx - y - xz \\ \frac{dz}{dt} &= xy - bz \end{aligned} \tag{2.18}$$

where the meaning of each of the values in the equations is as follows. The variable x is proportional to the intensity of the convective motion, while y is proportional to the temperature variation between rising and falling currents. The variable z is proportional to the vertical temperature gradient across the rolls. The parameter σ is the Prandtl number, which is a nondimensional ratio of viscosity of the fluid (the stickiness of a fluid, or its tendency to resist

motion) to the thermal conductivity of the fluid (the ability to conduct heat). The parameter b is a term dealing with physical proportions of the region. The parameter r is proportional to the Rayleigh number, which is a measure of imposed temperature difference across a layer of fluid, the measure actually represents the ratio of stabilizing to destabilizing forces in the fluid. A more detailed explanation of the process of simplification to this system with the variables and parameters discussed above can be found in Lorenz's original article [15], as well as in other books about chaos including Appendix D of Bergé et al [6].

In Chapter Four the behavior of the Lorenz equations will be discussed as well as visualized as the values of the three parameters σ, r, and b are changed. It will be seen that for certain values a strange attractor is present.

2.22 Rössler Equations

Another three dimensional system that contains a strange attractor was studied by Rössler. Rössler's intention was to develop a model which would explore dynamical properties associated with chaos. His equations are simple and originally were not intended to model any physical system. The model is

as follows:

$$\begin{aligned} \frac{dx}{dt} &= -y - z \\ \frac{dy}{dt} &= x + ay \\ \frac{dz}{dt} &= b + z(x - c) \end{aligned} \tag{2.19}$$

With certain values of a,b, and c these equations will also demonstrate a strange attractor and the phenomenon of chaos.

2.23 Silnikov Equations

A third set of equations that have a strange attractor are

$$\begin{aligned} \frac{dx}{dt} &= y \\ \frac{dy}{dt} &= z \\ \frac{dz}{dt} &= -az - y + bx(1.0 - cx - dx^2) \end{aligned} \tag{2.20}$$

called the Silnikov equations. These equations are a smooth version of a system of equations studied by Arneodo, Coullet, and Tresser [16] and [17]. The equations are models that describe forced oscillators with feedback effects. For certain values of the parameters a,b,c, and d in Equations (2.20), a strange attractor is present in phase space. Arneodo et al use a theorem by Shil'nikov to propose an explanation for the origin and structure of the chaotic behavior that these and other third-order systems such as Rössler's equations exhibit.

The equations then became known as the Silnikov equations.

This chapter was intended to introduce some terms and behaviors associated with dynamical systems. The most interesting type of behavior discussed was the strange attractor. Three types of systems that contain a strange attractor were introduced with some background, the Lorenz, Rössler, and Silnikov equations. An important idea discussed in this chapter was that in order for strange attractors to appear, there must be three or more variables. Therefore, in order to view the strange attractors it is best to be able to visualize them not as two dimensional projections but as full structures in three dimensional space. The next chapter will discuss the importance of a visual tool with capabilities to view strange attractors in this manner. It will then introduce the use of some new software created to view the attractors in three dimensions.

Chapter Three

Visualization

In the previous chapter, some important terms associated with dynamical systems and chaos were defined. Also, some nonlinear systems that exhibit chaos were introduced, namely the Lorenz, Rössler, and Silnikov systems. These systems that exhibit chaotic motion have three variables, so it becomes a hard task to visualize the solution trajectories and the full three dimensional phase space in which they are located.

This chapter will present a method of visualizing strange attractors in three dimensions. First, however, there will be a few introductory discussions. The first will discuss the importance of visualization to science, as well as present some definitions for scientific visualization. The next sections will discuss the reasons why visualization is so beneficial for viewing dynamical systems, especially for those exhibiting chaos. Finally, a brief section on viewing objects in three dimensions will lead into the discussion of the method

devised for the subject of this thesis.

3.1 Scientific Visualization

In a general sense, visualization of any quantity of data is an important tool for understanding. As early as pre-calculus the graphing of functions is a valuable tool for learning. Seemingly simple sets of numbers can have revealing structure when plotted. Edward Tufte's *The Visual Display of Quantitative Information* [18] is just one of the many books written on the subject of visualization. This book starts out with a discussion on pictures of data as "often the most effective way to describe, explore, and summarize a set of numbers". Tufte says that "at their best, graphics are instruments for reasoning about quantitative information". This infers that visualization of data is not necessarily just a pretty picture, but it can be a powerful tool to aid in learning important information.

When it is used as a tool, visualization becomes scientific visualization. As computers and their power have advanced tremendously in the past decade, so has the ability to solve more complex problems. However, in many cases this results in huge amounts of numerical data. With the use of these same computers, this information can now be viewed as a picture which is easier to understand and manage. This process of exploring and manipulating the visualization for some new information about the data is scientific visualiza-

tion. Haber [19] defines it as "an iterative, exploratory process in which a user experiments with a variety of abstractions to seek insight into a given data set." This process can not only produce new insight but can aid in solving a research problem. Kriz [20] describes the problem solving arena as an intersection of theoretical requirements, experimental results, and supercomputer simulation with scientific visualization. Many areas of science are finding this methodology to be very useful, especially in areas like fluid flow, physics, and chemistry.

It is also useful for dynamical systems. As has been mentioned, phase portraits are an important tool for understanding the types of motion the system will have. When dealing with nonlinear systems, especially those with three dimensions or more, the task of solving and visualizing the system becomes more difficult. The computer must be used for both processes. First, it must be used to numerically integrate the system to solve for each point of the trajectory. This process generates large quantities of numbers for which it is very useful to have a visual image. Due to the nonlinearity of the systems, the structures that arise from the trajectory can be very complex. The power of computers can be used again, this time to view the structure.

For many systems, the solutions change in many ways as parameter values change. Therefore the visual picture of the trajectory will change as well. By using the power of computers, solutions can be automatically generated and then visualized. This can lead to an understanding of the

factors that lead to motions like chaos. It is for systems that behave chaotically that the computer is even more important when visualizing dynamical systems.

As was discussed in Chapter Two, some nonlinear systems can exhibit chaos. The type of structure associated with chaos is a strange attractor. These strange attractors have very complex structures. For the case of a system of three variables, the attractor has dimension somewhere in between two and three. Therefore the object is not flat, but has some depth to it. The computer is now very important because of its abilities to show depth. There are many ways to present depth for an object on the computer screen. Haber [19] mentions a few such as occlusion (overlaying of objects), perspective, and manipulation of surfaces (shading, lighting). Another excellent way to see depth is through rotation of the object. As the object turns, it is easy to see the depth and dimension of the object. The next section of this chapter will discuss the tools created to see solutions to the Lorenz, Rössler, and Silnikov equations with the ability to continuously rotate the strange attractors to examine their structures.

3.2 AVS Tool

In the visualization laboratory, there are many different software packages for viewing data. After considering this particular problem, it was

decided that the tool best suited for the task was the use of a package called AVS (Version 4.0) by Advanced Visual Systems. The first part of this section will introduce the package and its uses. The final section will describe how it was customized to be used to view the specific dynamical systems of Lorenz, Rössler, and Silnikov.

3.21 AVS

As the Introduction in the AVS User's Guide [21] states, AVS is a package designed mostly to be used as a tool. Its main goal is for users to get quick visual results for data sets while spending little if any time programming. AVS allows users to combine individual software components into a flow network that is specific to their problem.

Each of the components is called a module which is designed for a specific function in the flow. These modules are comprised of FORTRAN or C programs with AVS language incorporated in the code. Some modules filter data into a usable form, some map data to produce a geometrical representation of the data, and others render the images into pictures on the screen. Some can either take data as input or create data within itself. In addition to these tasks, the modules also allow interaction through parameter values. These values are represented by an onscreen control widget such as a dial or slider. As the user change the values, the module will recompute and send the new information to the next module in the flow, which eventually leads to the

generation of a new image on the screen.

This image becomes an object in the Geometry Viewer subsystem which allows interaction with the object. The user can move the object anywhere on the screen, rotate it in any direction, or zoom up close or back out. Other ways to interact include changing the eye point, lighting or shading.

The above features of AVS are attractive to anyone who wants to be able to view and interact with a large data set. They simply have to find all of the right built-in AVS modules and create a flow in the Network Editor (see Figure 3.1). In many cases, users do not have to program anything in order to create an entire visualization application. However, there are cases when there is not one module in the AVS Library that will do what the user wants. For this reason AVS allows users to create their own modules that fit the specific needs of the problem. This module can then be loaded into AVS and can be used with other modules already present.

3.22 Development of New Modules

In order to view the three dimensional phase portraits of the dynamical systems, new modules had to be created [22]. First, in order to make use of AVS and its widget functions, modules were created to specifically compute trajectories for the Lorenz, Rössler, and Silnikov equations. Then, modules were created that would draw the phase trajectories. Each of them will be discussed separately in order to present their functions as well as show the

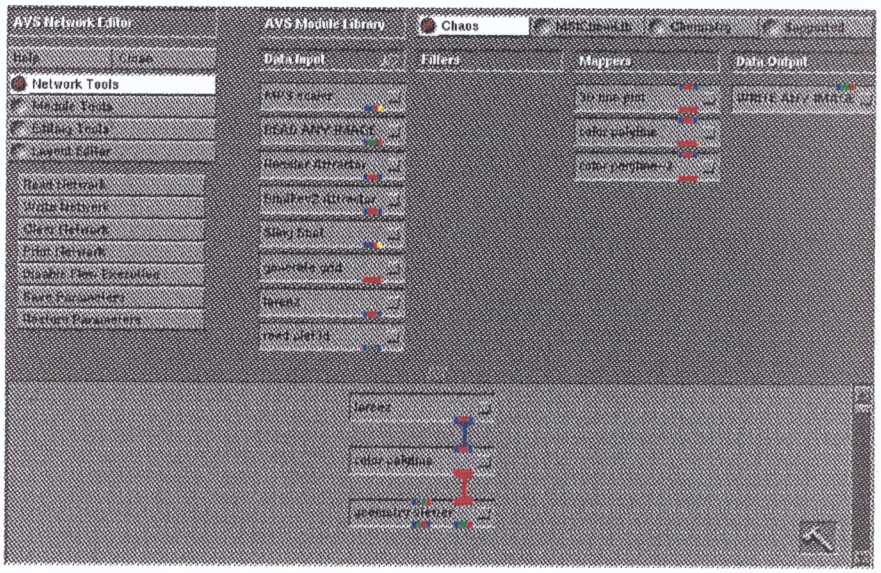

Figure 3.1: Network Editor screen in AVS

screens associated with each module.

The Lorenz module is designed to compute the trajectory for the Lorenz equations. The user interface for this module is illustrated in Figure 3.2. It allows the user to change any of the values on the dial through use of the mouse. It is not easy to make accurate small changes in parameter values by using the mouse to turn the dial to a new position. Since for dynamical systems a large change can occur in the solution for a small change in parameter, it is necessary to be able to input parameter values with precision. If the dial is pressed in the center, a box appears as shown in Figure 3.3 and the value can be typed in the appropriate space.

As shown in Figure 3.2, it is possible to change the initial condition for x, y, or z, the value of the parameters r,s, and b, and the amount of time for which to compute the trajectory. Initial time always starts at zero, so the total time will be from zero to the final time. The timestep and accuracy dials both have to deal with the integration routine in the C program. The choice of timestep results in smooth or choppy visual output, while the accuracy controls the precision of the integration. The two buttons control which integration routine will be used - the Runge Kutta fourth order or the Bulirisch Stoer method -clicking on either one turns the button on or off.

The Rössler and Silnikov modules have similar functions, just different equations and parameters. The interfaces look similar, but the dials for parameters have different names. Also, the integration routine for these

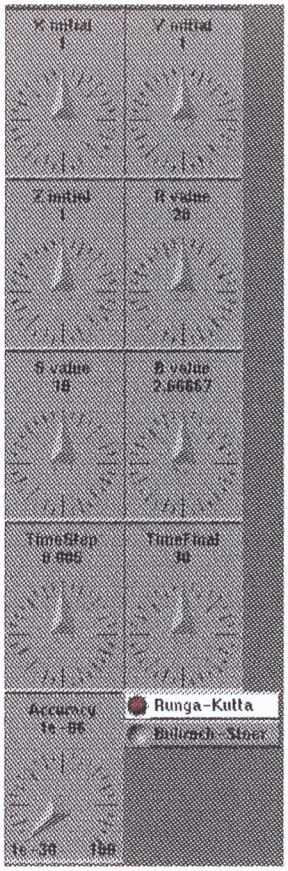

Figure 3.2: User interface screen for the Lorenz module

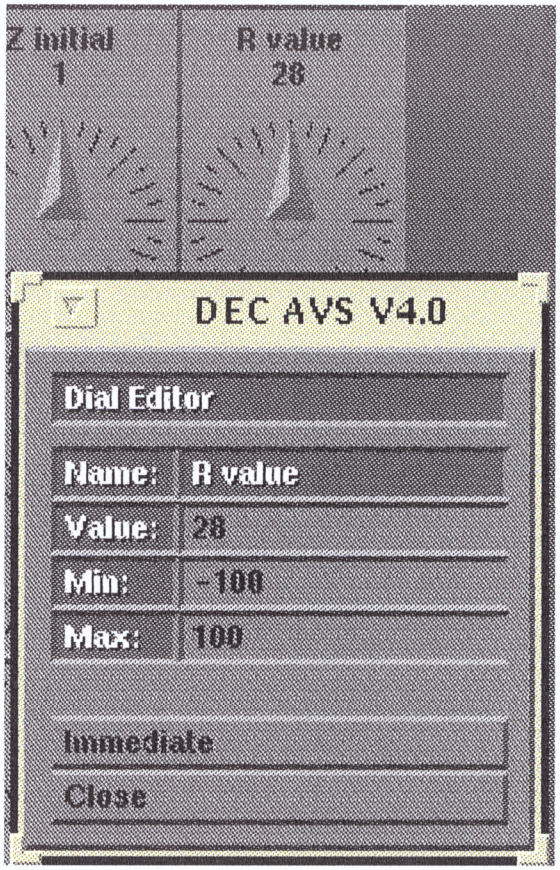

Figure 3.3: Dial Editor box for the parameter r in the Lorenz module

modules is Runga Kutta only, there is not a button available for choice of integration routine as there was for the Lorenz module.

Every time a parameter is changed, the module recomputes and sends the information to the next processor which will produce a three dimensional geometrical representation of the data. This module also had to be created. Two modules were created to allow more variety in the presentation of the object. The first is called Colorpolyline. The user interface is illustrated in Figure 3.4. This module creates a geometry in either black and white, or color. If the monochrome button is "on"(lit up), then the image will be in black and white. If the button is "off", then the image will be in color. The image will be in three colors - blue, green and red. The blue represents the first third of the time interval, the green the next third, and the red the final third. The blackout button allows for removal of the trajectory from its beginning to its end. This function is essentially for removing transients that occur at the beginning of the orbit. If the remove button is on, then the program actually removes the colored lines. If it is off, the program just replaces the color of the lines with black, which is the same color as the background. Therefore, for a change in background color, the black lines will appear if the button was off.

Colorpolyline-2 is the other module that creates a geometry. The interface for this module is illustrated in Figure 3.5. It is somewhat more difficult to explain without actual interaction. The dials init red, init green, and init blue essentially give the initial color of the trajectory. If all of the

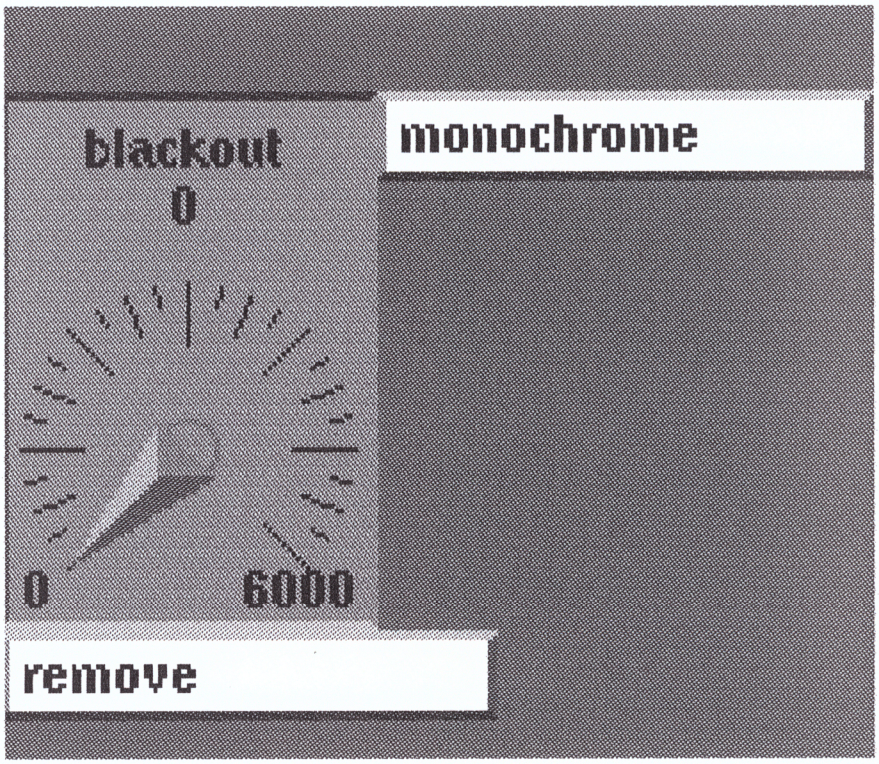

Figure 3.4: User interface screen for the Colorpolyline module

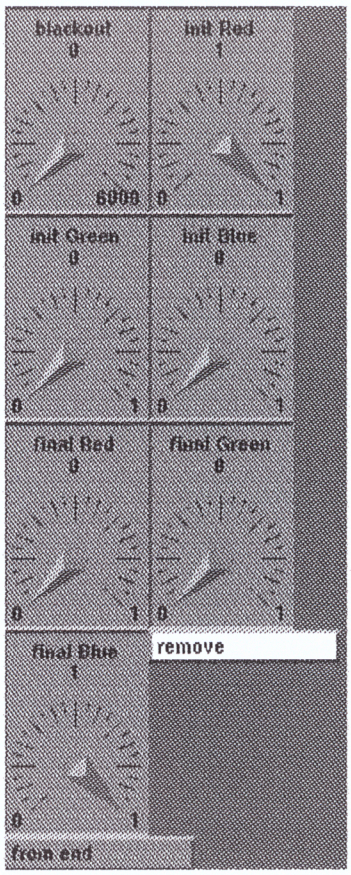

Figure 3.5: User interface screen for the Colorpolyline-2 module

dials are on 1, then the color is a total combination of red, green, and blue. If red is on 1 and the other two are 0, then the color is red. In-between colors can be made through different combinations of the numbers on the dials. The final color buttons work in the same way, but represent the final color.

The blackout dial works in the same way it did for the colorpolyline module, but with a slightly different twist. If the dial is at zero, then the trajectory's color will be entirely represented by the color set indicated by the final buttons. As the dial is turned to positive blackout values, the trajectory starts to be removed from its initial position. If the remove button is on, then the lines being removed become black (the color of the background) if the remove from end button is off. If the remove button is on and if the remove from end button is on, then the lines are completely removed. For either case, it looks like the trajectory is disappearing. The latter case presents much more solid lines for the trajectory since it does not have to intersect black lines that would show up where it intersected the color. If the remove button is off, then the trajectory being "removed" becomes the color represented by the initial buttons. Although it appears complicated, once used a few times it becomes easy to use.

Either Colorpolyline or Colorpolyline-2 create a geometry that can be used by a built-in AVS module called Geometry Viewer which will render the image into a picture on the screen. Figure 3.1 shows the network flow connection of modules set up to visualize the Lorenz attractor using Colorpoly-

line. Once the image has been created, it can be rotated, moved and scaled in order to study the trajectory. AVS is designed so that the user can rotate the object continuously, and then change a parameter and the object will be restructured accordingly while in motion. This allows the user to be able to watch the orbit evolve as the parameter value(s) change.

This chapter covered many areas. First it discussed the meaning and importance of scientific visualization. The next section talked about the importance of visualizing dynamical systems, especially those with a strange attractor that need three dimensions for the phase portrait. Next the AVS package was discussed and then its use with this particular problem was introduced. The next chapter will discuss some of the solutions to the Lorenz equations while discussing the aid of the AVS tools to visualize the solutions, especially the strange attractor. The Rössler and Silnikov equations and the visualization of their strange attractors will also be discussed.

Chapter Four

Theory and Application

In the last chapter, the importance of visualization for dynamical systems, especially those with strange attractors, was discussed. There was also an introduction to new types of tools for three dimensional visualization of the attractors. This chapter will discuss the Lorenz equations and the changes that occur in the system as parameter values change. The Rössler and Silnikov equations will also be discussed, but not in as much detail. It should be noted here that this chapter is also supplemented by an instructional video created through use of the software plus other tools in the scientific visualization laboratory. This video visually runs through the Lorenz system with changing parameter values and rotates the structures for full three dimensional effect. It also shows the rotation of the Rössler and Silnikov strange attractors.

4.1 Lorenz Equations

The Lorenz equations have been studied by many different mathemeticians and dynamicists because their solutions exhibit such a wide variety of behaviors. In order to go through the solutions as parameters change, it is best to first discuss some global properties of the system. Much of the following is due to Sparrow[23], with some material from Baker et al [5], Drazin[7], Schuster[24] and Jackson[8].

4.11 Properties of the Lorenz equations

First, recall the Lorenz equations are represented by

$$\begin{aligned} \frac{dx}{dt} &= \sigma(y - x) \\ \frac{dy}{dt} &= rx - y - xz \\ \frac{dz}{dt} &= xy - bz \end{aligned} \tag{4.1}$$

The first property to notice is that the equations have symmetry about the z axis, that is they are the same for (x,y,z) and (-x,-y,z). This property will become important later on when discussing certain types of behavior.

Next, it should be mentioned that the Lorenz equations have the following two important properties. First, it can be shown the equations have

negative divergence by use of Equation (2.10) from Chapter Two,

$$\begin{aligned} D &= \frac{\partial}{\partial x}\left(\frac{dx}{dt}\right) + \frac{\partial}{\partial y}\left(\frac{dy}{dt}\right) + \frac{\partial}{\partial z}\left(\frac{dz}{dt}\right) \\ &= \frac{\partial}{\partial x}(\sigma(y-x)) + \frac{\partial}{\partial y}(rx - y - xz) + \frac{\partial}{\partial z}(xy - bz) \\ &= -\sigma - 1 - b \end{aligned} \tag{4.2}$$

Since σ and b are both positive, this affirms that the equations have negative divergence and so are dissipative. Therefore, volume elements in phase space are contracted as time progresses. Also, it can be shown that there is a bounded region that all trajectories eventually enter. This is done by use of a Lyapunov function and is discussed in Appendix C of Sparrow [23]. These two together show that there is a bounded set with zero volume towards which the trajectories are attracted. This is important for a strange attractor to be present, as was discussed in the introductory chapter about chaos.

Next, it is necessary to examine the equilibrium points. Recall that equilibrium points of a system occur where

$$\frac{d\mathbf{X}}{dt} = 0 \tag{4.3}$$

For the Lorenz system, this is where

$$\begin{aligned} \frac{dx}{dt} &= \sigma(y-x) = 0 \\ \frac{dy}{dt} &= rx - y - xz = 0 \\ \frac{dz}{dt} &= xy - bz = 0 \end{aligned} \tag{4.4}$$

Solving these equations, it can be seen that the equilibrium points are (0,0,0) for all r and $(\pm\sqrt{b(r-1)},\pm\sqrt{b(r-1)},r-1)$ for all r>1. For future reference the points $(+\sqrt{b(r-1)},+\sqrt{b(r-1)},r-1)$ and $(-\sqrt{b(r-1)},-\sqrt{b(r-1)},r-1)$ will be referred to as c1 and c2 respectively.

Now that all the equilibrium points have been found, the next step is to check the stability of these points. In order to check for the stability, the system can be linearized around each of the equilibrium points. To linearize the system, the following procedure will be used

$$\frac{d\mathbf{X}}{dt} = f(\mathbf{X}) \approx f(\mathbf{X}_{eq}) + \left.\frac{\partial f}{\partial \mathbf{X}}\right|_{\mathbf{X}_{eq}} \mathbf{X} \tag{4.5}$$

After the linearized equations have been obtained, the eigenvalues of the system must be checked. If all of the eigenvalues have negative real parts, then the system is asymptotically stable around the equilibrium values. The sign of the real parts can be checked using the method of Routh [25].

For the first look at stability, the system will be linearized around

x=y=z=0. The linearized system is

$$\begin{aligned} \frac{dx}{dt} &= \sigma(y-x) \\ \frac{dy}{dt} &= rx-y \\ \frac{dz}{dt} &= -bz \end{aligned} \tag{4.6}$$

From this it can be seen right away that z decays with time (since b>0), more specifically the solution for z is

$$z = z_o e^{-bt} \tag{4.7}$$

This shows that any trajectory started on the z-axis (x=y=0) will always decay to zero as time reaches infinity.

Now the system must be checked in the x-y plane. The eigenvalues λ can be obtained from the remaining two equations by assuming that the values of x and y are proportional to $e^{\lambda t}$. The equations can be put in the form

$$\begin{bmatrix} \lambda+\sigma & -\sigma \\ -r & \lambda+1 \end{bmatrix} \begin{pmatrix} x \\ y \end{pmatrix} = 0 \tag{4.8}$$

Setting the determinant of the eigenvalue matrix equal to zero yields the following characteristic equation

$$\lambda^2 + (1+\sigma)\lambda + (\sigma - \sigma r) = 0 \tag{4.9}$$

whose two roots represent the remaining two eigenvalues of the system. Routh's method involves placing the coefficients of the terms of λ in the

following form

$$\begin{matrix} 1 & \sigma(1-r) \\ 1+\sigma & 0 \\ \sigma(1-r) & 0 \end{matrix} \tag{4.10}$$

In order to have an asymptotically stable system the terms in the left hand column must all be greater than zero. Since $\sigma>0$, the second term is positive. The third term in the column implies that for asymptotic stability $r<1$. Since r is also a positive term, this shows that the equilibrium point (0,0,0) is stable for $0<r<1$. Figure 4.1 shows a picture of an orbit for r=.5 decaying directly into this point attractor.

Now the system must be linearized around the equilibrium points c1 and c2. The linearized system is

$$\begin{aligned} \frac{dx}{dt} &= -\sigma(x-y) \\ \frac{dy}{dt} &= x-y-(\pm\sqrt{b(r-1)})z \\ \frac{dz}{dt} &= (\pm\sqrt{b(r-1)})x+(\pm\sqrt{b(r-1)})y-bz \end{aligned} \tag{4.11}$$

After some algebraic manipulation, the characteristic equation turns out to be

$$\lambda^3+(\sigma+b+1)\lambda^2+b(r+\sigma)\lambda+2\sigma b(r-1)=0 \tag{4.12}$$

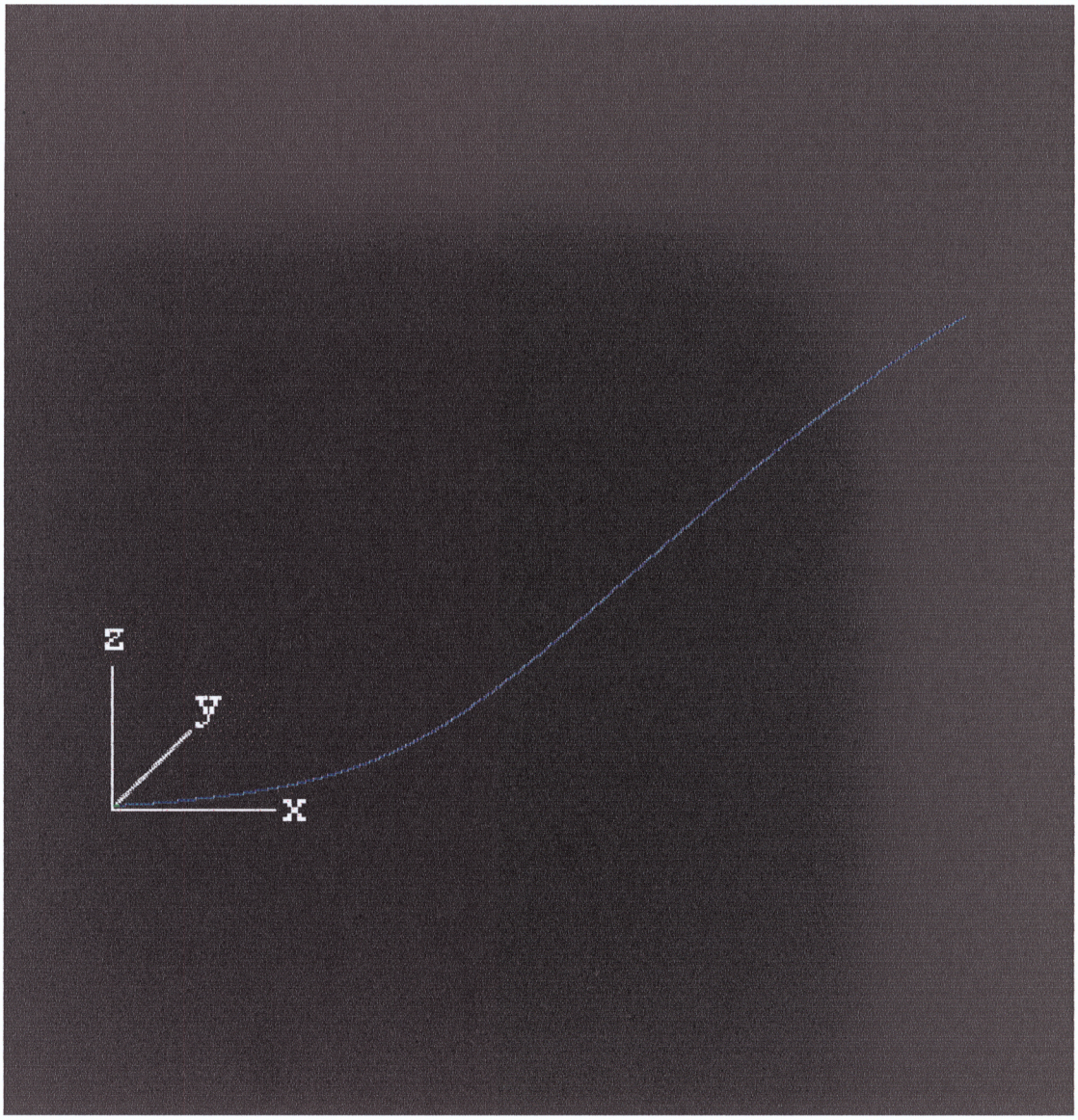

Figure 4.1: Lorenz solution for r=.5, initial (x,y,z)=(1,1,1)

Routh's form for Equation 4.12 yields

$$\begin{array}{ll} 1 & b(r+\sigma) \\ \sigma+b+1 & 2\sigma b(r-1) \\ b[(\sigma+b+1)(r+\sigma)-2\sigma(r-1)] & 0 \\ 2\sigma b(r-1) & 0 \end{array} \tag{4.13}$$

The values in the left-hand column must all be greater than zero for the system to be asymptotically stable (and therefore to be attracted by the equilibrium points c1 and c2). Since σ and b are both greater than zero the second term is greater than zero. The fourth term yields r>1, which is redundant since c1 and c2 don't exist unless r>1. The third term yields the following two conditions for the points to be stable and attracting

$$\begin{array}{l} \text{i) } \sigma < b+1 \text{ and } r>1, \text{ OR} \\ \text{ii) } \sigma > b+1 \text{ and } 1<r<\dfrac{\sigma(3+b+\sigma)}{\sigma-b-1} \end{array} \tag{4.14}$$

The first condition infers for any $\sigma<b+1$ and r>1, a trajectory will either spiral into c1 or c2. The second condition gives many more types of behaviors as parameter values are changed. The most studied case of the Lorenz attractor is for the values $\sigma=10$ and $b = \frac{8}{3}$. Sparrow[23] studies these with great detail in the book *The Lorenz Equations: Bifurcations, Chaos, and Strange Attractors*. The rest of this section will use these same values for σ and b and describe the changes for the solution of the system as r goes from zero to infinity. Figures from the visual tool will be included to help explain some of

the changes, although the visualization of the structures is more beneficial with the interactive use of the rotational tool.

4.12 Lorenz solutions for 0<r<24.74

For values of r between zero and one, the solution has already been discussed. The trajectories are all attracted to the equilibrium point (0,0,0). Above r = 1, the point (0,0,0) becomes unstable while the points c1 and c2 become stable and attracting. This type of change in the solutions to a system is known as a pitchfork bifurcation. The trajectories will either terminate at c1 or c2, depending on the initial conditions. For σ=10 and b = $\frac{8}{3}$, part ii of Equation 4.14 is true so the points c1 and c2 are fixed point attractors for 1<r<24.74. At this point, another type of bifurcation will occur. Before discussing what happens at this critical value, r will be followed more carefully in the interval (1,24.74).

As r increases past one, the equilibrium point (0,0,0) loses its stability. One of the eigenvalues has a positive real part, while the other two have negative real parts. A sketch of the phase portrait near the origin is illustrated in Figure 4.2. The figure shows that while two paths lead to the origin, another path leaves the origin. An equilibrium point that exhibits this type of behavior is called a saddle point. The eigenvalues with negative real parts represent orbits that are attracted, while the eigenvalue with positive real part represents an orbit that is repelled since the solution would grow as

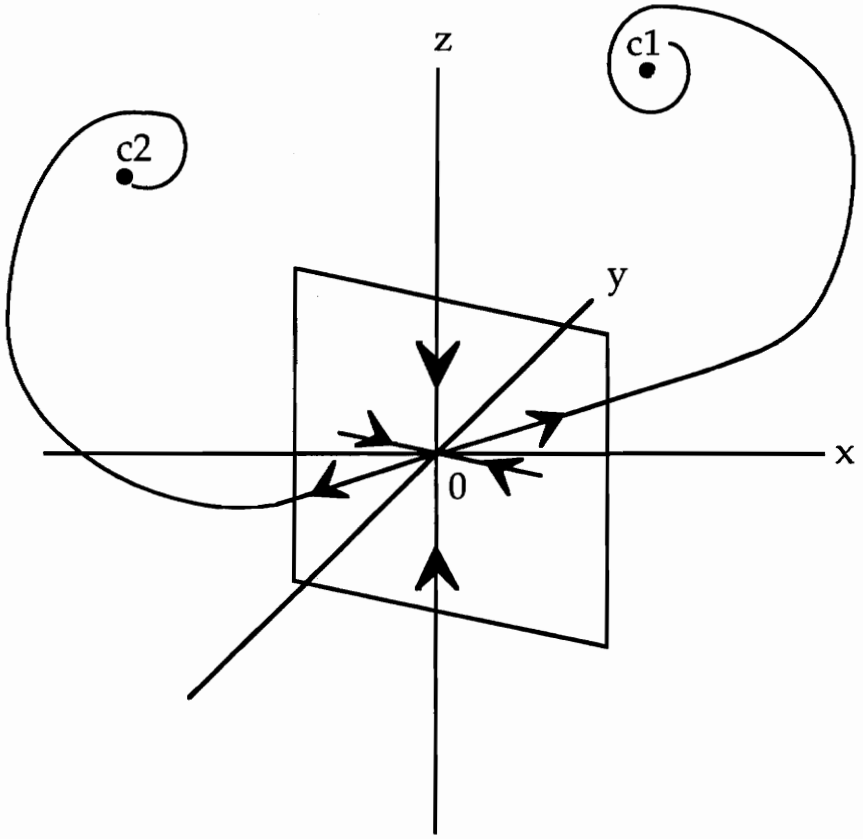

Figure 4.2: Phase portrait near the origin for 1<r<13.92..

$e^{\lambda t}$. In three dimensions, the two eigenvalues with negative real parts represent orbits that lie in a sheet which is called the stable manifold of the origin. All trajectories started on this manifold will move toward the origin. There is also an unstable manifold at the origin, for the eigenvalue with positive real part. This is a one-dimensional manifold. All trajectories started on this either spiral to c1 or c2.

For values of r fairly close to one, the stable manifold divides the phase space into two halves (see Figure 4.2). On one half the trajectories tend to c1, and on the other half they tend to c2. For an r value greater than 13.926... trajectories that start spiralling to c1 cross over and become attracted to c2, and vice versa (see Figure 4.3). Since these trajectories on the unstable manifold cannot go through the stable manifold (then they would tend toward the origin), an interesting event occurs. At 13.926..., in order to make this transition the unstable manifold of the origin must lie in the stable manifold of the origin. That is, trajectories started on the unstable manifold will return to the origin (see Figure 4.4). This type of orbit is known as a homoclinic orbit and it is associated with the unstable equilibrium point (0,0,0).

Because the stable manifold is a two dimensional sheet, any small deviation from the manifold will cause the trajectory to eventually leave the stable manifold. Therefore, it is difficult if not impossible to see this numerically since numerical integration routines make approximations. Figure 4.5 shows a trajectory that stays near the origin for a while, before continuing

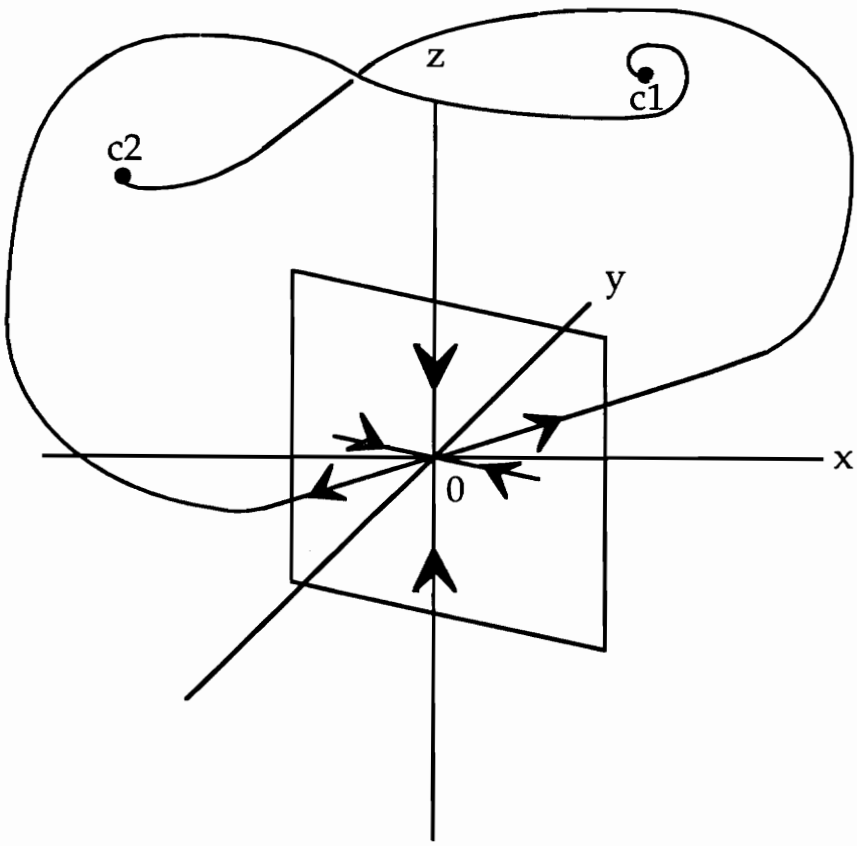

Figure 4.3: "Crossover" of trajectories to the opposite equilibrium point

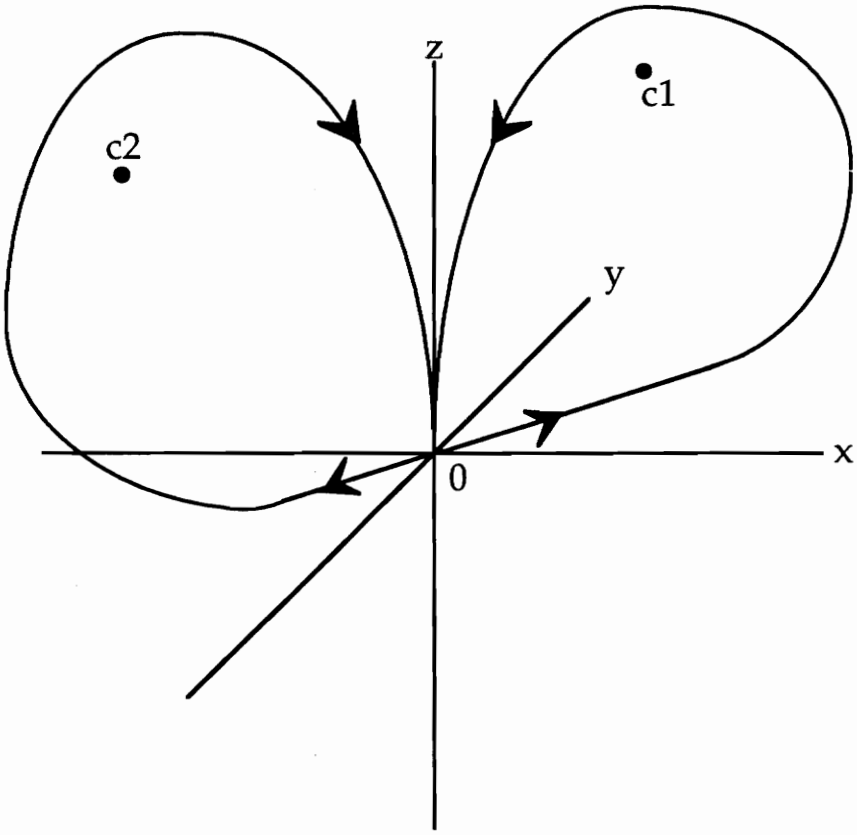

Figure 4.4: Homoclinic orbit for r=13.926..

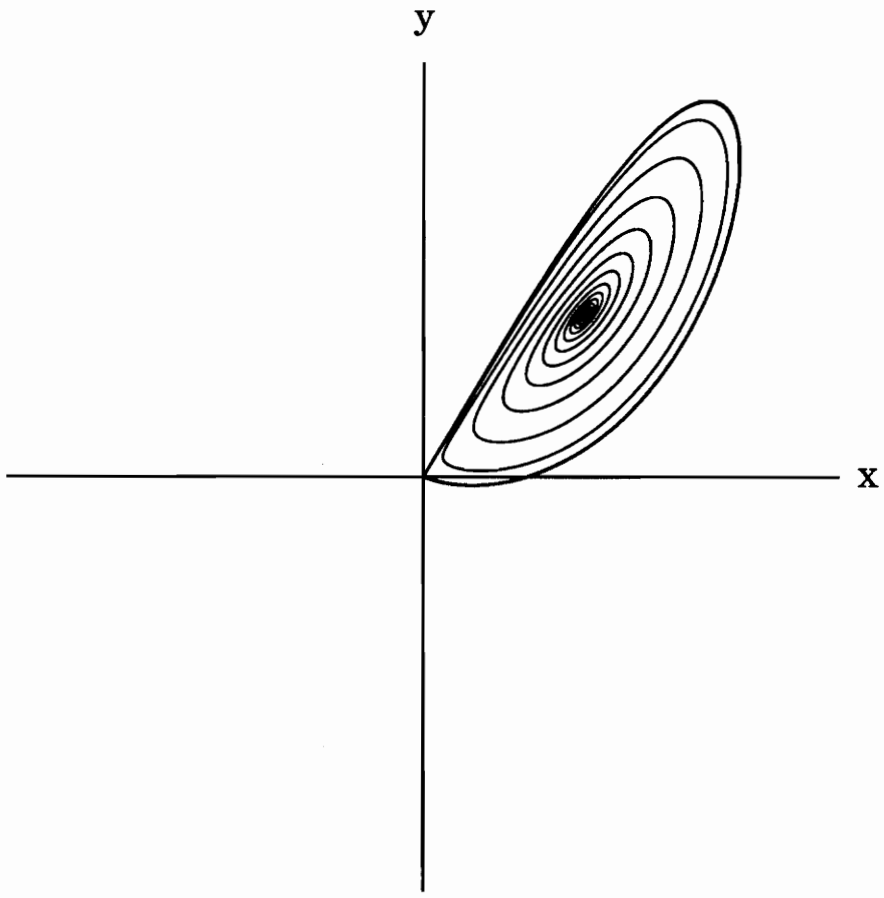

Figure 4.5: Trajectory near the homoclinic orbit

on to either c1 or c2, depending on which side of the manifolds the trajectory ends up.

Sparrow[23] talks at length about this homoclinic orbit and the "explosion" that results from it. A mathematical study of the region very close to the homoclinic orbit will reveal the following. There is a small "box" around the origin for which trajectories will leave through the side and enter again through the top (see Figure 4.6). By studying the return of the trajectories through the top of the box, a section of the face can be found for which trajectories that start in the box will return again through the same section for all time. All the trajectories that start and stay in this section make up what Sparrow calls a strange invariant set. These trajectories will either proceed directly to the origin, become periodic orbits, or become aperiodic orbits. All of the orbits and trajectories are nonstable, therefore the strange invariant set is nonstable. So for practical purposes, the visualization of this invariant set at this value of r is not obtainable, since trajectories that fall into the area eventually get "bumped off" and then spiral into c1 or c2.

However, as r increases, some trajectories will take longer and longer to leave this region. Trajectories exhibiting this type of behavior are said to be preturbulent. Authors like Kaplan and Yorke [26] and Yorke and Yorke [27] have shown that the average time that the trajectories wander near the strange invariant set approaches infinity as r approaches 24.06. It is at this point that the strange invariant set becomes a strange attractor. Therefore for

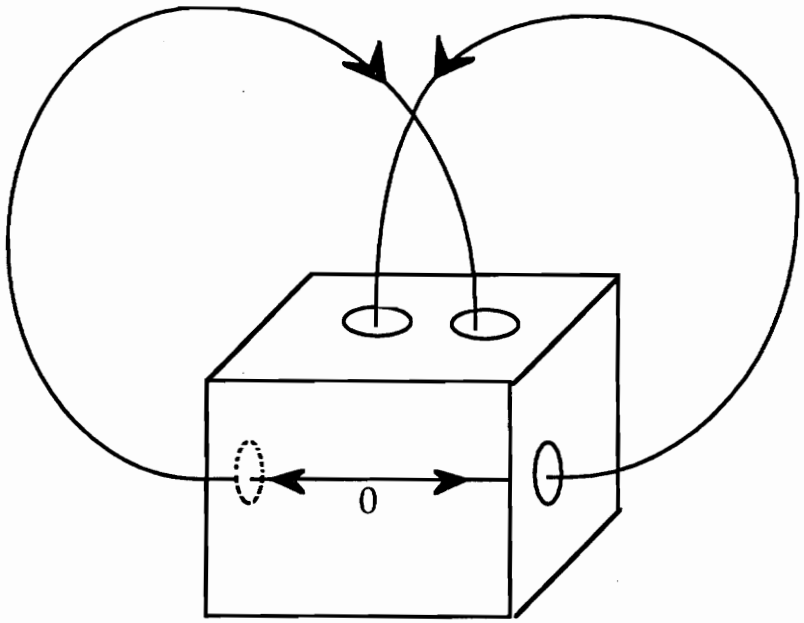

Figure 4.6: Local box enclosing origin

r>24.06, there are trajectories which lie in the strange attractor for all time t. Recall that c1 and c2 are stable until the value of r becomes 24.72. Therefore, for 24.06<r<24.72 the strange attractor and the two fixed point attractors c1 and c2 coexist. That is, some trajectories are still attracted to c1 and c2, while the rest are attracted to the strange attractor (see Figure 4.7).

At r=24.72, c1 and c2 lose their stability. A look at the changes in the eigenvalues of the system reveals the method in which they lose stability. For $\sigma=10$, $b = \frac{8}{3}$ and r less than 24.72, there is one real negative eigenvalue and two complex eigenvalues with negative real parts. The real eigenvalue is negative for all r. As r increases past 24.72 the real parts of the complex eigenvalues become positive and the points lose their stability. This type of bifurcation is known as a Hopf bifurcation. There are two types of this bifurcation. If it is supercritical, then each point loses its stability by giving off a stable periodic orbit. If it is subcritical, then they lose their stability by absorbing a non-stable periodic orbit. It has been shown (Marsden and McCracken [28]) that the Hopf bifurcation is subcritical in the Lorenz equations. Sparrow talks at length about the fact that the two non-stable periodic orbits (one for each fixed point) must come from the strange invariant set. The result of all of the above, is that as r increases past 24.74, the strange attractor exists by itself, attracting all orbits.

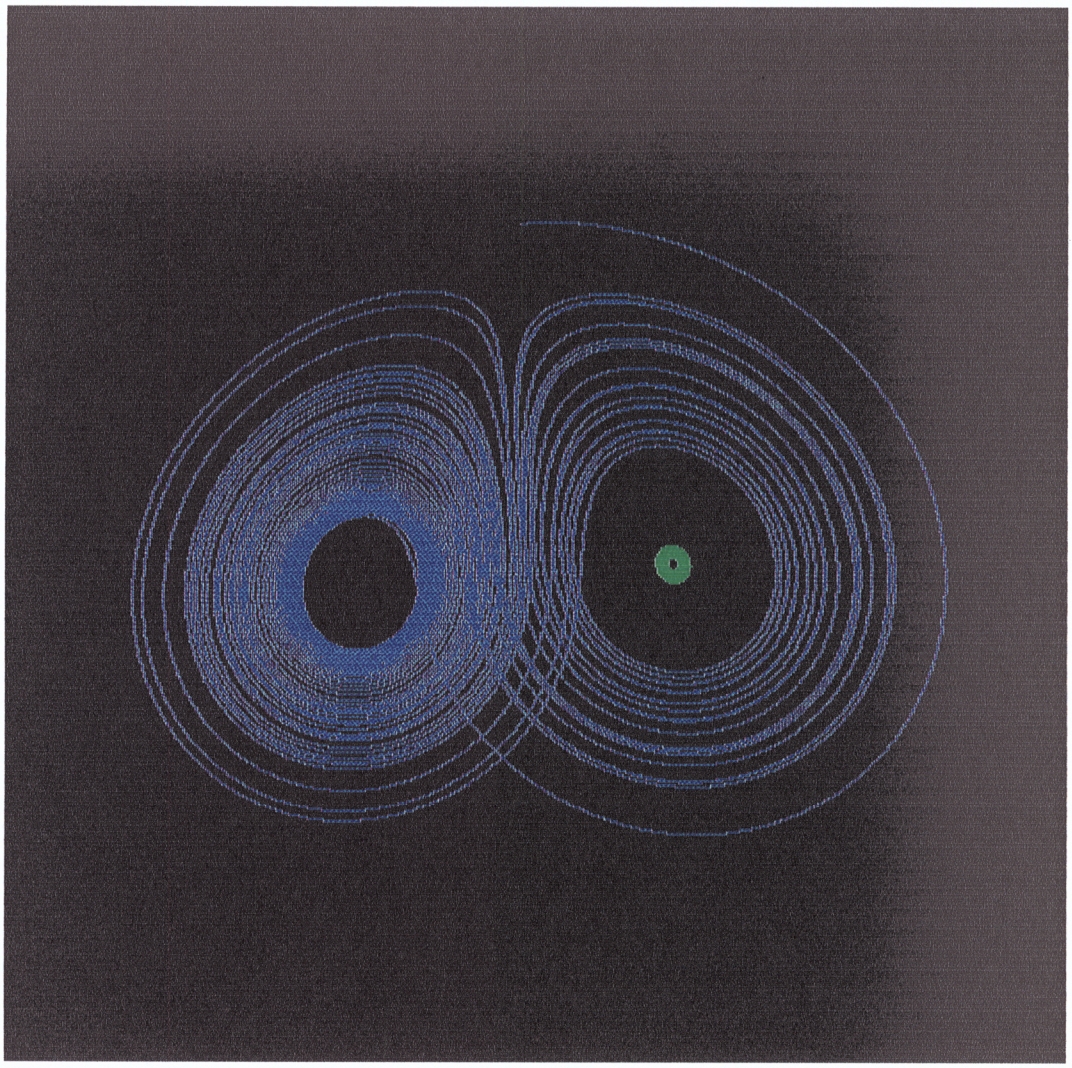

Figure 4.7: Two trajectories for 24.5 - blue attracted to strange attractor, green attracted to fixed point c1

4.13 Lorenz strange attractor

Before continuing with increasing values of r, the structure of the Lorenz strange attractor must be examined. Recall that a strange attractor has non-integer dimension. Lorenz [14] obtained the value d = 2.06 ± 0.01 for the dimension of the Lorenz strange attractor. Use of the visualization tool and its rotational abilities indeed show that the attractor takes up very little of the phase space. Certain rotations show the Lorenz attractor as almost a plane, which agrees with the value of its dimension. Figures 4.8 and 4.9 show a projection of some of these images, although the full effect is much better through user interaction.

The strange attractor also necessarily exhibits sensitivity to initial conditions. Many different researchers including Frøyland and Alfsen [29] have calculated one of the Lyapunov exponents of the Lorenz system to be positive for the chaotic periods of the motion. This condition is illustrated in Figure 4.10 with the use of two colors; red represents one initial condition (1,1,1), while blue represents an initial condition very close to the red, (1.01,1.01,1). The two trajectories do not stay on the same path but diverge rather quickly.

4.14 Lorenz solutions for 24.74<r<∞

This strange attractor does not remain the same for increasing values of r. It turns out that as r gets larger, there are periods when the behavior



Figure 4.8: A rotated view of the Lorenz strange attractor for r=28

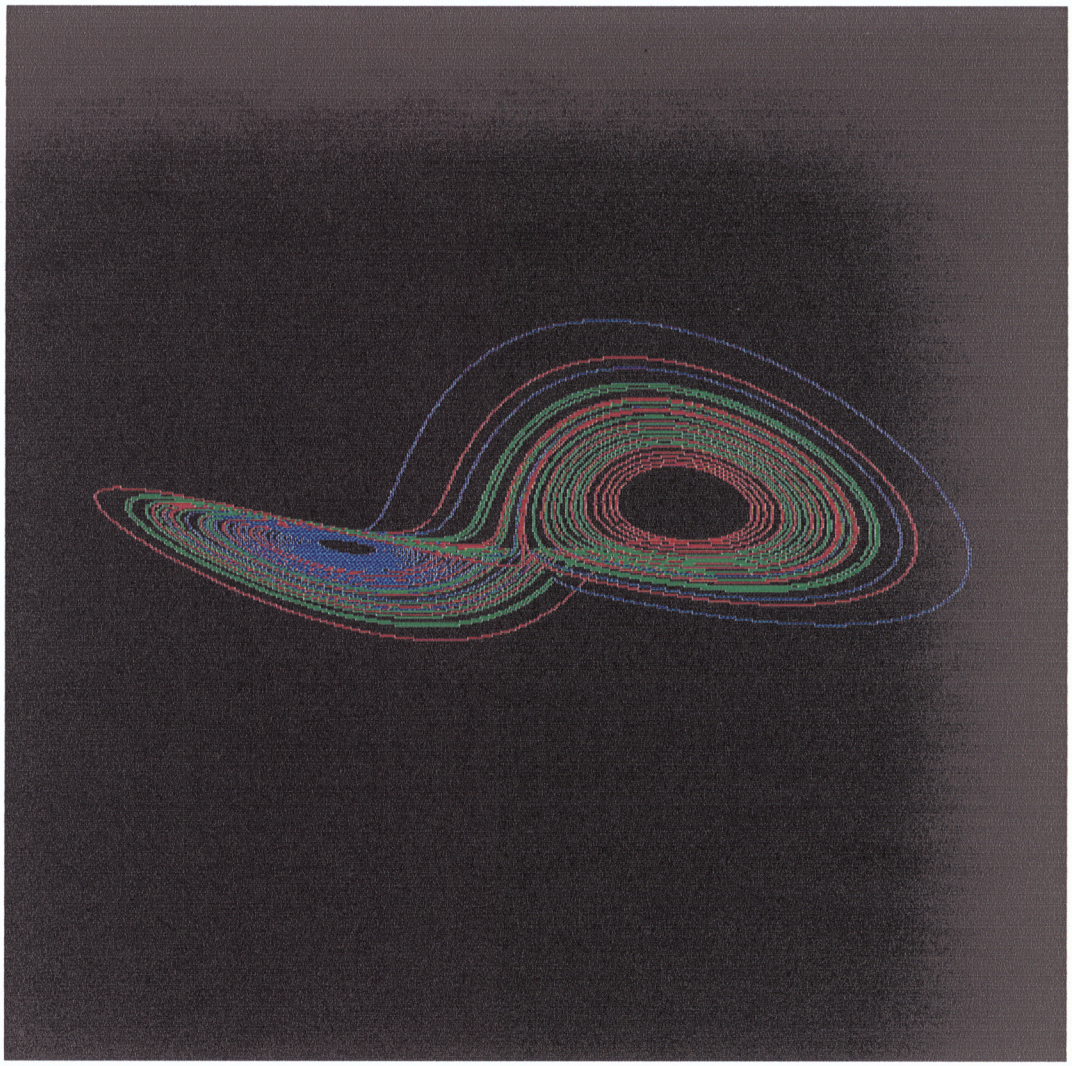

Figure 4.9: A rotated view of the Lorenz strange attractor for r=28

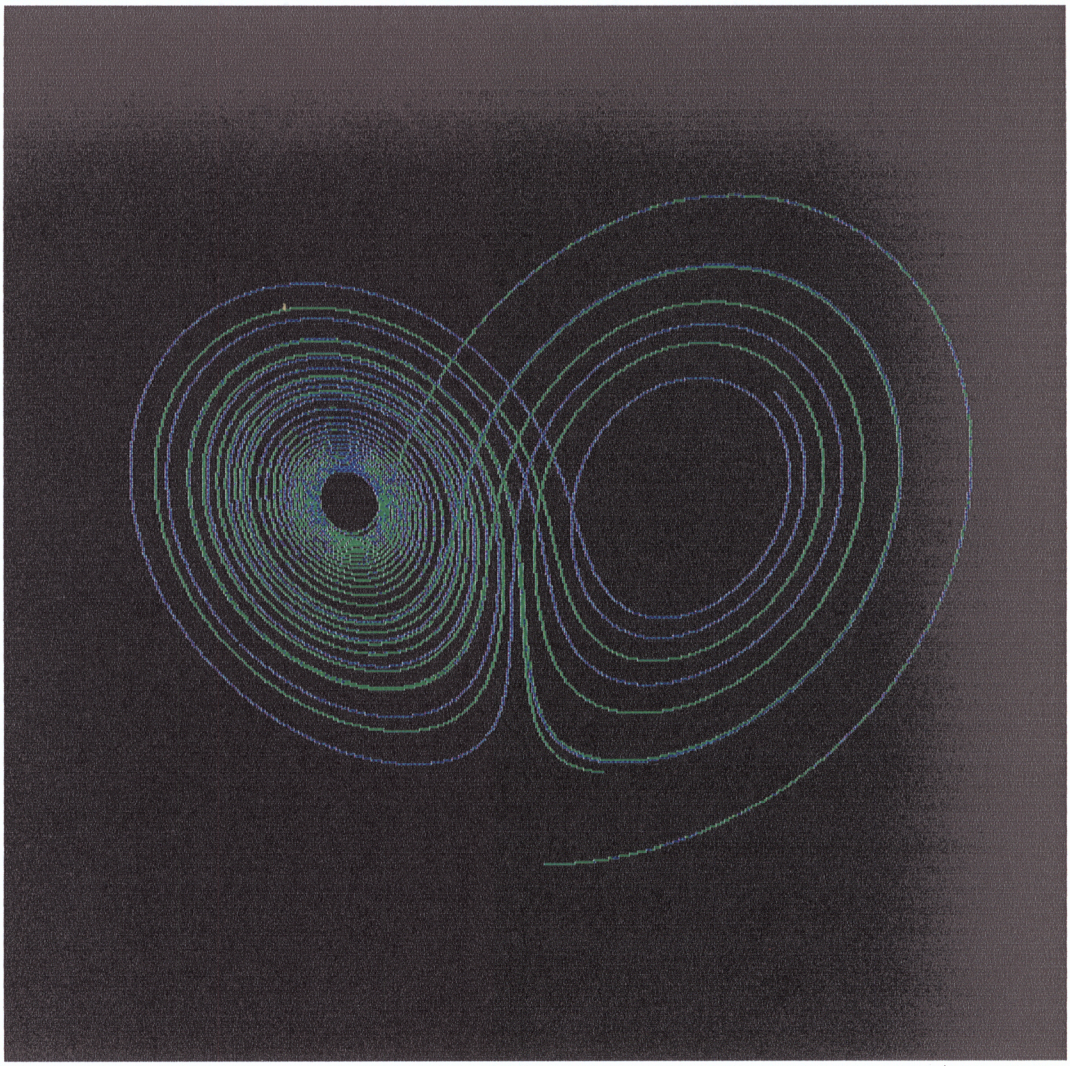

Figure 4.10: Lorenz attractor for r=28, blue initial (x,y,z)=(1,1,1), green initial (x,y,z)=(1.01,1.01,1)

goes from a strange attractor to stable periodic orbits. Sparrow[23] talks about three of the more easily found "windows" with stable periodic orbits, and discusses an orbit locating program that finds others, two of which are mentioned.

These periodic orbits do not occur as a simple jump from a strange attractor, to periodic orbit, and then back to a strange attractor as r changes. Instead, the periodic orbits appear in certain intervals, or windows of r values in which period doubling occurs. A trajectory in phase space experiencing period doubling has the following property. First, the solution is attracted to an orbit with period one. Then as the parameter changes, the orbit doubles its period to two. As the parameter is changed even more, the period of the orbit continues to double (4,8,16...) until eventually the orbit is chaotic again. The solutions to the Lorenz equations show this same type of behavior in intervals of r values where period doubling occurs as r decreases. Since r is followed with increasing value, the windows are thought of as period halving windows. There are three large windows of this nature that many authors have discussed.

The first occurs for $99.524<r<100.795$. Sparrow calls it the x^2y period doubling window, where the x and y are symbolic and represent the trajectory spiralling into $x>0$ space or $x<0$ space (see Figure 4.11). This is a nonsymmetric periodic orbit, so there is also a y^2x periodic orbit, since the Lorenz equations possess symmetry. For r approximately between 99.98 and 100.795

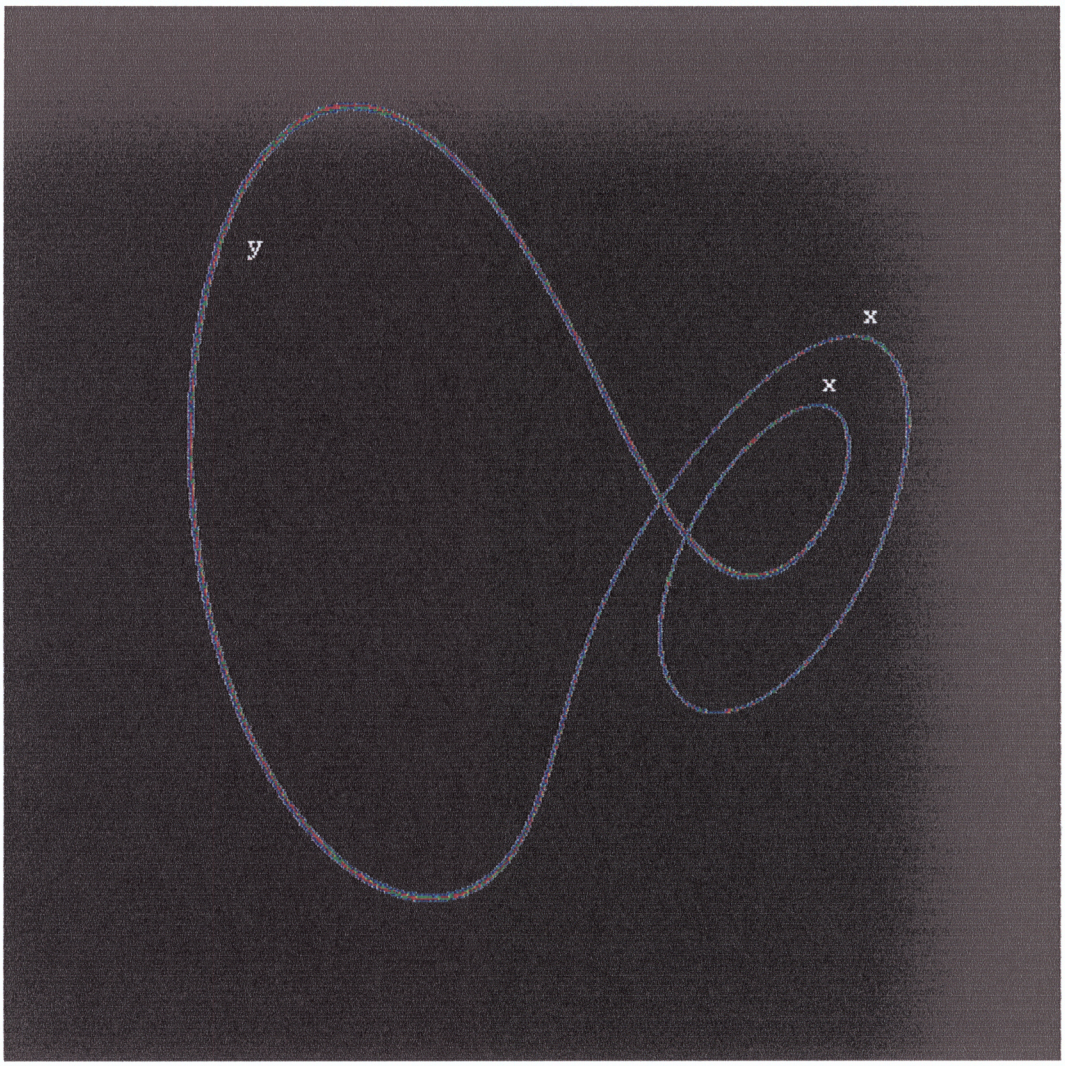

Figure 4.11: An x^2y periodic orbit for r=100

the trajectories are attracted to either one these stable periodic orbits. For r less than 99.98 but greater than 99.629, period doubling occurs and the periodic orbits are now x^2yx^2y and y^2xy^2x. These periodic orbits are illustrated in Figures 4.12 and 4.13. (Although the trajectories appear to be crossing in these pictures, three dimensional views of the objects show that they do not since the trajectories must maintain the uniqueness condition discussed in Chapter Two). As r is decreased even further, period doubling continues until r is approximately 99.524, below which the motion is chaotic again.

The next large window occurs for $145<r<166$ and involves an x^2y^2 symmetric orbit. For $154.4<r<166.07$ this symmetric orbit is stable and all trajectories are attracted to it. At approximately 154.4, this symmetric orbit becomes two stable nonsymmetric x^2y^2 orbits, which then double in period continuously as r is decreased, similar to the previous period doubling window. When r is about 145, the system is chaotic again.

Before discussing the last period doubling window that the system encounters, some other smaller period doubling windows will be discussed. Sparrow used an orbit finding routine (numerical), and mentioned a few very short windows with stable periodic orbits that this program found. At r=126.52 there is a stable x^2y^2xy orbit, at r=114.0 there is a stable x^2yxy orbit, and a stable x^2yxy^2xy orbit is present at r=132.5. These orbits are illustrated in Figures 4.14 through 4.16. After Sparrow discusses these, he suggests that other period doubling windows can be found using the same technique. He

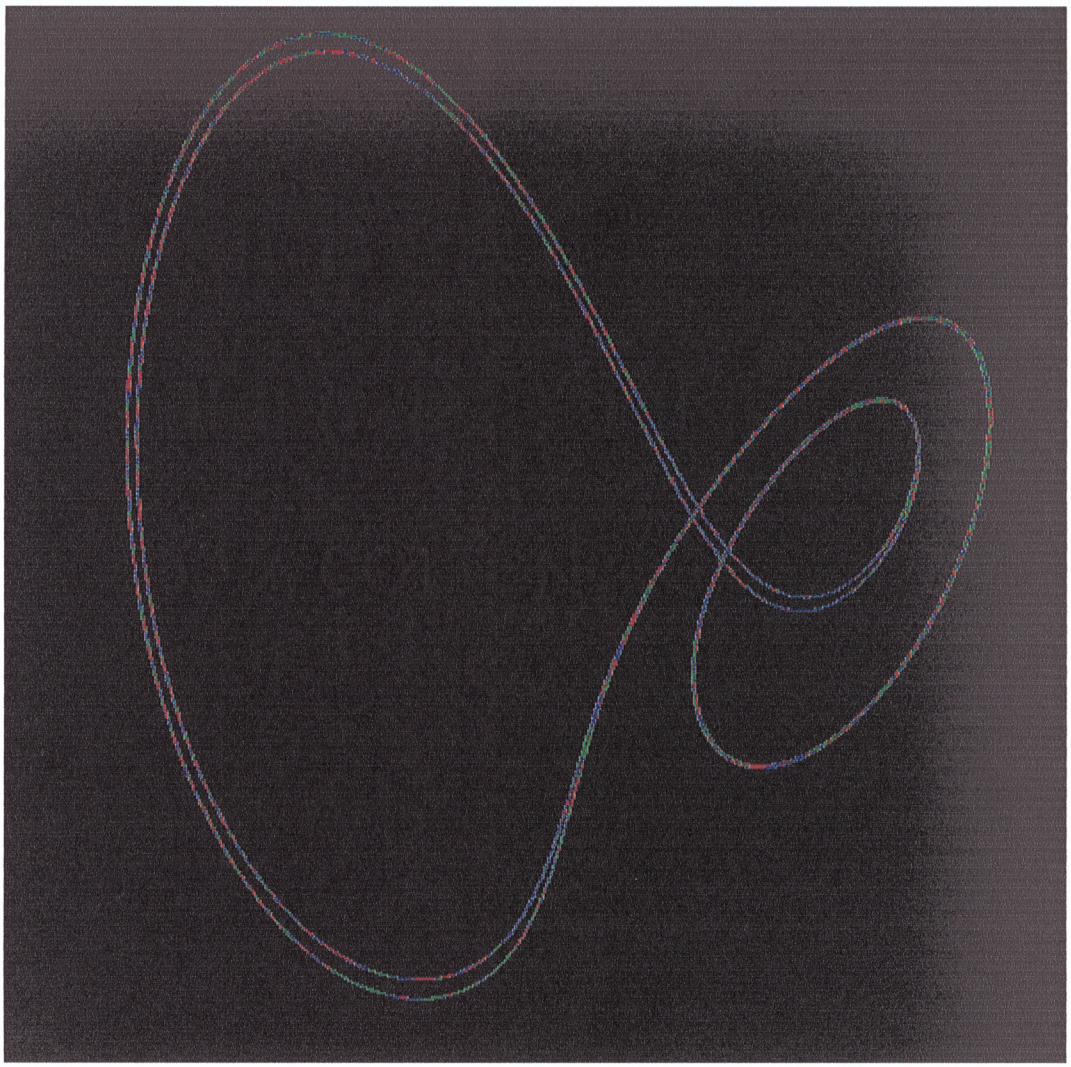

Figure 4.12: An x^2yx^2y periodic orbit for r=99.7

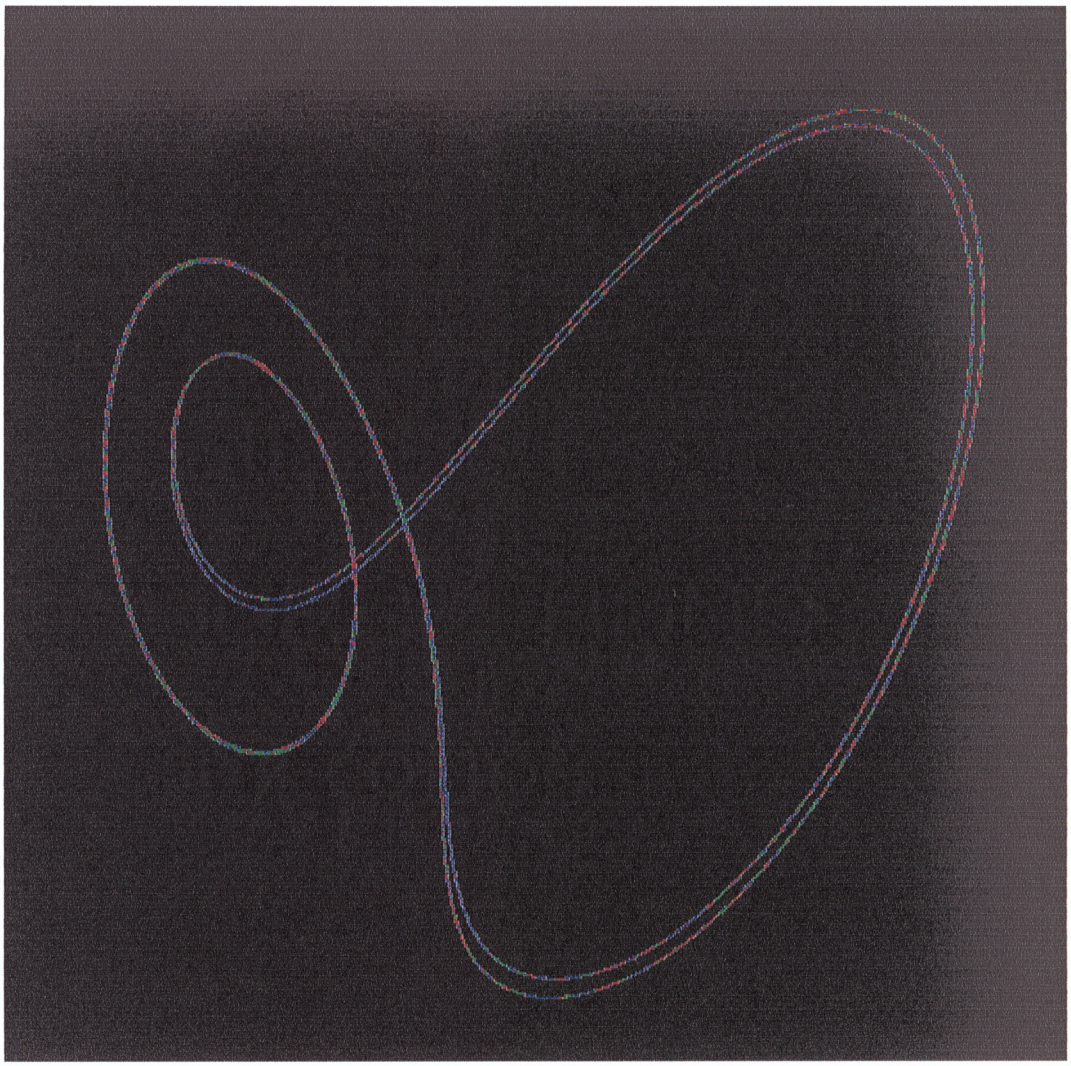

Figure 4.13: A y^2xy^2x periodic orbit for r=99.7

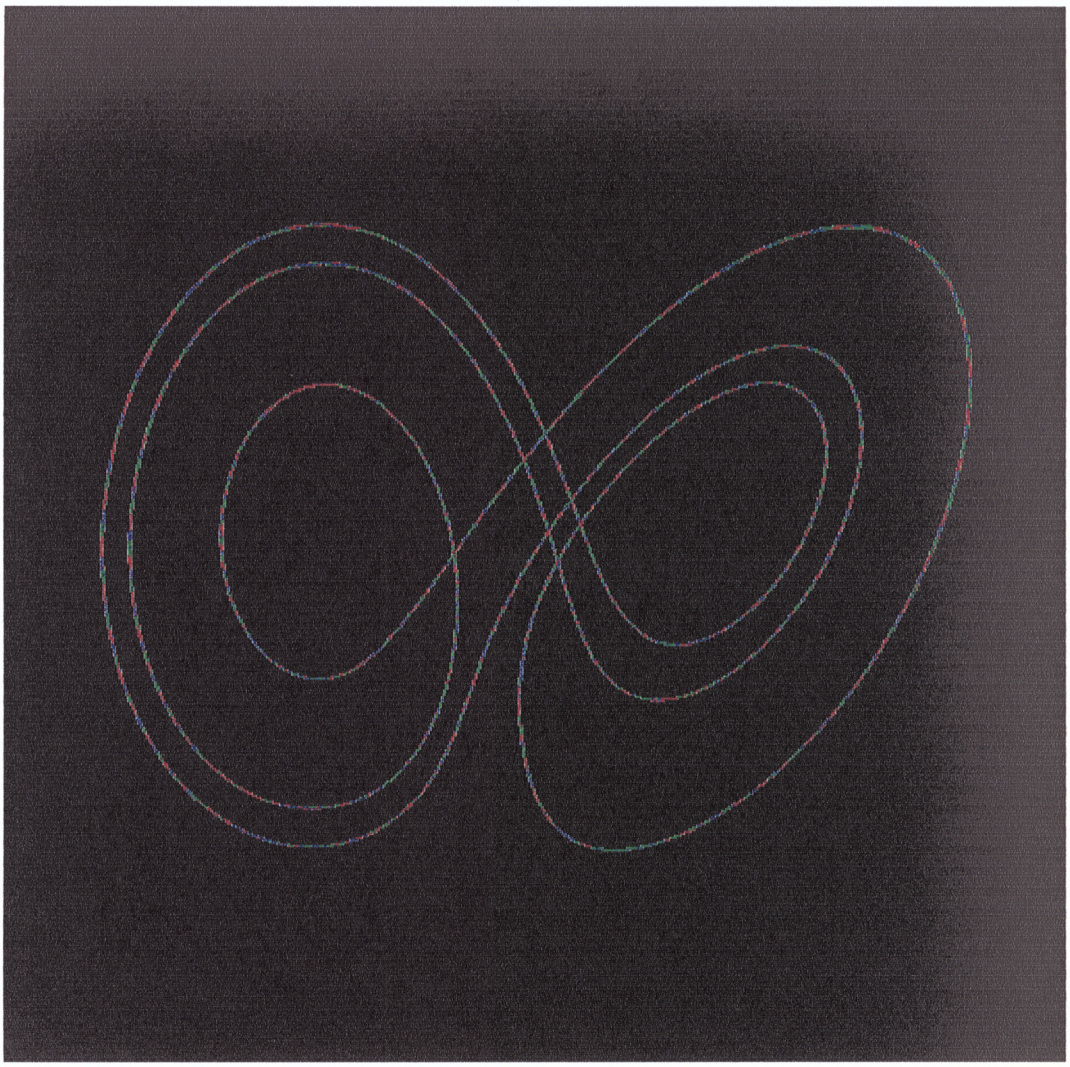

Figure 4.14: An x^2y^2xy periodic orbit for r=126.52

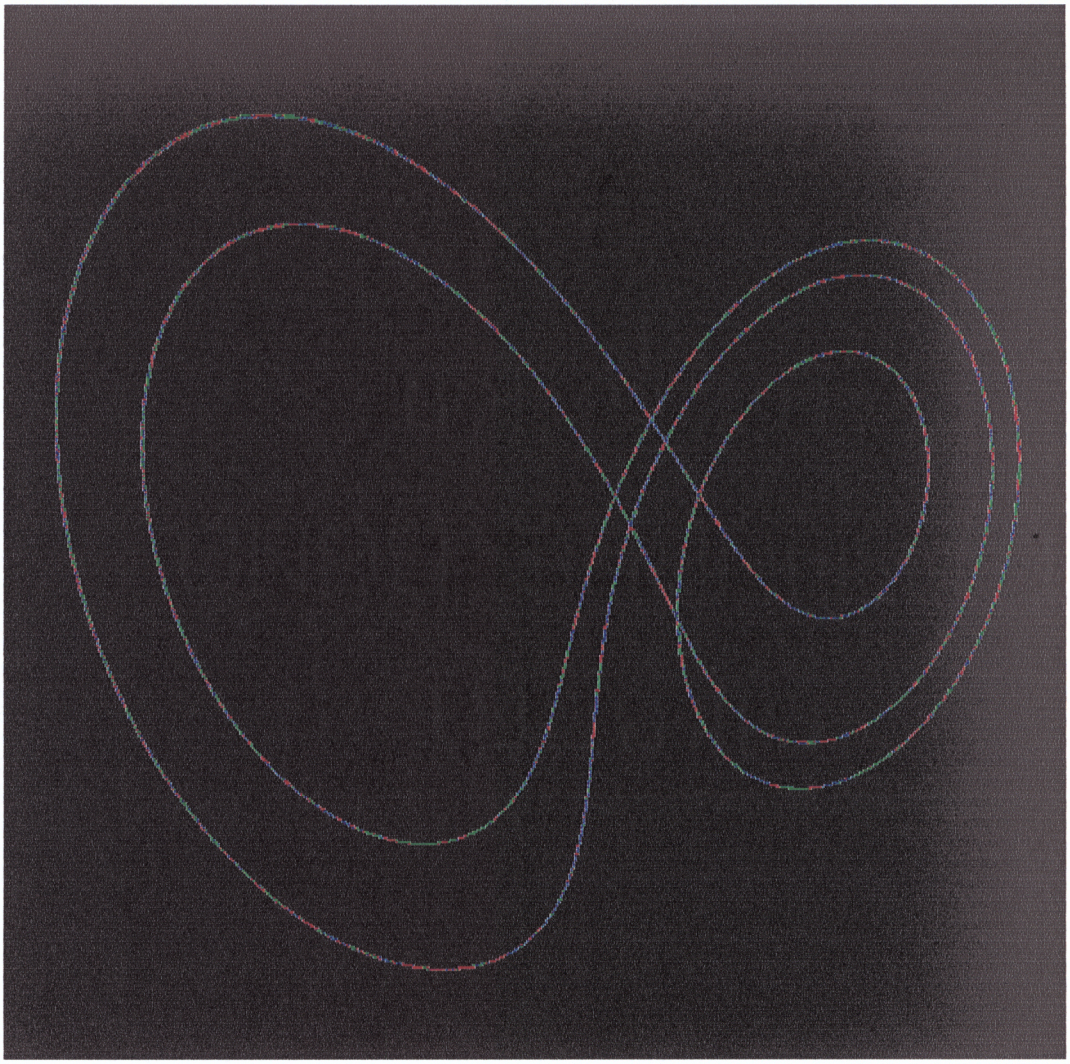

Figure 4.15: An x^2yxy periodic orbit for r=114.0

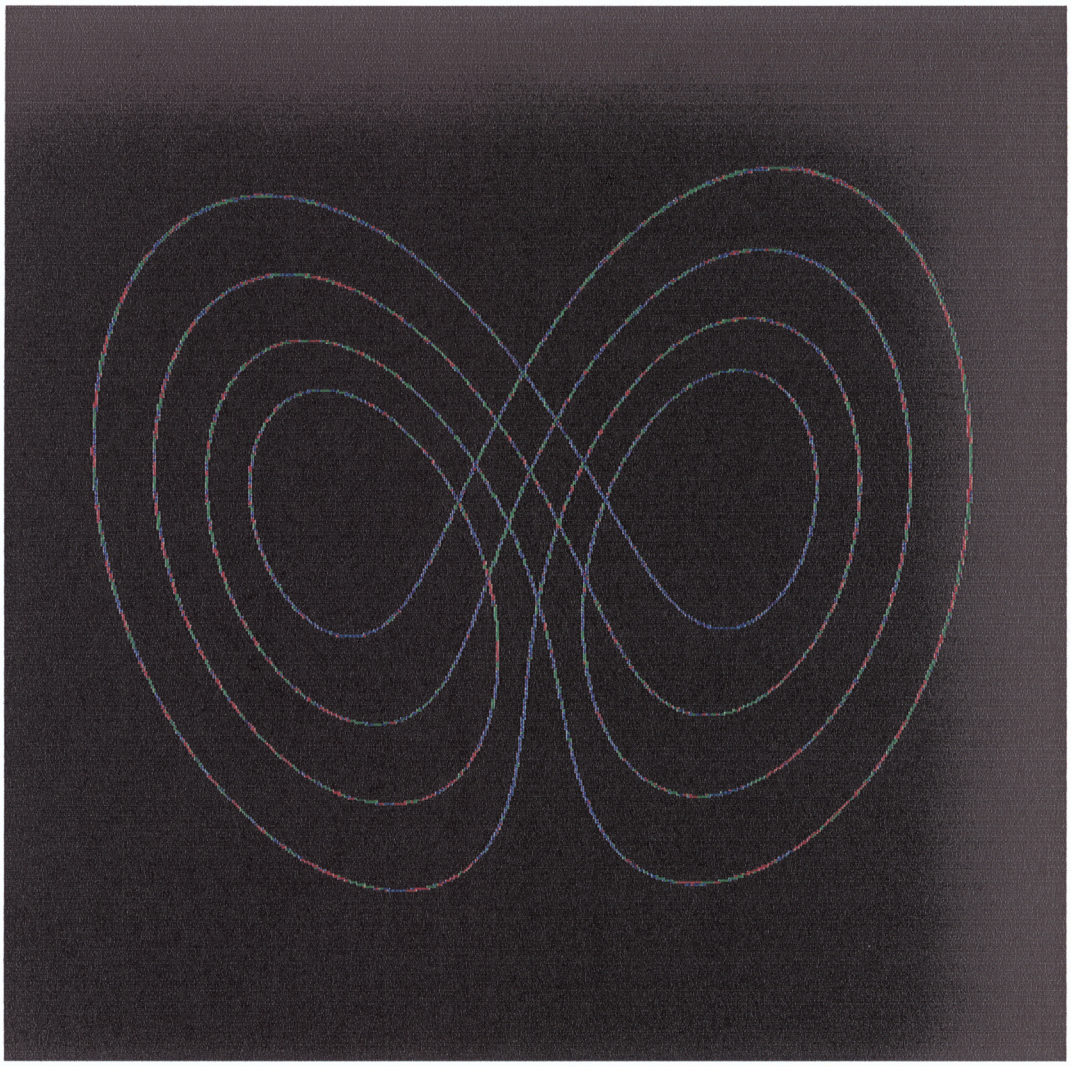

Figure 4.16: An x^2yxy^2xy periodic orbit for r=132.5

also mentions that period doubling windows for r<99 are expected for which the orbits will have more than two consecutive x's or y's in their symbolic representation. The routine he used could not locate any of these orbits. Through the use of the visual tool, five different short windows were found for r<99.

The first was located at r=58.7. Following the notation of Sparrow, it is represented symbolically by x^5y^5. This orbit appears to be symmetric. The next was found at r=69.8 and is symbolized by x^4y^4. For an r value around 71.4 to 71.5 there is a nonsymmetric x^3y orbit as well as a y^3x orbit, due to the symmetry of the Lorenz equations. In this window the trajectories are attracted to one or the other, depending on the initial conditions. At r=86.4, there is a y^2xyx^3 and an x^2yxy^3 orbit. Finally, at r=92.2, a stable, periodic x^3y^3 orbit was found to exist. See Figures 4.17 through 4.21 for the two-dimensional projections of these orbits. The structure of these objects is appreciated much more through the use of the visual tool.

The visual tool is also beneficial for observing the following. As r increases past 166.07 and becomes approximately 198.0, the trajectories will only spiral around each fixed point once and then return to the other point once, and back again. This behavior is illustrated in Figure 4.22. The trajectory's exact path around each point cannot be predicted, so the motion is still chaotic. However, the trajectory is not randomly spiralling around each fixed point anymore but following a simple pattern. Lorenz [30] describes the

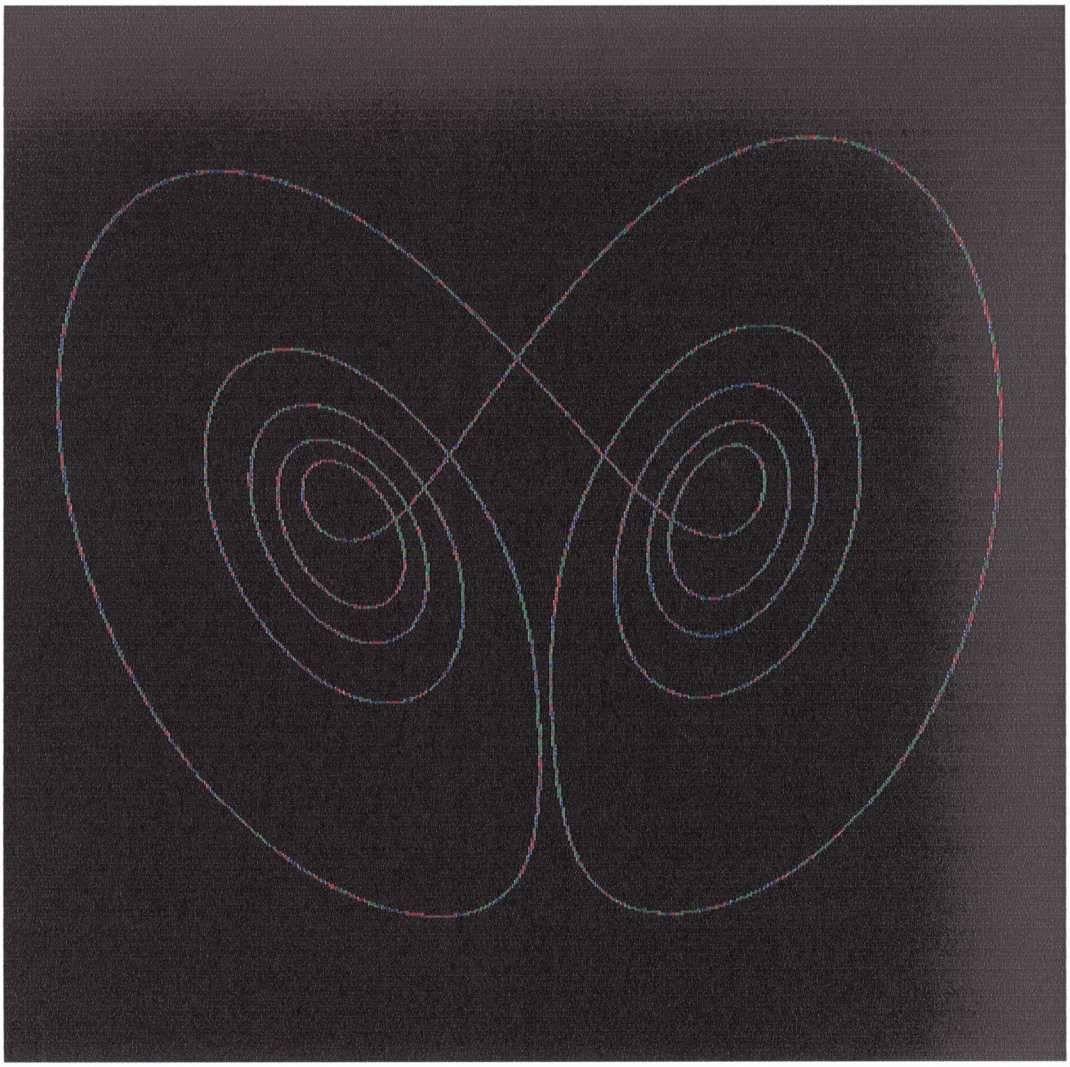

Figure 4.17: An x^5y^5 periodic orbit for r=58.7

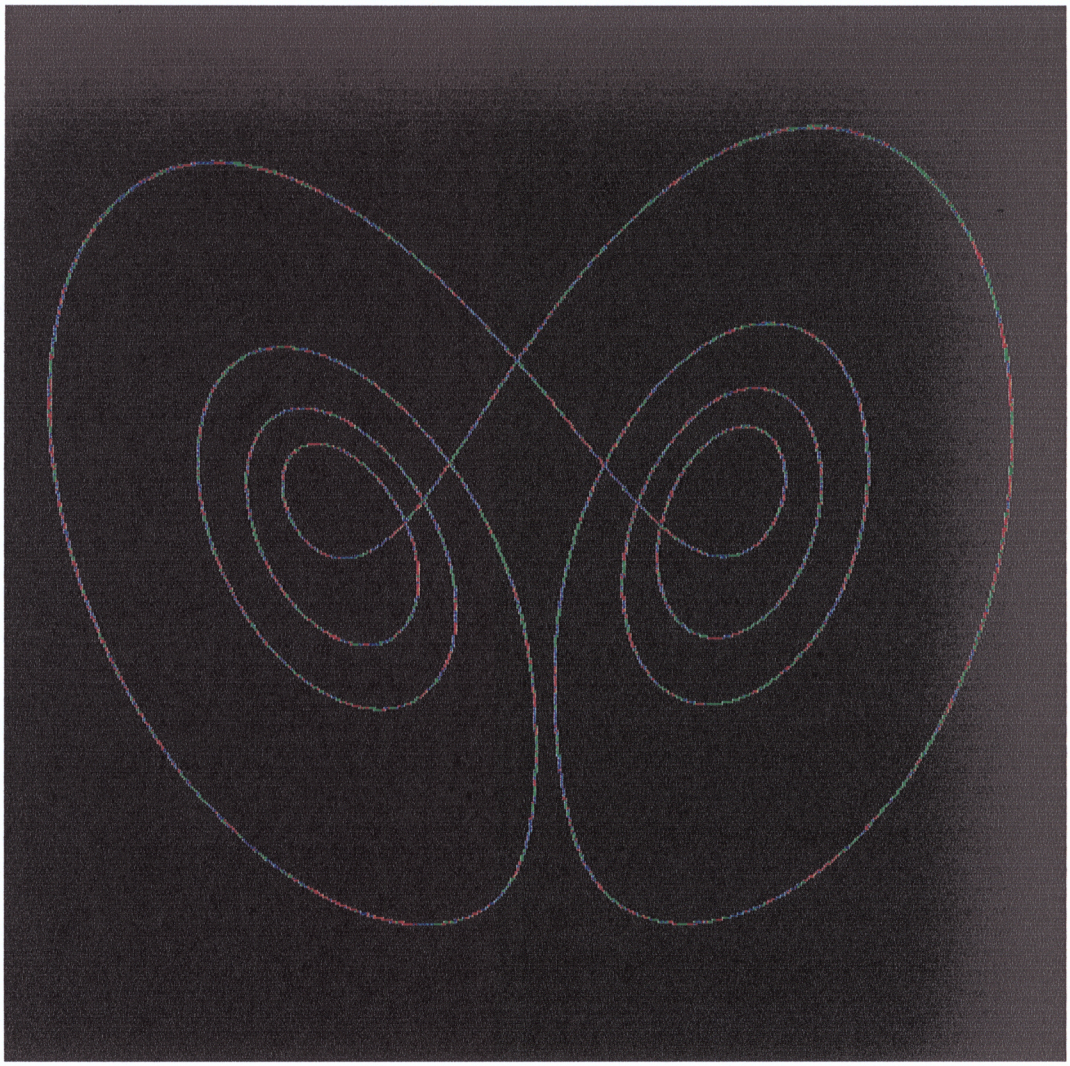

Figure 4.18: An x^4y^4 periodic orbit for r=69.8

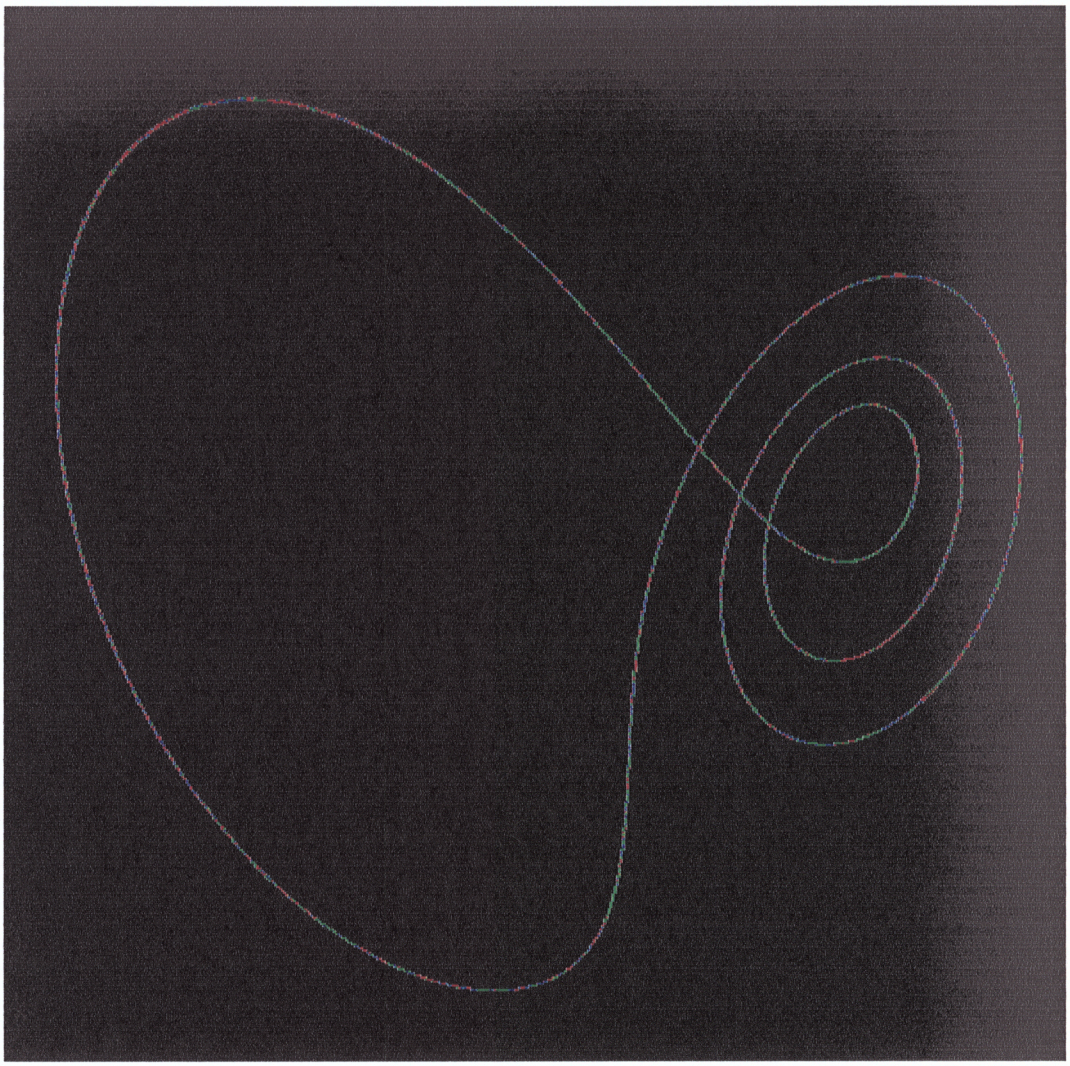

Figure 4.19: An x^3y periodic orbit for r=71.5

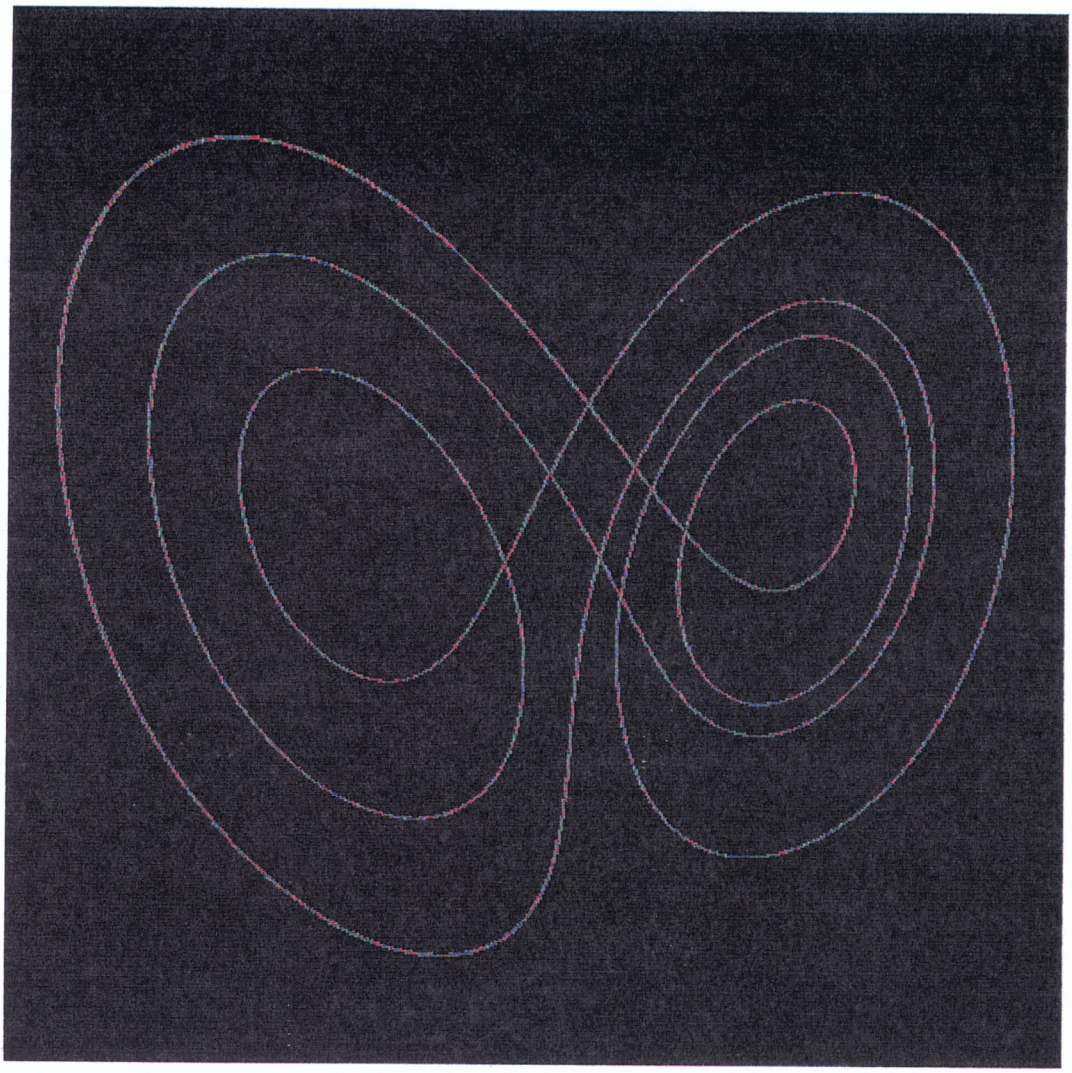

Figure 4.20: A y^2xyx^3 periodic orbit for r=86.4

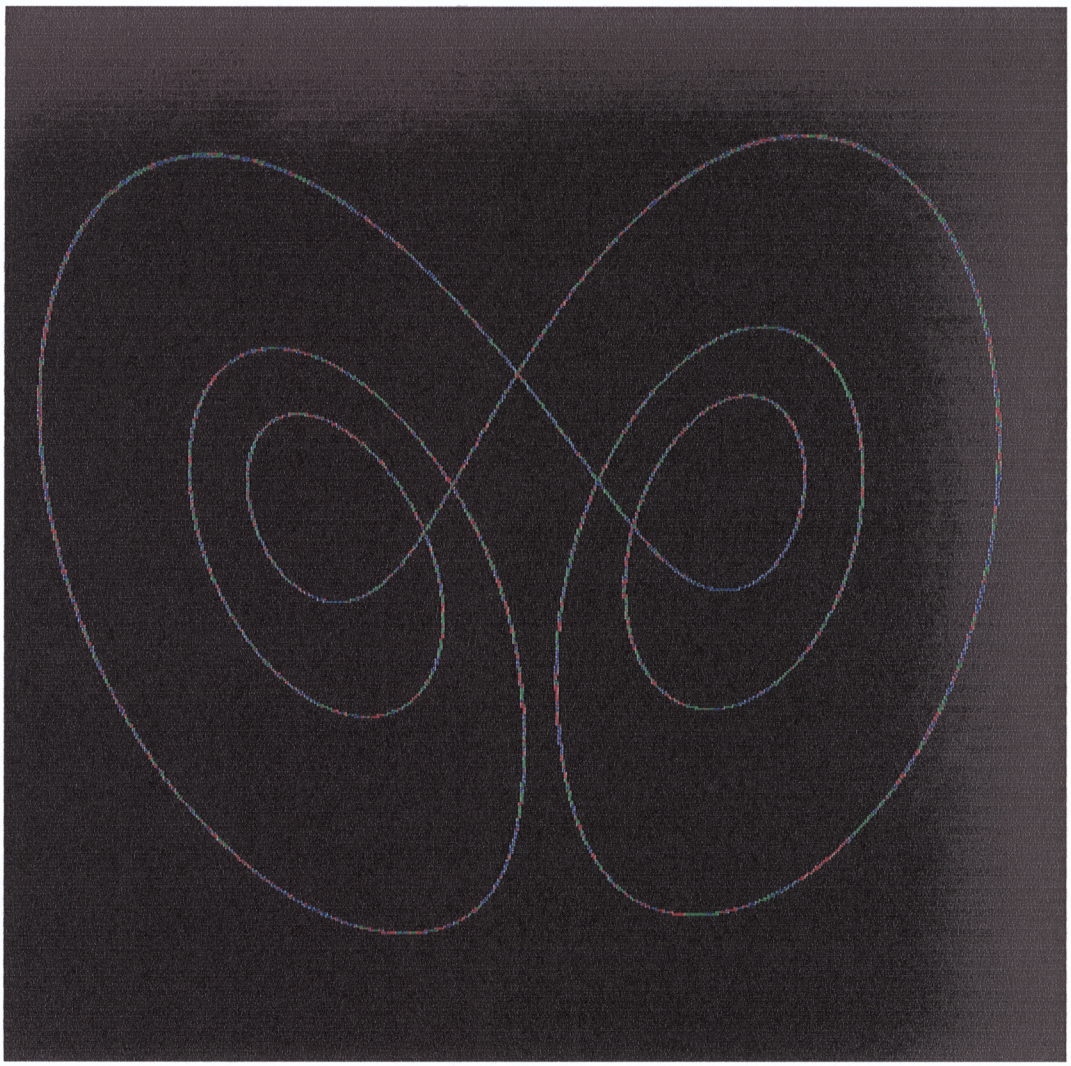

Figure 4.21: An x^3y^3 periodic orbit for r=92.2

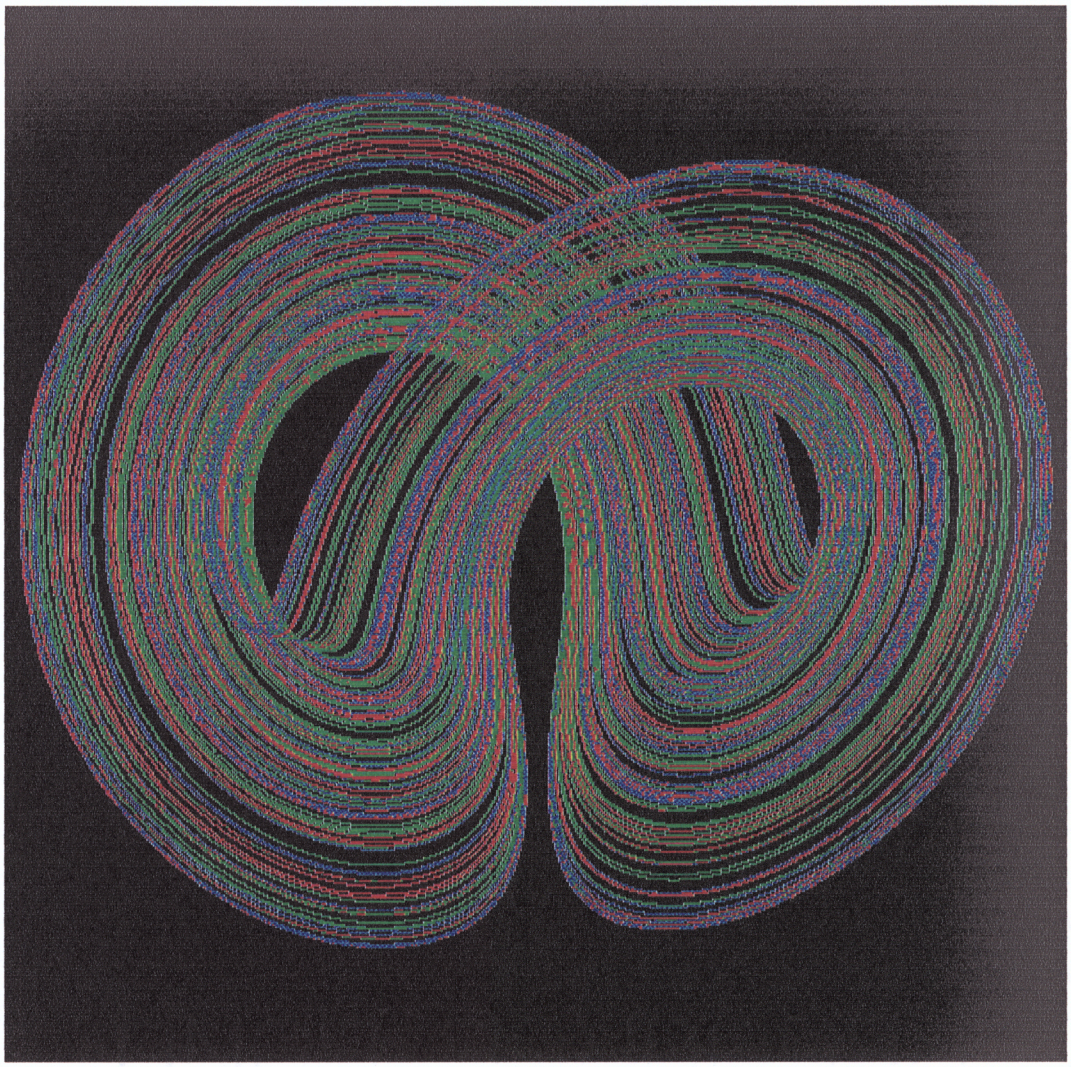

Figure 4.22: Semi-periodicity in the Lorenz attractor for r=199

system at this point as being semi-periodic. This can also be observed below other period doubling windows, but is much more prominent and can be observed for a longer period of time for the parameter range 198<r<215.

At r approximately 214.364, the period halving starts to occur and stable periodic orbits of $(xy)^n$ can be observed. The final bifurcation occurs at r=313 for which a symmetric xy orbit is produced (see Figure 4.23). This orbit is stable and attracting for 313<r<∞.

The above section followed the solutions of the Lorenz equations for values of σ=10 and b = $\frac{8}{3}$ from the discussions in Sparrow [23], with the visual tool being used to understand the behaviors being discussed. A video was developed to reproduce the process of visualizing the solutions.

4.2 Rössler equations

The solutions to Rössler equations were also visualized in phase space with the AVS tool, though only for a few changes in parameter value. Recall that the equations are

$$\begin{aligned} \frac{dx}{dt} &= -y - z \\ \frac{dy}{dt} &= x + ay \\ \frac{dz}{dt} &= b + z(x - c) \end{aligned} \tag{4.23}$$

For fixed values of a=.2, b=.2, the solution will exhibit chaotic behavior with

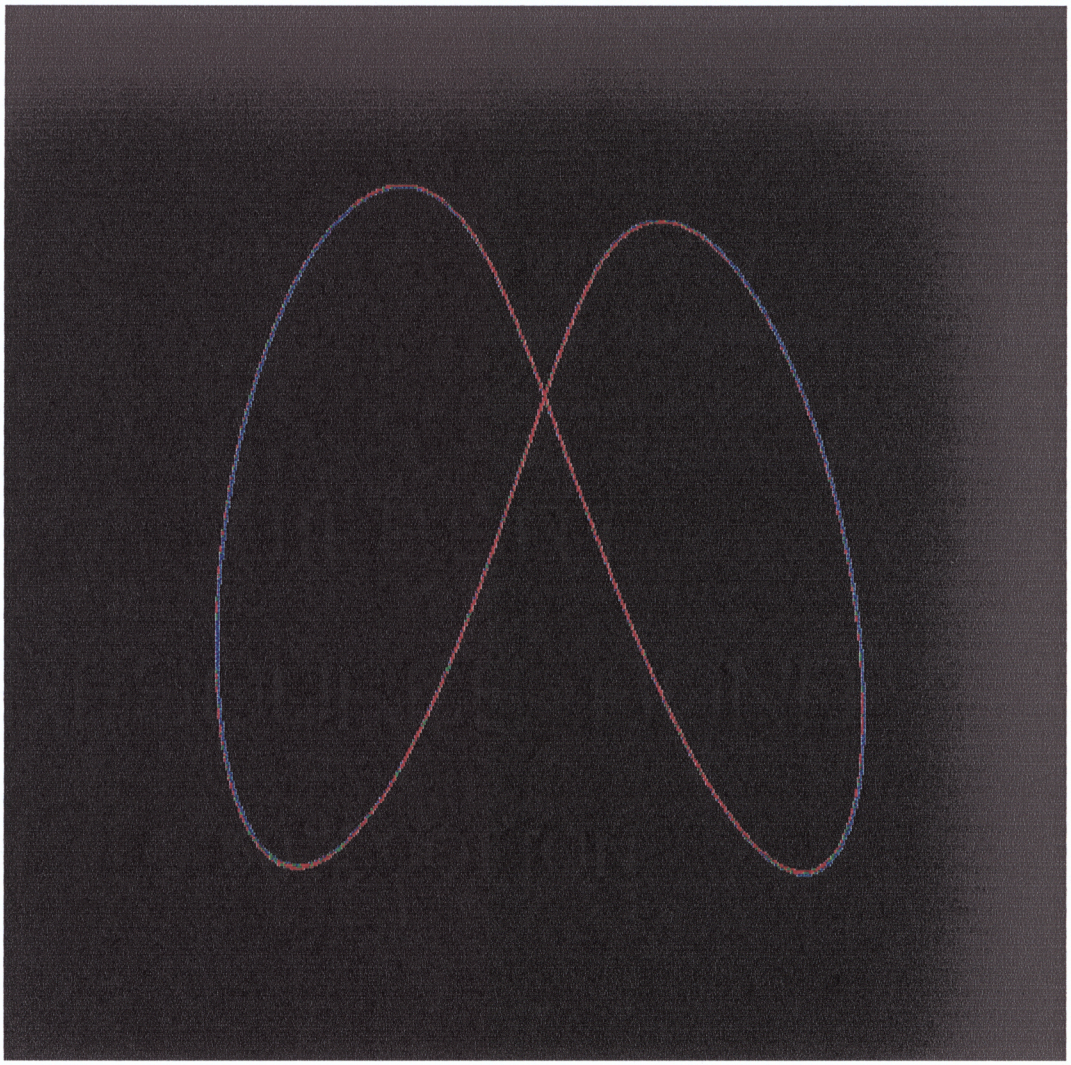

Figure 4.23: Final xy periodic orbit for r>315

varying values of c. The route to chaotic behavior in this case is a period doubling route. At c=2.5, there is a single periodic orbit present. (See Figure 4.24). As c increases to about 2.8, period doubling occurs and the orbit has period 2. This period doubling continues until a c value of approximately 4.26 when the solutions become chaotic and a strange attractor is present as illustrated in Figure 4.25. These two dimensional pictures do not accurately represent the structure of this attractor, but most illustrations in books show this picture. A better view of the attractor is shown in Figure 4.26 where it has been rotated. The trajectory, when entering positive z space actually lifts off of the base of the attractor with varying heights. As c increases, the elevation increases even more.

Rössler designed the equations this way in order to show the type of motion that can lead to chaos. The solution spirals in the xy plane of phase space and then leaves the spiral in the z direction, only to return again to the spiral. Past a certain parameter value, the system becomes chaotic and the returns to the plane become irregular and unpredictable. Rössler called this type of attractor a 'spiral-type chaos' [8]. Rotations of this attractor in real time exhibit this spiral quality of the attractor.

The strange attractor is not present for all values of c past the critical value. Exploration of the system showed various period doubling windows, each with different types of original periodic orbits, as in the Lorenz Equations. Figures 4.27 and 4.28 illustrate these different orbits.

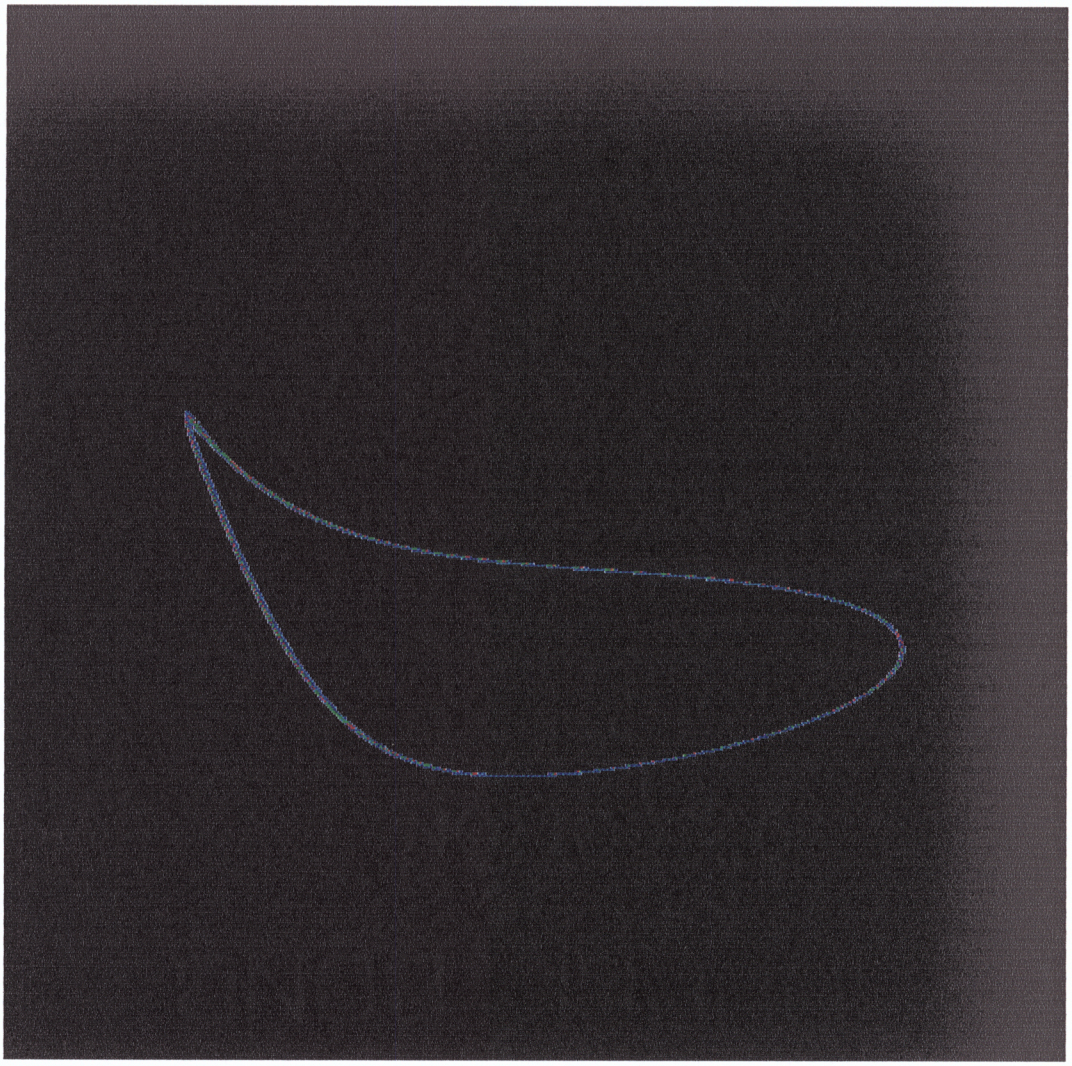

Figure 4.24: Periodic orbit of the Rössler system for c=2.4

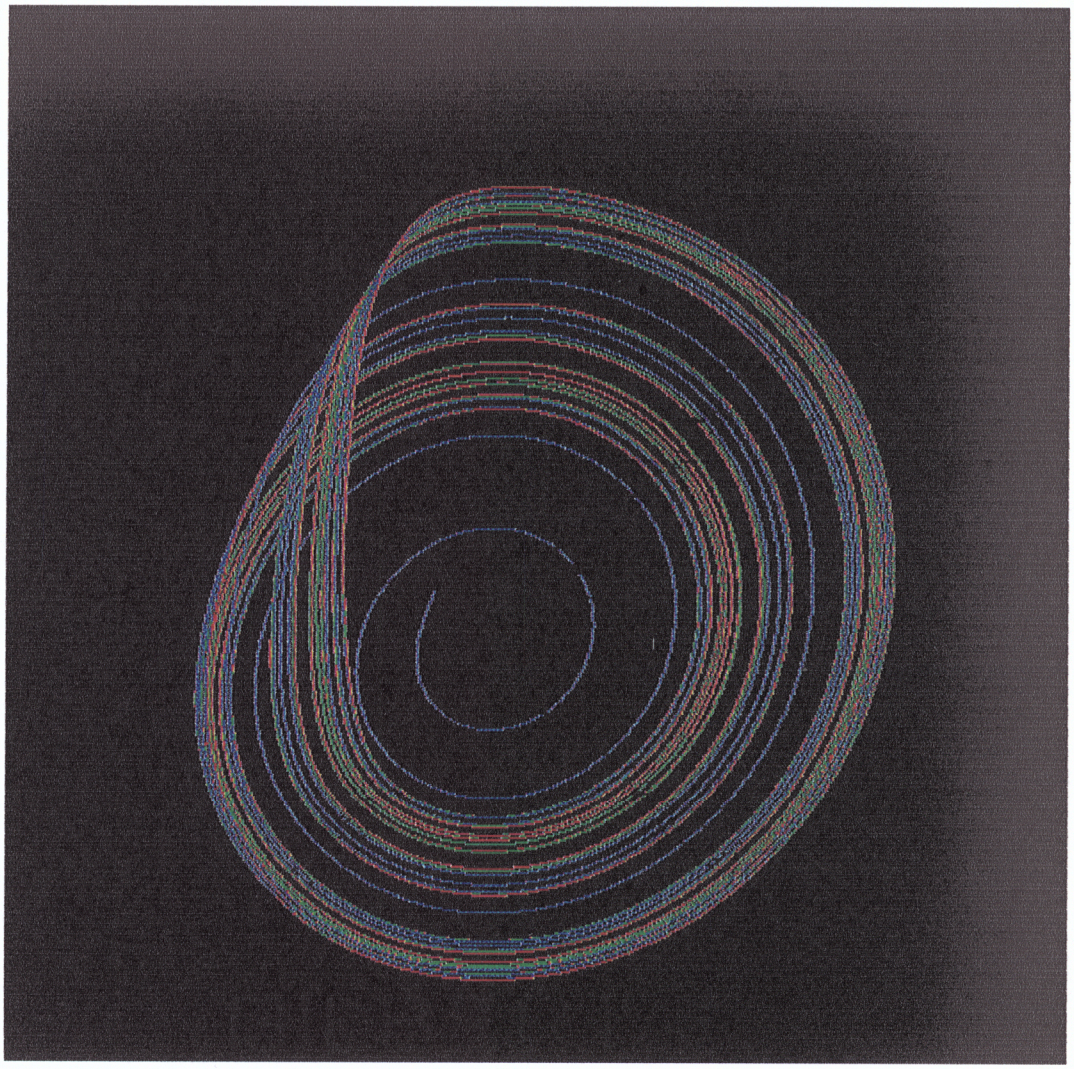

Figure 4.25: Rössler strange attractor for c=4.26

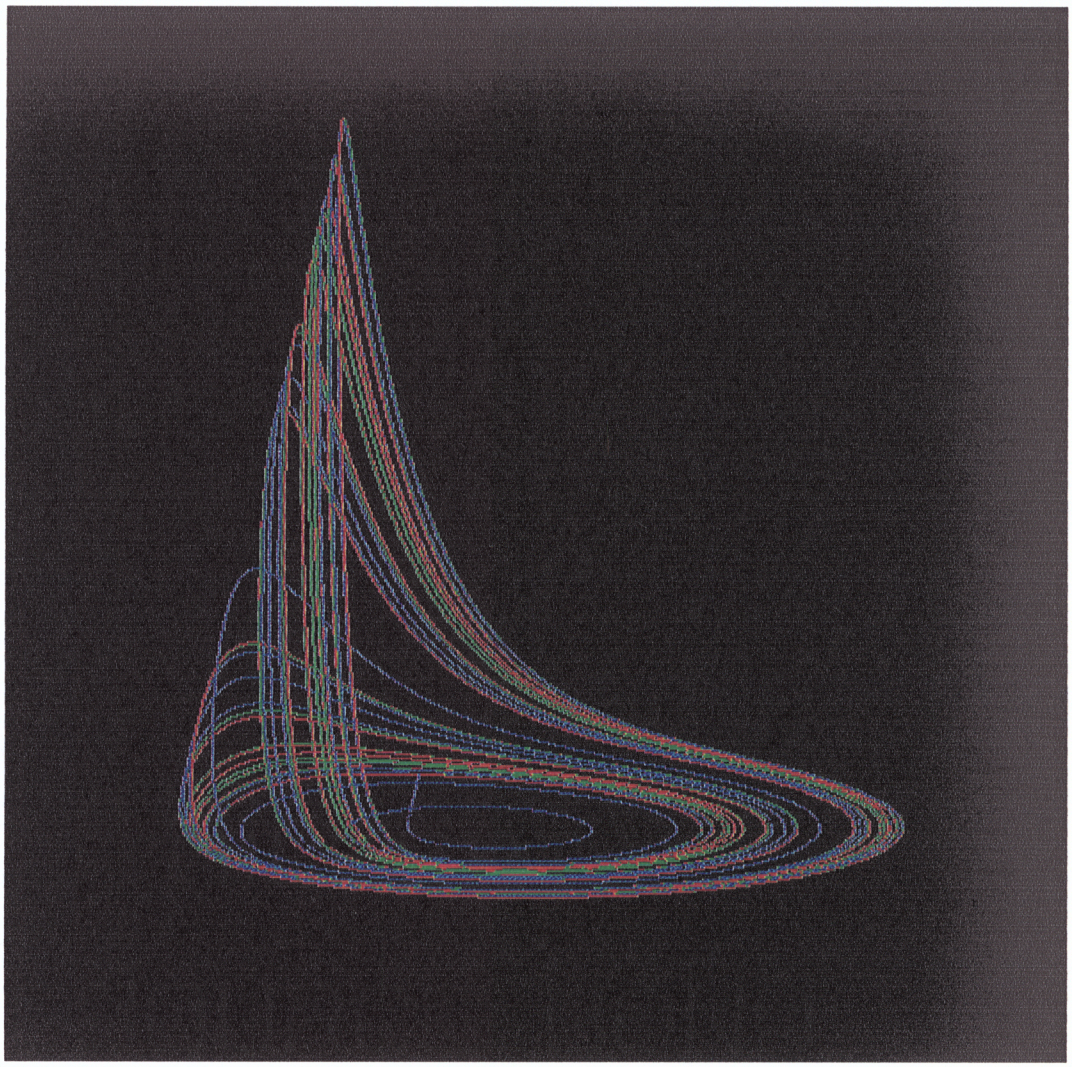

Figure 4.26: A rotated view of the Rössler strange attractor for c=4.26

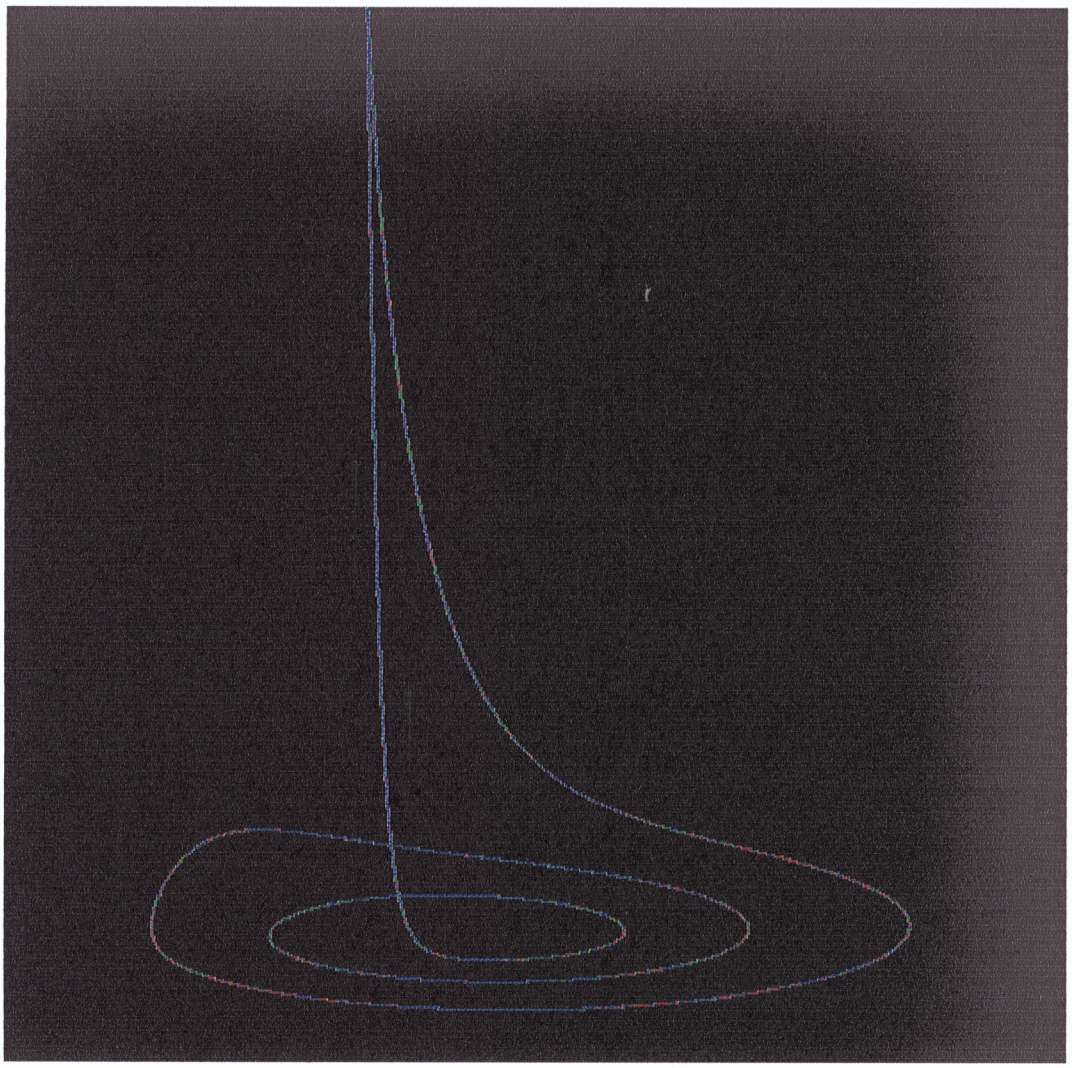

Figure 4.27: A periodic orbit of the Rössler system for c=5.3

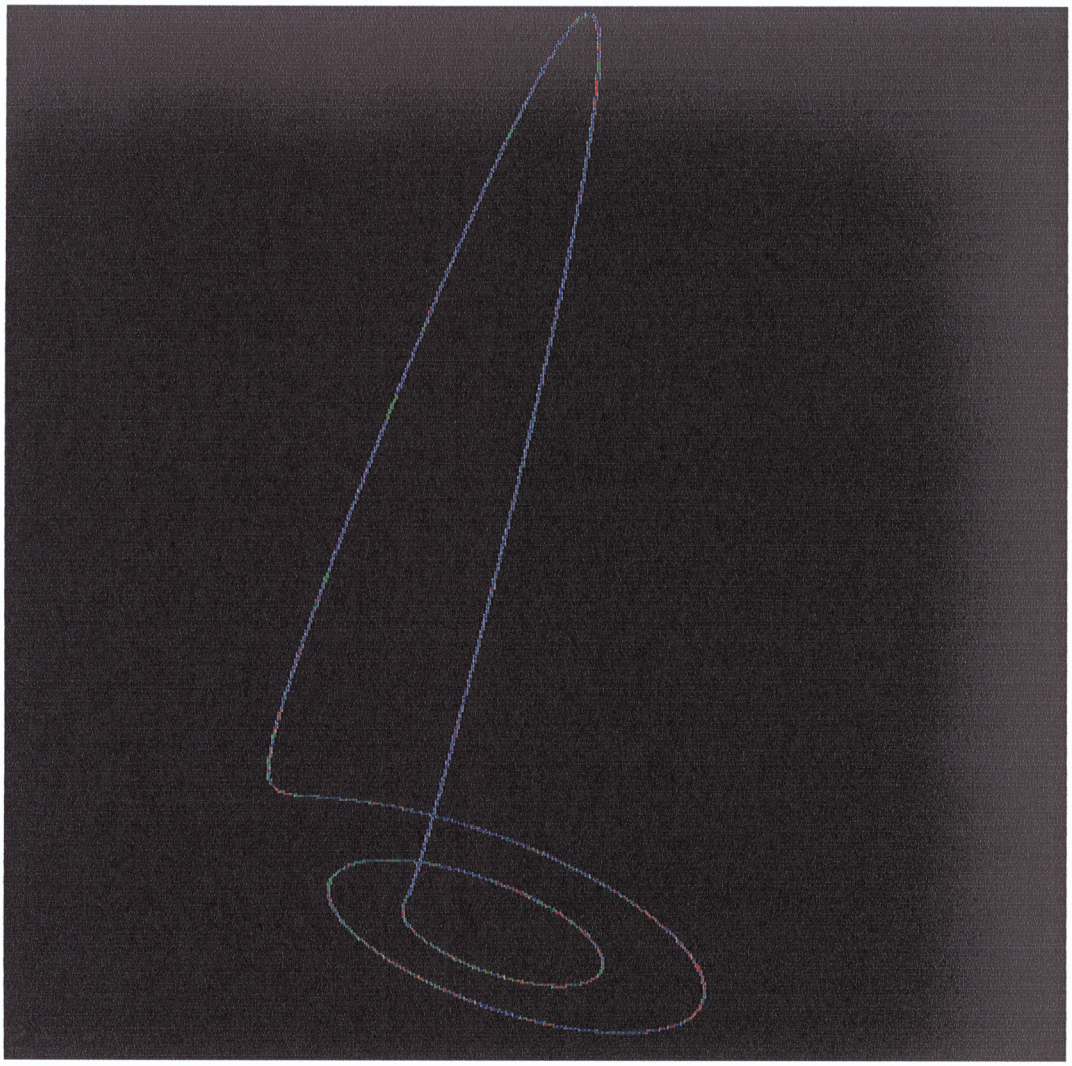

Figure 4.28: A periodic orbit of the Rössler system for c=30

As c is increased even further, the spikes become higher and higher. Past a certain value of c, the following behavior is observed. Some of the trajectories returning to the xy plane do not spiral around the center. This produces a funnel like structure, as illustrated in Figure 4.29. Rössler called this a 'skrew-type chaos'. Once again, two-dimensional images do not give full justice to the structure of this unique attractor.

4.3 Silnikov Equations

Another attractor with an even different structure is the Silnikov attractor. The equations for this system are

$$\begin{aligned} \frac{dx}{dt} &= y \\ \frac{dy}{dt} &= z \\ \frac{dz}{dt} &= -az - y + bx(1.0 - cx - dx^2) \end{aligned} \tag{4.24}$$

The solutions to these equations were not explored with any great detail. The equations are somewhat stiff, so regular integration routines run into trouble for many parameter values. A few trials were run in order to see the attractor in its full three dimensional space, and some interesting structures resulted. Some of the structures found for different parameter values are shown in Figures 4.30 through 4.32. These pictures do not reveal the three dimensional quality of the interesting funnel-like behavior found for this system as well as

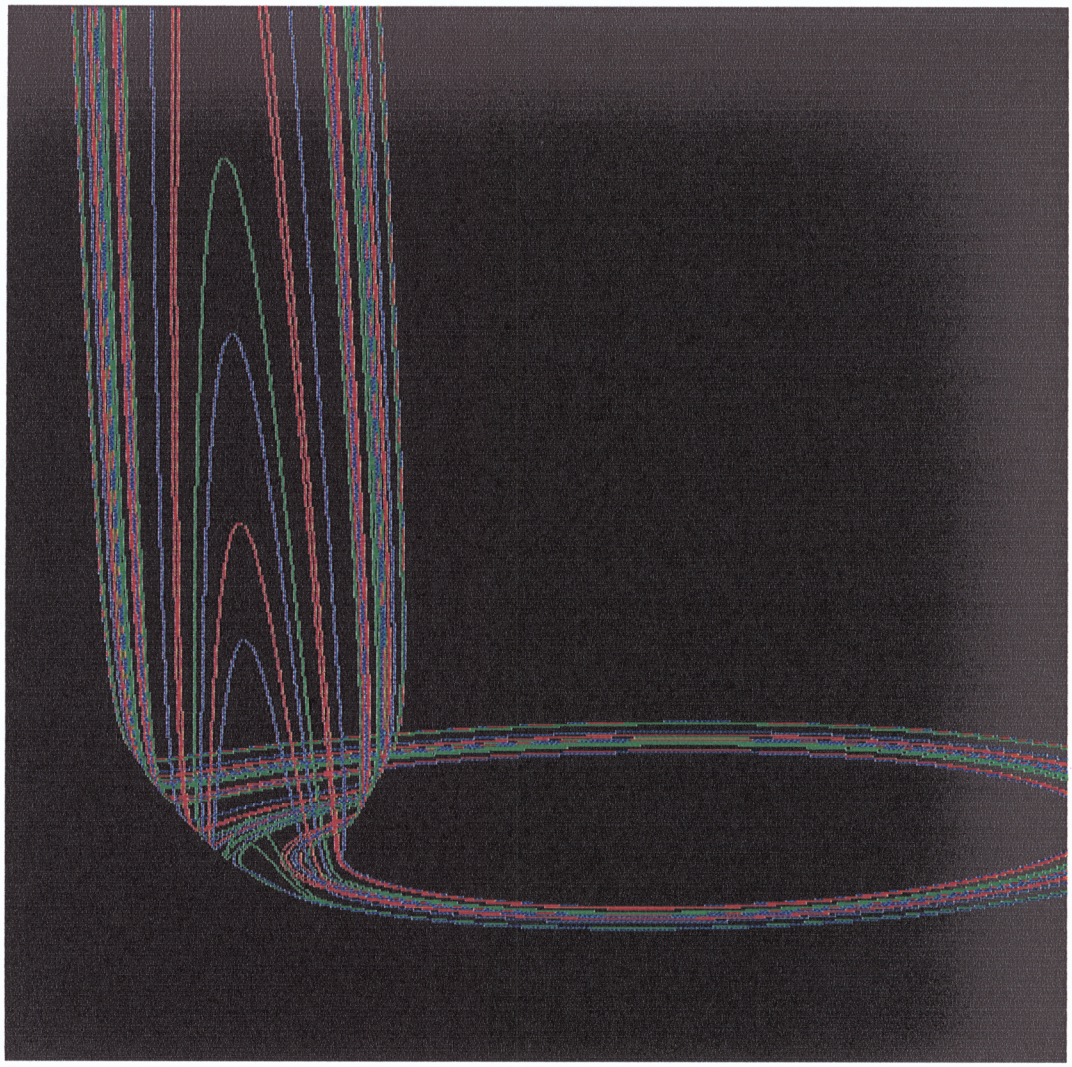

Figure 4.29: Funnel-like structure of the Rössler system for c=150

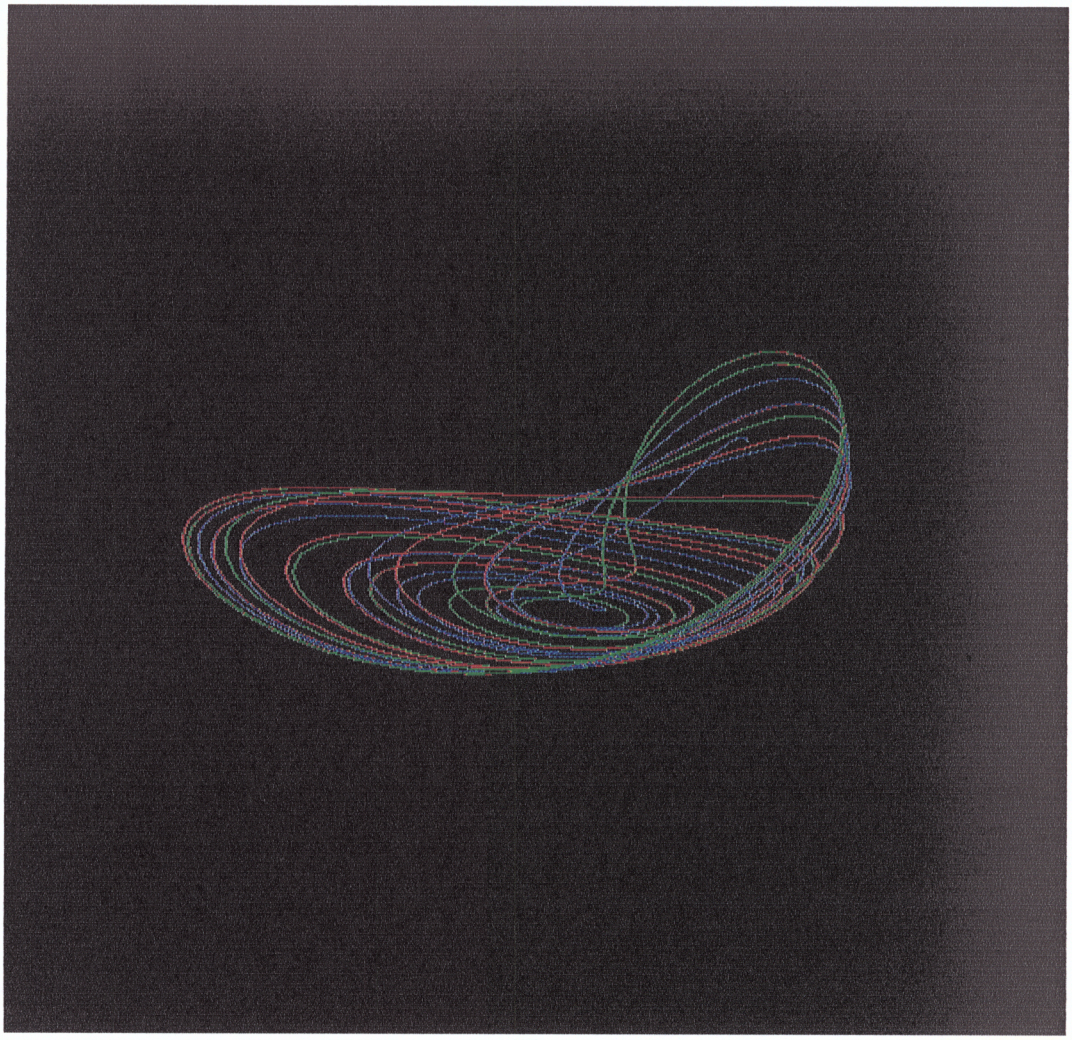

Figure 4.30: Silnikov strange attractor for a=.4, b=.65, c=1, d=1

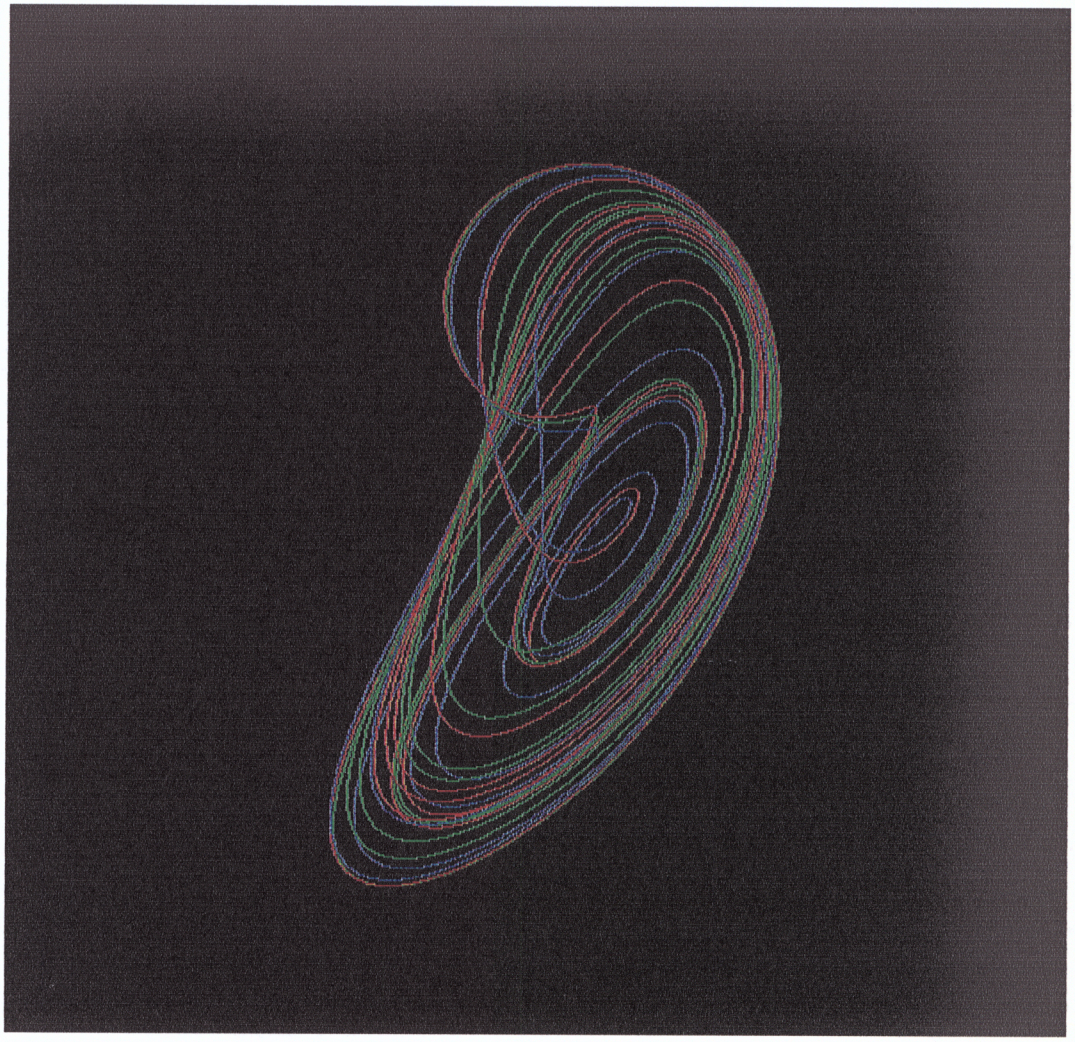

Figure 4.31: Silnikov strange attractor for a=.37, b=.65, c=1, d=1

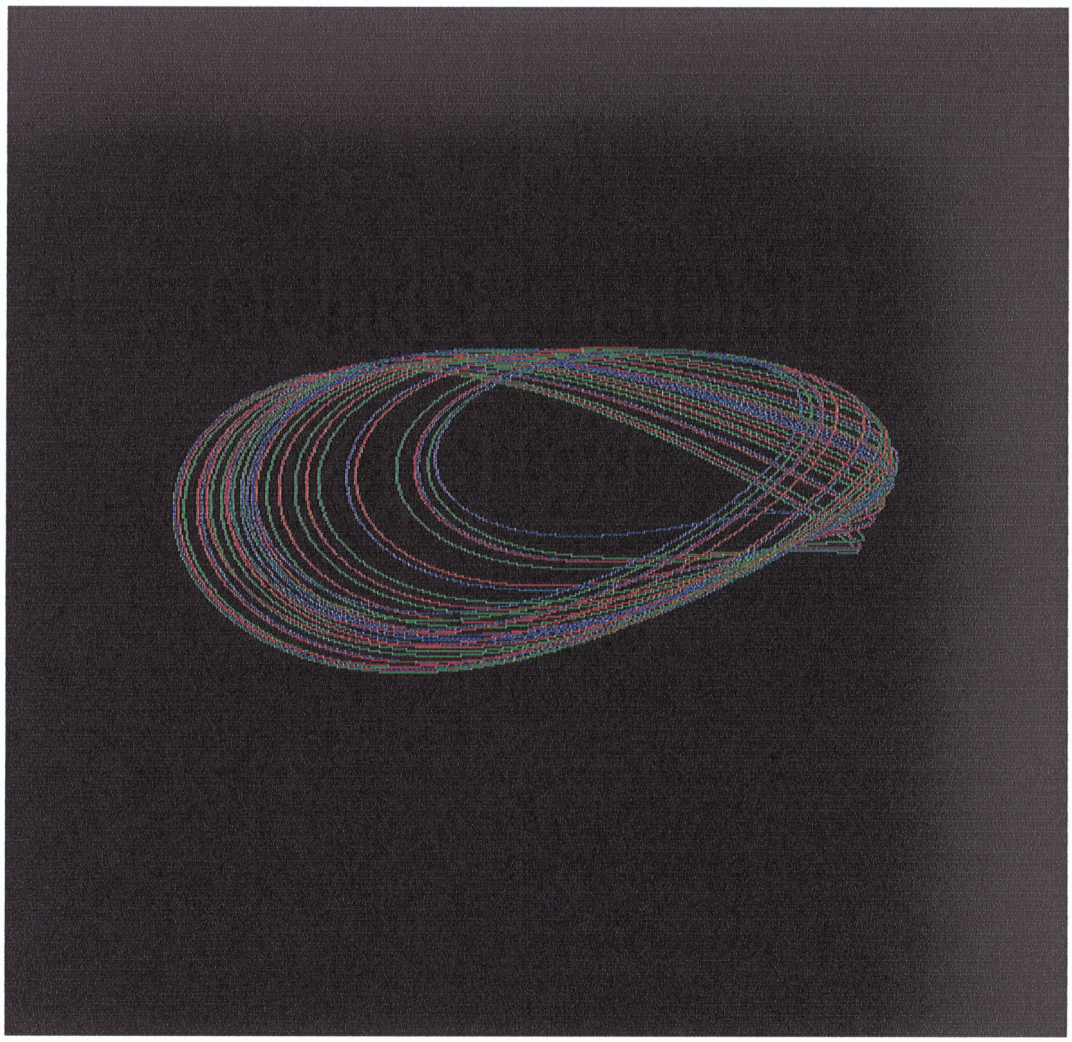

Figure 4.32: Silnikov strange attractor for a=.4, b=.7, c=2, d=1

rotation of the object does. During the visualization of the system's solutions periodic orbits were found as in the Lorenz and Rössler systems. The visualization of this strange attractor provided yet another structure for which the three dimensional capabilities of the AVS tools proved very useful, although further studies and exploration of the Silnikov solutions should be performed in the future.

This chapter discussed in detail the solutions to the Lorenz equations for changing parameter value r with fixed values of σ and b. The Rössler and Silnikov systems were also briefly mentioned and the visualization of some of the solutions to these systems was presented. Two dimensional figures were included in this report in order to give a feel for the structure of the attractors. The visualization is much more striking and educational when seen in three dimensions using the AVS tools. The final chapter makes a comparison of the AVS visualization tools with currently available methods for viewing strange attractors. A conclusion about the new tools will also be made, and suggestions for future work will be presented at the conclusion of the thesis.

Chapter Five

Conclusion

5.1 Discussion and Literature Review

In this thesis, the use of new tools to visualize strange attractors resulting from chaotic behavior of dynamical systems was introduced. After introduction of terms associated with chaos and dynamical systems, the importance of visualization of the phase space of these systems was discussed. Then AVS was introduced along with the new modules created for the purpose of viewing chaotic systems. Finally, the solutions to the Lorenz equations for $\sigma=10$ and $b=8/3$ were discussed, with figures from the AVS visualization used to attempt to illutstrate the benefits of the tool. The attractors of other systems like Rössler and Silnikov were also explored in three dimensions.

What conclusions can be made about the new way to view strange attractors? In order to show the advantages of this tool, it will be compared

with other methods currently used to visualize strange attractors.

5.11 Poincaré maps

One of the most basic and popular ways to view systems exhibiting chaos is with the use of a cross section of the orbit. A point is plotted each time the trajectory crosses a plane of interest. Periodic orbits will appear as a finite number of dots. For example, if the orbit is period one there will only be one point on the Poincaré map. If the orbit is period two, then two points will appear on the Poincaré map for all values of time. For chaotic orbits, a more complicated infinite set of points occurs. The points lie on an attractor of some shape. Figures 5.1 through 5.3 show the Poincare maps for the Lorenz Rössler, and Silnikov systems respectively. These maps are beneficial in revealing the attraction of the orbit to a strange attractor, but offer very little information about the dimensionality and shape of the attractor. The visualization of the attractors by the AVS tool not only shows the attraction of the orbits to a certain structure but also reveals the full three dimensional structure of the object in three dimensional phase space.

5.12 Other Available Software Packages

There are methods other than the Poincaré map that can be used to view strange attractors. Software packages are available to view solutions to many dynamical systems, including chaotic systems. Some of these include

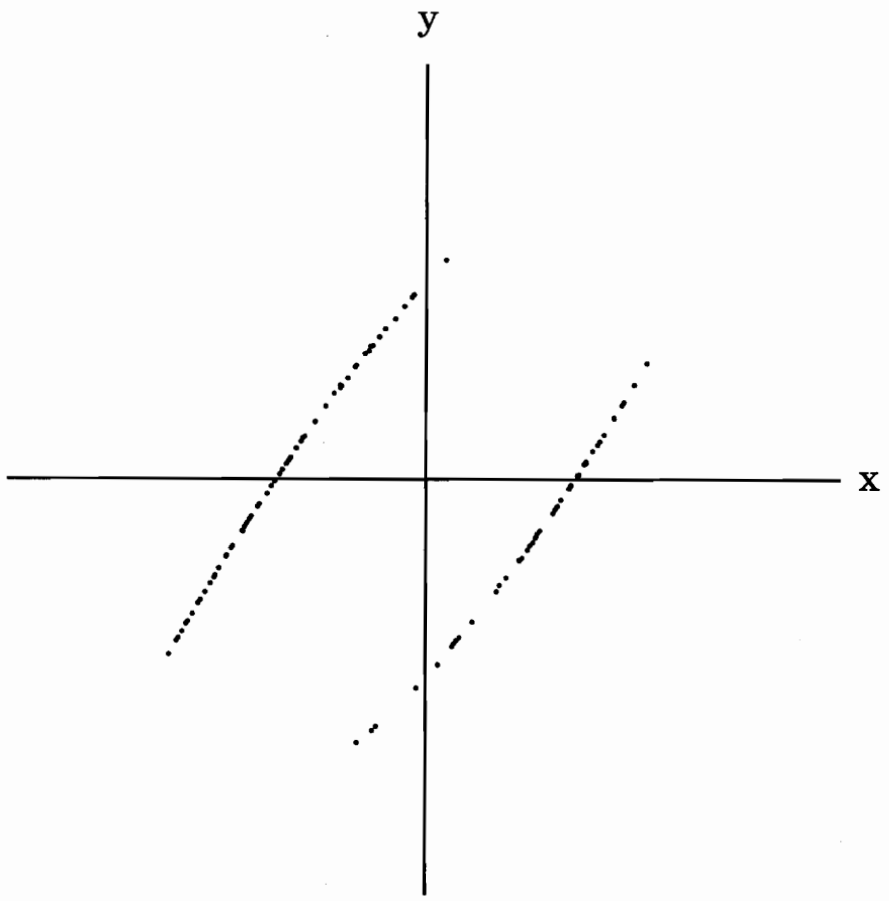

Figure 5.1: Poincaré map of the Lorenz strange attractor for the plane z=r-1, with r=28, σ=10, b=2.6667

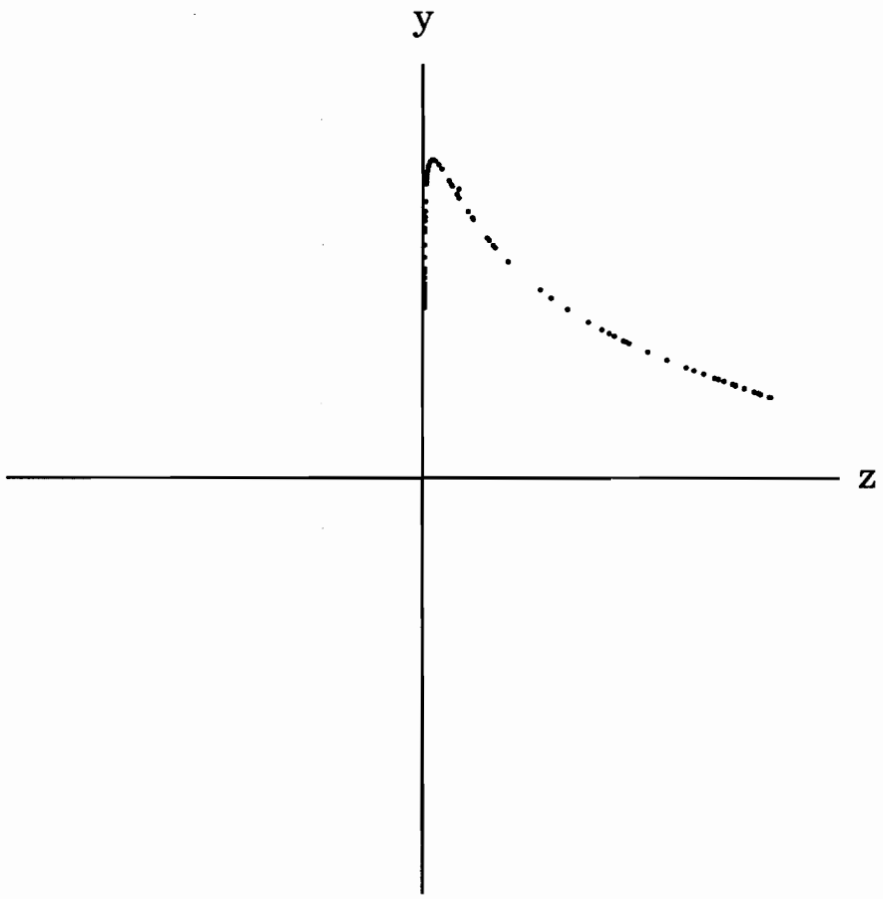

Figure 5.2: Poincaré map of the Rössler strange attractor for the plane x=0, with a=b=.2, c=5.7

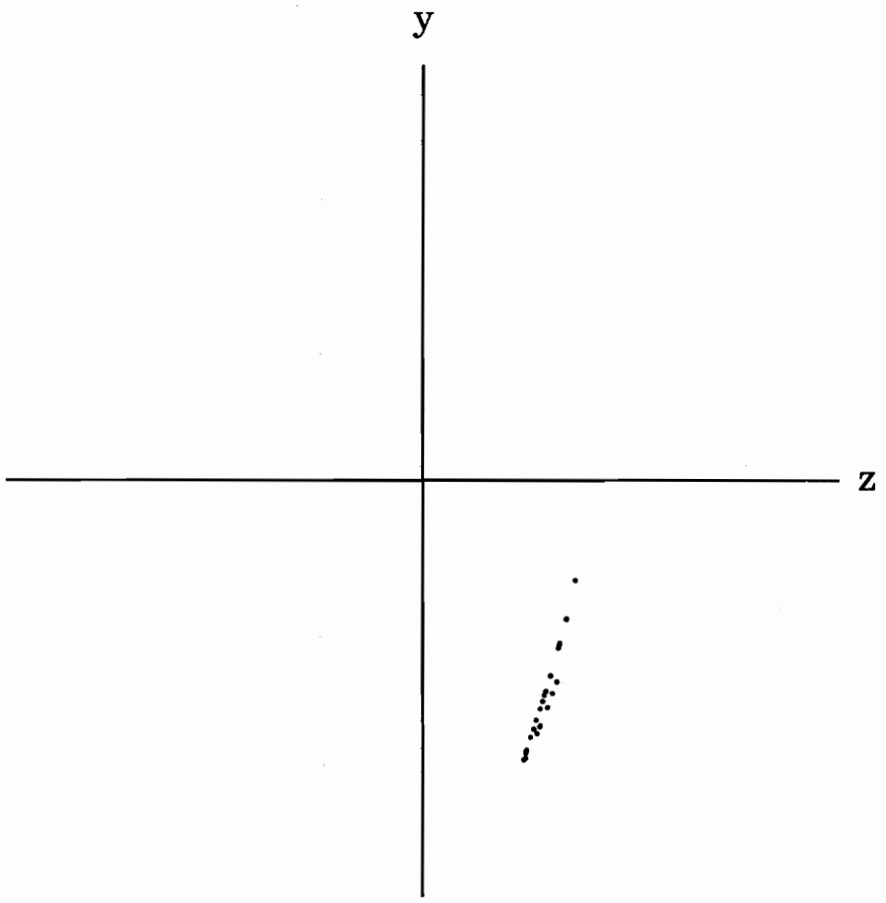

Figure 5.3: Poincaré map of the Silnikov strange attractor for the plane x=.2, with a=.4, b=.7, c=2, d=1

systems like Phaser [3] and PhasePlane [4]. Both of these packages include interactive panels that allow the user to change equations, parameters, initial conditions, and various other conditions. The display shows the trajectory developing in time, but only on a two dimensional projection. For systems with three dimensions or higher, this is a hard way to visualize the structures, especially strange attractors.

Recognizing this, Phaser and Phaseplane both allow the user to type in a certain value to see a particular rotation. For example, the viewer can type in a number to rotate about the x-axis. The problem in these programs is that the computer redraws the figure for each new rotation. So the attractor is seen as subsequent two dimensional projections which still makes it difficult to visualize the shape and dimension of the attractors. AVS, on the other hand, first draws the structure and allows the user to continuously rotate this object in any direction with a mouse button. The full structure of the attractor is more easily perceived through continuous rotation. Figure 5.4 shows a number of different rotations for the attractor. The reader can imagine these pictures in continuous animation, so that the attractor is rotated in real time. This is also supplemented by the fact that the user can also interactively stop the rotation at an interesting view and zoom in or out, and then continue by only using the mouse button, instead of having to type in values for rotation and scaling. For someone who has used both methods, the perception of a strange attractor and its dimensionality is much easier and more revealing

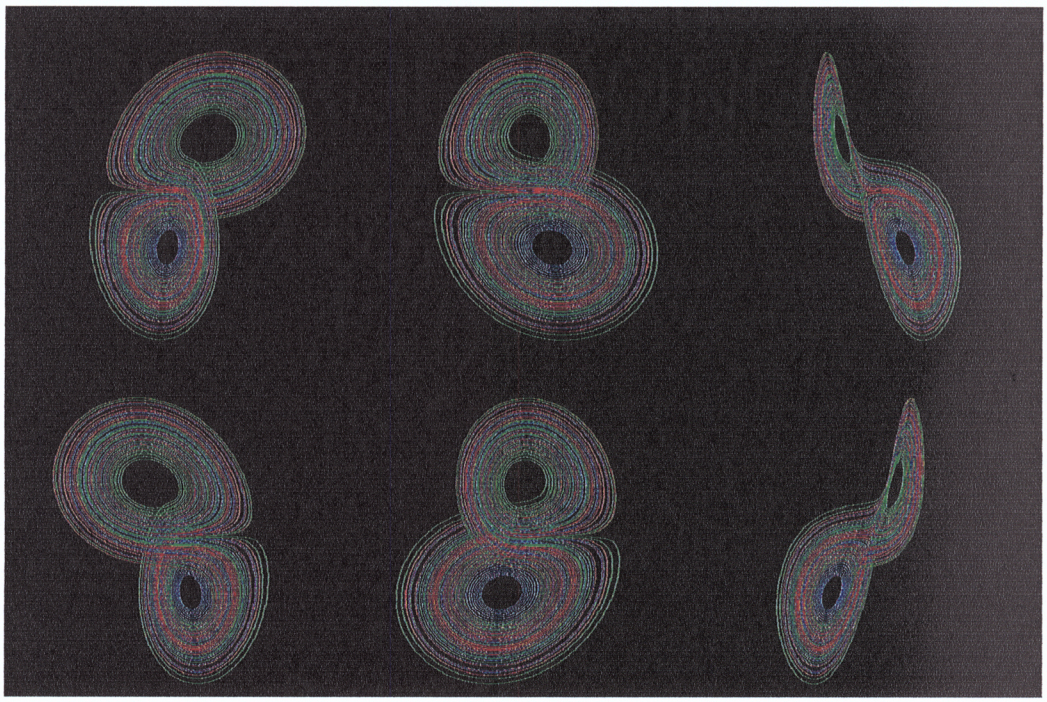

Figure 5.4: Six different rotated views of the Lorenz strange attractor

with the use of AVS and the individual modules.

Many researchers recognize the need for interactive programs that enable the user to change parameters and other conditions for immediate visual results of solutions to dynamical systems. Guckenheimer [31] authored an article titled "Computational Environments for Exploring Dynamical Systems" that suggested future possibilities for computer programs that visualize dynamical systems. The article included suggestions for interactive user interfaces, such as setting parameter values and initial conditions for computations, launching computations, and visualization of data and manipulation of graphical displays. The AVS package and the new modules created accomplish some of these tasks that are needed for better visualization of dynamical systems, especially those with strange attractors.

5.13 Other attempts

There have been other attempts to show strange attractors and their shape. Guckenheimer [31] suggests using color for depth, and Novak tries this technique in his article "The Improved Rendering of the Lorenz equations" [32]. Novak includes pictures that he developed that are two dimensional projections for two variables, with the third being mapped as a color. For example, he plots x versus z and then the depth, y, is represented by color changes. Figure 5.5 shows his attempts to show the structure. Once again, by the use of better graphics tools like AVS, a much better way to look at the attractor's shape is

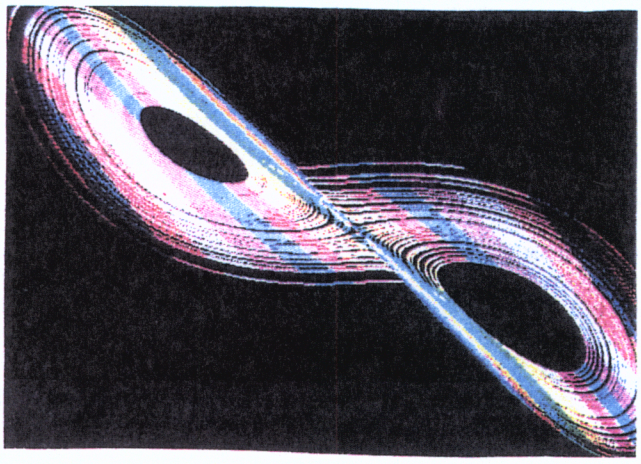

Figure 5.5: The projection of the Lorenz attractor onto the x-y plane, with color representing the variation of z; from Novak [32]

with continuous rotation. Color can be used to add another aspect of the attractor as in Colorpolyline, where it is used to show the development of the attractor over time.

There are also researchers working on programs to visualize attractors with multidimensional parameter space. Challinger [33] wrote a program on a Silicon Graphics Iris 4D/50GT to experiment with the approach of interactive visual exploration. She recognized the need for software that provides easy user interaction with sliders and the mouse button for user input and included this in her software. Also, she maintained that "rotation is extremely important for facilitating clear human perception of three dimensional objects"[33]. Her software includes sliders for which a type-in rotation about a certain axis can be made and a button for which auto-rotation can be turned on or off.

Mullin and Skeldon [34] also recognized the need for visualization of multidimensional systems and created a program on Winchester Graphics System that allows for changes in parameters and initial conditions, with quick figure generation and rotation and zooming abilities. Unfortunately, both of these researchers are dealing with multi-dimensional phase space problems, and focus on the fact that their program will plot three of the many parameters while holding the others constant. The pictures created are isosurfaces revealing sub-spaces of the system, not trajectories of solutions to dynamical systems. Their work is more geared towards possible uses for control theory.

5.2 Conclusion

In conclusion, the above comparisons show the benefits and contributions of the new tools toward the comprehension of the structure of strange attractors. It is also obvious by some of the above work that researchers find much value in the visualization of dynamical systems. The tool created in this thesis allows for some of the more important aspects of exploring solution sets visually. There are user interface panels which allow for change of initial conditions, parameter values, time step, and integration time for the solution set. Color can be used in various ways, including the relationship of color to time. Perhaps more importantly, though, is the ability to use the mouse to control rotation and scaling properties. Studies about chaos and strange attractors could be more revealing through use of all of these exciting aspects of the tool.

For this research, the Lorenz equations were explored with the visual tool in the most detail. Since these are the most famous nonlinear equations exhibiting chaos, many researchers over the past ten or twenty years have studied the complex behavior of these equations. In this sense, the AVS tool was useful as an aid to understanding the intricacies others have found. The tool was also used to visualize some of the behavior for the Rössler and Silnikov systems, revealing some of the differences in structure that strange attractors can exhibit. Simple Poincaré maps or two dimensional projections

will not reveal as many observable features of the attractors.

Finally, the video created to show these features is very educational for those who have the chance to watch it. In this thesis the attempt was made to show the outstanding features and benefits of the AVS tool, but full appreciation is most noteworthy when the user can see the tool at work.

5.3 Suggestions for Future Work

This tool, although a nice first step to new ways to explore chaos can be expanded into a more general system for exploring any dynamical systems. This writer's suggestion is that an entire AVS structure be designed solely for the use of dynamical systems. The modules could consist of the following areas:

1. A group of modules that are each different dynamical systems.

2. A group of modules that are different integration routines.

3. A group of modules that perform the plotting of the phase trajectories, like the Colorpolyline and Colorpolyline-2 modules. Also, a module that will show the trajectory plotting in real time, instead of the entire structure being plotted all at once.

4. A module to be used with this data that would include a set of x,y, and z axes on the structure if desired. (This is available for other structures in AVS but to this date was not working with the data created by the unsupported modules for this research).

5. Other interesting modules including those that slice the structure for Poincaré maps, modules that would calculate the Lyapunov exponents and reveal this as parameter values are changed, and modules that would allow the user to type in a set of equations not part of the library.

The user could then use as many of the above as needed to create a specific network that would be specialized for their problem. This added to the capabilities of AVS for rotation and scaling as well as the interactive dials would be an outstanding development for those interested in exploring dynamical systems and chaos.

References

[1] Gleick, J., 1987, *Chaos: Making a New Science*. Penguin Group, New York.

[2] Fisher, A., 1985, Chaos: The Ultimate Assymmetry. *Mosaic*, Vol. 16, p.25.

[3] Koçak, H., 1985, *Phaser*. Springer-Verlag, New York.

[4] Ermentrout, B., 1990, *PhasePlane: The Dynamical Systems Tool, Version 3.0*. Brooks/Cole, CA.

[5] Baker, G.L., and Gollub, J.P., 1990, *Chaotic Dynamics: An Introduction*. Cambridge University Press, Cambridge.

[6] Bergé, P., Pomeau, Y., and Vidal, C., 1984, *Order Within Chaos*. John Wiley and Sons, New York.

[7] Drazin, P.G., 1992, *Nonlinear Systems*. Cambridge University Press, Cambridge.

[8] Jackson, E.A., 1990, *Perspectives of Nonlinear Dynamics, Vol. 2*. Cambridge University Press, Cambridge.

[9] Ruelle, D., and Takens, F., 1971, On the Nature of Turbulence. *Communications in Mathematical Physics*, Vol.20, p.167.

[10] Liapounov, A.M., 1947, The General Problem of the Stability of Motion. Reprinted in *Annals of Mathematical Studies*, Vol. 17.

[11] Benettin, G., Galgani, L., and Strelcyn, J., 1976, Kolmogorov Entropy and Numerical Experiments. *Physical Review A*, Vol.14, P.2338.

[12] Hirsch, M.W., and Smale, S., 1965, *Differential Equations, Dynamic Systems, and Linear Algebra*. Academic Press, New York.

[13] Mandelbrot, B., 1982, *The Fractal Geometry of Nature*. Freeman, San Francisco.

[14] Lorenz, E.N., 1984, The Local Structure of a Chaotic Attractor in Four Dimensions. *Physica*, Vol. 13D, p.90.

[15] Lorenz, E.N., 1963, Deterministic Non-Periodic Flows. *Journal of the Atmospheric Sciences*, Vol. 20, p.130.

[16] Arneodo, A., Coullet, P., and Tresser, C., 1981, Possible New Strange Attractors with Spiral Structure. *Communications in Mathematical Physics*, Vol. 79, p.573.

[17] Arneodo, A., Coullet, P., and Tresser, C., 1982, Oscillators with Chaotic Behavior: An Illustration of a theorem of Shil'nikov. Journal of Statistical Physics, Vol. 27, p.171.

[18] Tufte, E.R., 1983, *The Visual Display of Quantitative Information.* Graphics Press, Conn.

[19] Haber, R.B., 1990, Visualization Techniques for Engineering Mechanics. *Computing Systems in Engineering*, Vol. 1, p.39.

[20] Kriz, R.D., 1990, Computer Simulation and Visualization of Stress Wave Propagation. *Scientific Computing and Automation*, Vol. 6, p.19.

[21] Advanced Visual Systems, Inc., 1992, *AVS User's Guide.* Advanced Visual Systems, Inc., MA, (617) 890-4300.

[22] Module Computer Codes were written by John Shalf, 1993, Blacksburg, VA.

[23] Sparrow, C., 1982, *The Lorenz Equations: Bifurcations, Chaos, and Strange Attractors.* Springer-Verlag, New York.

[24] Schuster, H.G., 1984, *Deterministic Chaos: An Introduction.* Physik-Verlag, Weinheim.

[25] Routh, E.J., 1897, *On the Stability of a Given State of Motion.* Macmillan, New York.

[26] Kaplan, J.L., and Yorke, J.A., 1979, Preturbulence: A Regime Observed in a Fluid Flow Model of Lorenz. *Communications in Mathematical Physics*, Vol. 67, p.93.

[27] Yorke, E.D., and Yorke, J.A., 1979, Metastable Chaos: Transition to Sustained Chaotic Behavior in the Lorenz Model. *Journal of Statistical Physics*, Vol. 21, p.263.

[28] Marsden, J., and McCracken, M., 1976, *The Hopf Bifurcation and Its Applications*. Springer-Verlag, New York.

[29] Frøyland, J., and Alfsen, K.H., 1984, Lyapunov-exponent Spectra for the Lorenz Model. *Physics Review*, Vol. A29, p.2928.

[30] Lorenz, E.N., 1980, Noisy Periodicity and Reverse Bifurcation. *Annals of New York Academy of Science*, Vol. 357, p.282.

[31] Guckenheimer, J., 1991, Computational Environments for Exploring Dynamical Systems. *International Journal of Bifurcations and Chaos in Applied Sciences and Engineering*, Vol. 1, p.269.

[32] Novak, M.M., 1991, Improved Rendering of the Lorenz Equations. *Image and Vision Computing*, Vol. 9, p.169.

[33] Challinger, J., 1992, Interactive Graphical Exploration of Multidimensional Nonlinear Dynamical Systems. *International Journal of Bifurcations and Chaos in Applied Sciences and Engineering*, Vol. 2, p.251.

[34] Mullin, T., and Skeldon, A., 1992, Phase Portraits for Parametrically Excited Pendula: An Exercise in Multidimensional Data Visualization. *Computers and Graphics*, Vol. 9, p.169.

Vita

Tracy Stauffer Halsey was born Tracy Ann Stauffer on June 5, 1969 in Allentown, PA. She was raised for the next seventeen years in the nearby town of Emmaus, where she graduated from High School in 1987.

After high school, she attended Penn State University, much to the delight of her Dad the Nittany Lion fan. It was not until her fourth and final year at Penn State that Tracy finally decided "what she wanted to be when she grew up." Being a Supplementary Instructor for freshman Calculus during her senior year helped her to realize how fulfilling teaching was, especially at the collegiate level. She realized, however, that this would require more education so she spent her senior year applying to graduate schools.

Fortunately she was accepted by a few along with her fiance and high school sweetheart, Andy Halsey. After much discussion, they decided to attend Virginia Tech, where Andy was finishing up his Bachelor's Degree in Aerospace Engineering. With that decision made, Tracy enjoyed the rest of her senior year and graduated cum laude with a Bachelor of Science in Science.

Tracy spent the next two intense years pursuing her Master's Degree in Engineering Mechanics at Virginia Tech. In the summer between she married Andy Halsey, a dream she had since their very first date. After graduation from Tech in May, she plans to hopefully teach in Engineering Education, get a sister for her dog Hershey, and most importantly have a family.

Tracy Stauffer Halsey